# Evaluation of the Measurement Capabilities of an Autonomous Surface Vessel in Coastal Regions

A thesis
submitted in partial fulfilment
of the requirements for the degree
of
**Master of Science (Research)**
**in Earth and Ocean Sciences**
at
**The University of Waikato**
by
**MORGAN EMILY HARVIE**

THE UNIVERSITY OF
WAIKATO
*Te Whare Wānanga o Waikato*

2019

# Abstract

Reliable monitoring data underpins many coastal management decisions; such as decisions associated with development of defence strategies for coastal hazard protection or ecosystem-based estuarine management. For coastal monitoring, recent new technologies are providing opportunities to widen the scope of data collection. We assessed use of an Autonomous Surface Vessel (ASV), known as the JetYak, for taking a variety of measurements in two coastal environments. We examined the quality and reliability of data acquired by the JetYak and performance of steering for surveying in automated driving mode.

The JetYak can be programmed to run in autonomous mode and follow a predefined path. However, the turning angle of the JetYak was quite large and hence, the vessel can easily overshoot or undershoot the target path. A series of optimisation tests were run at Lake Ngaroto, New Zealand to optimise the of steering and throttle parameters for the JetYak. The driving parameters FF gain, P gain, navigation period, P throttle and cruise speed were systematically varied to examine the effect of each parameter on the straightness of the path to each waypoint. With the right parameters, this deviation was minimised, and an optimal set of parameters were saved for future research using the JetYak.

The JetYak was also tested for measuring flows around seagrass in the Tauranga Estuary, to investigate the possibility of resolving small-scale changes in velocity with a downward-mounted ADCP and independent GPS system. However, in this case, the performance of the instrumentation set-up proved inadequate. The JetYak was travelling too fast during the survey, and the influence of the vessel's motion was not entirely removed from velocity measurements. For future studies of this nature, we would recommend using the JetYak at a slower speed or using a purpose-built boat integrated boat-mounted system for better results.

Measurements of salinity, temperature and turbidity were taken in the Waihou River plume in the Firth of Thames, from low tide to high tide, using the JetYak and a research vessel. The JetYak successfully captured data inside and outside the surface plume, which revealed that as the flood stage of the tidal cycle progressed,

the plume was pushed towards the west of the Firth and then towards the southern end into the mangroves with the incoming tide. Measurements attained from the JetYak and vessel were in good agreement for salinity, although some of the turbidity measurements did not appear to be correct, likely owing to air around the sensor. Overall the JetYak was successful at resolving the how plume progressed over spatial and temporal scales.

The JetYak was proven to be a very useful tool for taking measurements in shallow coastal environments. However, it requires the appropriate set-up and the scientists and researchers need to be trained in both operational (piloting) skills and data processing skills. One advantage of the JetYak over a manned vessel is the precision of positioning, generally exceeding that of manual craft, thus allowing driving of near identical transects and to decrease errors in the data. Such data would suit monitoring over large temporal scales such as months to years to understand coastal dynamics and validate numerical models. Another key use of the JetYak would be in the completion of missions alongside a research vessel. Such an approach allows for the collection of data over multiple transects simultaneously, thus greatly increasing spatial resolution of measurements, without significantly increasing personnel requirements.

# Acknowledgements

Firstly, I would like to thank and acknowledge my supervisor Dr. Julia Mullarney. Julia, thank you for your helpful guidance, patience and your passion towards the project and coastal science. You are an inspiration to me and entertaining out in the field. I will be forever appreciative of you for being understanding and for allowing me to use the JetYak for this research.

I am also very grateful to the American Chemical Society for providing much needed funding for this research. I would also like to thank NIWA and The University of Waikato for providing instrumentation for this research.

Dean Sandwell, I am so grateful for the hard work and time you put into getting the JetYak up and running and user friendly. Thank you for being kind, even when you were super busy, which happened to be all the time. Your hard work ethic and friendly and approachable personality did not go unnoticed and I am so proud of how the JetYak performs and am excited for it to be used in future projects.

I would also like to thank my family and Nick for supporting me through this research and for being loving and supportive of my goals. Thank you for being understanding and for not asking too many questions.

Similarly, I would like to thank the nicknamed 'Julia Gang' that listened to me at each weekly meeting and spent time together in the field and in the office, Hemanth Bharadwaj, Berengere Dejeans, Tiago Dutra de Silva, Ben Norris, Peter de Ruiter, and Yuliana Ramirez.

Lastly, to all the friends I have made along the way, that have listened to me talk about the JetYak and have had no idea what I was talking about but, had listened anyway. Thank you for being supportive, encouraging and for getting me through this research with all your smiles and laughs.

# Table of Contents

# List of Figures

# List of Tables

# Chapter 1

# Introduction

## 1.1 Coastal Environments

The majority of the world's increasing population lives near to the coast (Nicholls & Hoozemans, 1996; Small & Nicholls, 2003). Coastal ecosystems are therefore, being subject to a growing number of stressors as a result of this growing population. Similarly, an increasing number of people are being exposed to coastal hazards (Nicholls & Small, 2002). Good quality measurements of key variables are required to underpin and develop robust coastal monitoring and protection strategies (Ellis *et al.*, 2012).

Coastlines can be extremely vulnerable to dangerous weather events including large storms, noting that hazards are only perceived as threats, if there are people or property to harm (Nicholls & Small, 2002). Consequently, in densely populated areas, the greater the coastal hazard is perceived to be. Overall analysis is determined by the severity of a hazard for a range of exceedance levels and the potential losses or consequences of the hazard (Shand *et al.*, 2015; Wainwright *et al.*, 2015). Accurately measuring and monitoring the coastal zone is consequently, important to quantify this risk (Wainwright *et al.*, 2015), and needs to be combined with consistent monitoring, to understand and quantify the substantial changes to the coastal zone as a result of human activity (Gornitz, 1991; Small & Nicholls, 2003). Other changes to the coast, including sea level rise could also endanger these coastal communities due to increased inundation and erosion. The consequences of sea level rise are not uniform from coastline to coastline therefore, it is important to monitor each individual coastline for resistance to these hazards as well as the changes in flow patterns and features (Gornitz, 1991).

An estuary is defined by Cameron and Pritchard (1963) as "a partially enclosed body of water that receives inflow of fresh water from land drainage and which has an open connection with the open sea." Estuaries are highly dynamic coastal environments, which are continually being modified as a consequence of their position at the boundary between the open ocean and the land. Individual estuaries

can be in a depositional or erosional regime: The erosion and deposition patterns are altered in response to changing of flow patterns and water depths as well as sediment inflow from land drainage. Estuaries are affected by river flows, tides, waves, wind and seiches and can be a sink for nutrients due to the long residence times (Nedwell *et al.*, 1999). Estuaries have been described as 'nurseries of the sea' by Boesch and Turner (1984); (Beck *et al.*, 2001), due to the sheltered environment and excess nutrients from fresh water inflow and run off from land drainage. Thus, estuaries can provide a good location for an abundance of fish and invertebrates to reproduce due to the high primary and secondary productivity (Beck *et al.*, 2001). Estuaries can be sheltered from large winds and waves and provide protection for fish and invertebrates species to thrive. Birds also rely on estuaries for food and nesting areas, therefore, changes to the estuarine system can impact the whole ecosystem and disrupt important food chain and life cycles (Klein & Nicholls, 1999).

## 1.2   Monitoring and Numerical Modelling

Reliable measurements of the coastal and estuarine zone are crucial for a number of purposes, for example: Measurements can be used in the prediction and prevention of coastal hazards (Geeraerts *et al.*, 2007). Coastal monitoring was determined to be the key to understanding the dynamics of coastal morphology and collections of survey data can be used to quantify long-term erosion and accretion rates in addition to rates of recession and recovery (Harley *et al.*, 2011). Along with these physical processes, it is also important to monitor marine ecosystems to assess how these valuable areas are being impacted by anthropogenic disturbances and whether the rate of change is exceeding marine organisms ability to adapt (Doney *et al.*, 2011). The effects of the growing population at the coast to ecosystems can vary over spatial and temporal scales, (Halpern *et al.*, 2009) therefore, reliable and consistent measurements are needed for prediction and prevention of changes to ecosystems and habitats (Claudet & Fraschetti, 2010). Changes to water quality can have an influence on ecosystems, which can then be assessed to evaluate the coastal environment, for example: Measurements of pollution levels within biomarkers (Cajaraville *et al.*, 2000). Data collection is often still lacking in potentially hazardous or remote areas of interest (Nicholls & Small, 2002; Moulton *et al.*, 2018).

Within New Zealand, regional councils are tasked with undertaking state of the environment monitoring to meet the obligations of the Resource Management Act (RMA) (Section 35(2)a). The RMA provides the framework for environmental planning and management and is the basis for new policy documentation (Memon & Gleeson, 1995). Policy documents at both the national and regional level, require monitoring of variables such as sedimentation levels (eg. Policy 22, New Zealand Coastal Policy Statement (NZCPS) (Department of Conservation, 2010), Chapter 7 in the Sea Change, the Hauraki Gulf Marine spatial plan), marine water quality (NZCPS, policy 7.2) and ecosystem health (Sea change chapter 6 (Sea Change Stakeholder Working Group, 2017)). The New Zealand Coastal Policy Statement 2 (NZCPS) is also used to monitor to inform coastal hazards management decisions by assessing coastal erosion and accretion as well as other additional factors (Shand *et al.*, 2015).

Monitoring over large spatial and temporal scales to show the changes to the coast as a requirement of the RMA, poses many challenges and there often lacks the time and resources to do so (Nicholls & Hoozemans, 1996; Harley *et al.*, 2011). However, standardised long-term records are essential to create new hypotheses of future hazards and protocol for hazard management (Wolfe *et al.*, 1987) as well as, monitor water quality aspects to identify changes in the environment occurring as a result of anthropogenic activity (Ellis *et al.*, 2012).

Numerical models are tools that are commonly employed by coastal managers, developers and planners. Modelling is the process in which often simplified mathematical equations are solved to provide insights into complex real processes (Blum & Ferri, 2009). Modelling has been proven to be a very effective tool in multiple situations such as:

- showing the main features and impacts of coastal hazards (Vickery *et al.*, 2009).
- showing how vulnerable different coastal environments are to coastal hazards (Nicholls & Small, 2002).
- predictions of how hydrodynamics will change in harbours following dredging (Mullarney & de Lange, 2018, 2019).

However, it is important to note that even with the best models and the best model inputs, there can still be errors in numerical modelling. Errors can be due to assumptions made when calculating the set of equations, which can give some uncertainty in the estimates of coastal hazard impacts (Resio *et al.*, 2009). Developing a process-based understanding for implementation into numerical models is needed for reliable predictions, and as a first step, reliable measurements are needed as inputs, calibration and validation data (Geeraerts *et al.*, 2007).

Flows in estuaries are strongly influenced by the bathymetry. Changing water depths within these coastal environments can alter the flows speeds as shown by Hernández-Dueñas and Karni (2011). Consequently, the depth of the estuary can be regarded as a first order input for any numerical model (She *et al.*, 2007).

### 1.2.1  Difficulties in Collecting Coastal Measurements

For accurate model predictions, good measurements are needed; however, obtaining such reliable measurements in these highly variable coastal environments can be particularly challenging. Difficulties arise due to the shallow water environment, rapidly changing water depth and the continuous wetting and drying from the incoming and outgoing tides (Moulton *et al.*, 2018). In order to achieve accurate results in these challenging environments, it is crucial to repeat experiments for an accurate representation of coastal features and to remove errors in the data (Nicholls & Hoozemans, 1996). It is also crucial to capture measurements over large regions, but, resolving the variety of spatial scales can also be challenging (Horner-Devine *et al.*, 2015) and time consuming (Devlin *et al.*, 2012). The time-consuming factor equates to a greater amount of resources spent, including costs of operation, and can be labour intensive, especially when using large vessels. Large vessels can also be limited to deep waters and generally more open seas (Moulton *et al.*, 2018). However, new technologies (both measurement techniques and instrumentation) are constantly being developed, which may assist in mitigating some of these difficulties.

### 1.2.2  Types of Measurements

Different styles of measurements can be used to their advantages when collecting data from difficult to measure areas and to capture the complexities of ocean

dynamics (Davis, 1994). Eulerian and Lagrangian measurements are two different methods that can be used with corresponding advantages and disadvantages. Eulerian measurements are collected in situ and collect data from one point over a period of time (Wu *et al.*, 2012). Data is collected as a time series and multiple instruments are required to capture data over spatial scales and resolve gradients. Eulerian measurements can be used in modelling to interpret the larger spatial scale changes. Instrumentation that can be used include acoustic doppler current profilers (ADCPs), echo-sounders, and water temperature, turbidity and conductivity sensors. These instruments are generally non-invasive and do not change the flow of water or move material and organisms (Falter *et al.*, 2008), outside of the immediate vicinity of the instrument. Lagrangian measurements are taken in a flow-following frame of reference, typically by attaching an instrument to a drifter which moves at (close to) the current speed (Mullarney & Henderson, 2013). Lagrangian methods measure changes over both spatial and temporal scales (Davis, 1994). These methods can be used to increase the area surveyed for a better representation of coastal processes. Difficulties surrounding Lagrangian methods are due to the motion of the drifter and subsequently, the instrument attached, affecting the data collection: This motion must be accounted for (removed) from the data. A time series of data is acquired that moves with location therefore, positioning data is also required throughout the survey. Lagrangian data can be complicated to process or interpret owing to the nature of changing over spatial and temporal scales, thus, it is advised to repeat transects to evaluate the data (Davis, 1994).

A separate type of measurement from Eulerian and Lagrangian is boat-mounted measurements. Boat mounted measurements are often classed as quasi-Lagrangian, as they do not follow the flow; however, similar to Lagrangian measurements, these measurements capture data from varying spatial locations (Riser & Rossby, 1983). Specific vessel-mounted (VM) instrumentation can be used to collect data of this type but, require specialised equipment. The motion of the vessel is measured when collecting current velocities. This vessel motion must be removed from the data. The speed the vessel is travelling can be found using bottom tracking techniques or from boat-movement tracks to remove the vessel's movement to attain actual velocities of the water column (Yorke & Oberg, 2002).

## 1.3   The JetYak

Environmental monitoring in these marine environments such as estuaries can be challenging (Moulton *et al.*, 2018), therefore, the right equipment and methods are needed for accurate results (Falter *et al.*, 2008). The spatial variability in the coastal zone entails monitoring to ideally include coverage of a vast area for comprehensive understanding of the coastal processes. Operations completed manually can be long, drawn-out processes that can be dangerous as well as costly (Moulton *et al.*, 2018). Low-cost autonomous research platforms have become increasingly prevalent in the marine sciences. Their uses include, but are not limited to, bathymetric mapping, habitat mapping and water quality data collection (Valada *et al.*, 2014).

We explored use of an Autonomous Surface Vessel (ASV) known as the JetYak to address some these problems with monitoring. The JetYak is a motor-powered instrument that has the ability to navigate autonomously in shallow water environments (Kimball *et al.*, 2014). Due to the JetYak's small size, power and fuel efficiency, the JetYak can be operated for extended periods. The JetYak can be operated to perform survey task missions with coverage of large areas at low cost, in comparison to the same mission carried out by a manned vessels (Ludvigsen *et al.*, 2018; Moulton *et al.*, 2018). Moreover, the JetYak can be used in addition to manned vessels to increase spatial scales to show the extent of hydrodynamic processes (Moulton *et al.*, 2018). We test the JetYak for two purposes described briefly below.

### 1.3.1   Hydrodynamics over Seagrass Beds

The JetYak was used to measure the flows over seagrass patches in the Tauranga estuary. The hydrodynamics within an estuary control transport, erosion and deposition of sediment in the bottom boundary layer (Cheng *et al.*, 1999). Seagrasses are thought to provide protection of the coast due to their ability to stabilise sediments in shallow coastal environments by altering the hydrodynamics (Bos *et al.*, 2007). Therefore, the monitoring of seagrass flows could benefit coastal communities and be used to inform mitigation strategies for coastal hazards by shifting away from traditional engineering structures to more natural coastal protection solutions. However, before such eco-engineering is implemented, a deeper understanding of how seagrass manipulate flow patterns is essential

6

(Ondiviela *et al.*, 2014). Due to the shallow water environment seagrass inhabit, traditional methods of flow measurements such as those on a manned boat are quite restrictive (Moulton *et al.*, 2018). We used the JetYak to collect data in the Tauranga estuary to examine if the JetYak could be used to show changes in flows over seagrass.

### 1.3.2 River Plume Monitoring

River plumes span substantial areas and are constantly changing with time and the incoming and outgoing tides. This coastal feature can be challenging to accurately monitor because of these characteristics (Moulton *et al.*, 2018). We used the JetYak alongside a research vessel to measure the extent of a river plume. We examined the Waihou River plume which debouches into the Firth of Thames. Rivers are primary mechanisms in delivering sediment (Milliman & Syvitski, 1992; Nittrouer *et al.*, 1995) and dissolved nutrients to the coastal environment and therefore, are heavily impacted by land development, urbanisation and agriculture (Lathrop *et al.*, 1990). There is a requirement for consistent monitoring (Lathrop & Lillesand, 1989) to understand the hydrodynamics of river plumes, and the impact of increased inputs of sediment, nutrients and contaminants on ecosystems (Lathrop *et al.*, 1990).

## 1.4 Aim

The overarching aim of this thesis is to test this new technology of the JetYak to see how it performs in two different coastal situations and therefore, to answer these questions:

1. How can the JetYak be operated to benefit future coastal research and used at maximum potential?
2. What are the limitations surrounding use of the JetYak and the data it can collect?

The Autonomous Surface Vessel (ASV) is evaluated on how these challenges in measuring and monitoring in marine environments can be overcome. We test the use of the automated JetYak in two situations:

1. The Tauranga estuary examining flows over seagrass.
2. The Waihou River plume which spreads into the Firth of Thames.

The two experiments will be covered in their respective chapters.

## 1.5   Thesis Outline

Chapter 2 is a review of the JetYak and instrumentation onboard the autonomous vessel for surveying. We discuss the uses, purpose, set-up and describe the procedures used and results from tests to optimise the internal driving parameters.

Chapter 3 provides background on the effects of seagrass in the process of disrupting flow patterns and the importance of seagrass in the region for sediment transport and deposition. This chapter also provides details of the methodology used in sampling and the instrumentation used to gather the data in the Tauranga estuary. It includes the results from the experiment and discussion of the findings.

Chapter 4 consists of the Firth of Thames river plume monitoring using the JetYak in addition to a research vessel and processing of the data collected, and the methods used. This chapter also includes the findings from the experiment.

The final chapter, chapter 5, summarises and concludes the results obtained in previous chapters and the final section is an overview from this study of the capabilities of the JetYak and recommendations for future use.

# Chapter 2

# JetYak Preparation & Optimisation

## 2.1 Introduction

Autonomous vehicles and vessels have been used for many decades for use for shipping, military, transport and scientific research (Tsai *et al.*, 2019). However, only recently in the past few years have they become relatively inexpensive and hence, more commonly used (Wang *et al.*, 2009; Valada *et al.*, 2014). The JetYak is an Autonomous Surface Vessel (ASV) which can provide new opportunities for marine studies especially within shallow water or dangerous conditions where boats and manned crafts cannot be operated (Kimball *et al.*, 2014). Therefore, the JetYak offers the opportunity to collect data and research areas of marine or fresh water environments that have been previously undisturbed (Kimball *et al.*, 2014; Ludvigsen *et al.*, 2018). The automation of the JetYak also provides increased accuracy and repeatability of transects and manoeuvres for optimal data collection (Kimball *et al.*, 2014). The JetYak also offers the possibility of being used as an extra tool, alongside other research vessels to increase surveying speeds and expand the area of surveys to attain large data sets without increasing the resources spent or increasing the number of personnel required to conduct such surveys (Ludvigsen *et al.*, 2018; Moulton *et al.*, 2018).

For repeatability of transects, it is important that the JetYak drives the same course to each waypoint, no matter the conditions. We established and tested the JetYak's operating procedures before attempting parameter optimisation. This process included developing start up procedures, equipment needed to run the JetYak as well as rescue vessels and user knowledge of the JetYak systems. Controlling the motion of an ASV can be challenging due to the nature of the small vessel in its dynamics and environmental disturbances such as currents, waves and differing wind speeds and directions (Shojaei, 2016; Moulton *et al.*, 2018). These challenges can be partly solved by optimising parameters used to automate the driving of the vessel. The JetYak uses Mission Planner by ARDUPILOT, an open source programme, originally designed for drones but which now supports use for planes, rovers, boats and helicopters. Mission planner allows pre-programming of missions

for the JetYak to follow as well as includes satellite images from google to be used as a guide (Kimball *et al.*, 2014). Rover firmware is used to control the JetYak and can be fine-tuned to optimise steering angle and throttle control based on proportional, integral and derivative (PID) feedback of cross track error. Throttle changes to increase or decrease speed of the JetYak are also controlled by PID feedback measured by GPS positioning (Kimball *et al.*, 2014). The control algorithm based on sensory output is critical for controlling the vessel in locations where conditions are not constant as a result of large waves, strong winds or currents (Moulton *et al.*, 2018).

### 2.1.1 JetYak Specifications

The JetYak was created and produced for the University of Waikato by Integrated Coastal Solutions located in the USA. Integrated Coastal Solutions used a model of a jet-powered kayak previously created by Mokai Manufacturing Inc. which was designed for individual use for recreational purposes. Integrated Coastal Solutions used the Mokai design and transformed the jet-powered kayak into the JetYak equipped with sampling and data collection methods and computer systems set up. These computer systems allow the JetYak to drive autonomously or to be controlled remotely. The autonomous auto-pilot mode requires a pre-determined track to be created and transmitted to the JetYak from Mission Planner.

The configuration and components of the University of Waikato JetYak are shown in Figure 2.1. The range of the data collection from the JetYak extends over large scales, both temporal and spatial with a run time of up to 8 hours at a speed of 3.6-5.6 metres per second (Ludvigsen *et al.*, 2018). Transects can be preprogramed into the computer system onboard for the JetYak to follow, as well as, remotely controlled from the shore or larger vessel. The instrument can easily switch between the two modes for sampling and safety (Shojaei, 2016; Ludvigsen *et al.*, 2018). The system is powered by two 12 V batteries for the control and navigation system. Scientific instruments for example, ADCPs or echo-sounders, can be easily added to the JetYak and powered by the large batteries. The University of Waikato JetYak also features a sea chest inside the JetYak allowing instruments to be positioned in the water without damaging electronics onboard (Figure 2.2). The communication

with the JetYak ranges up to 20 km through a low-bandwidth radio frequency modem (Kimball *et al.*, 2014; Ludvigsen *et al.*, 2018).
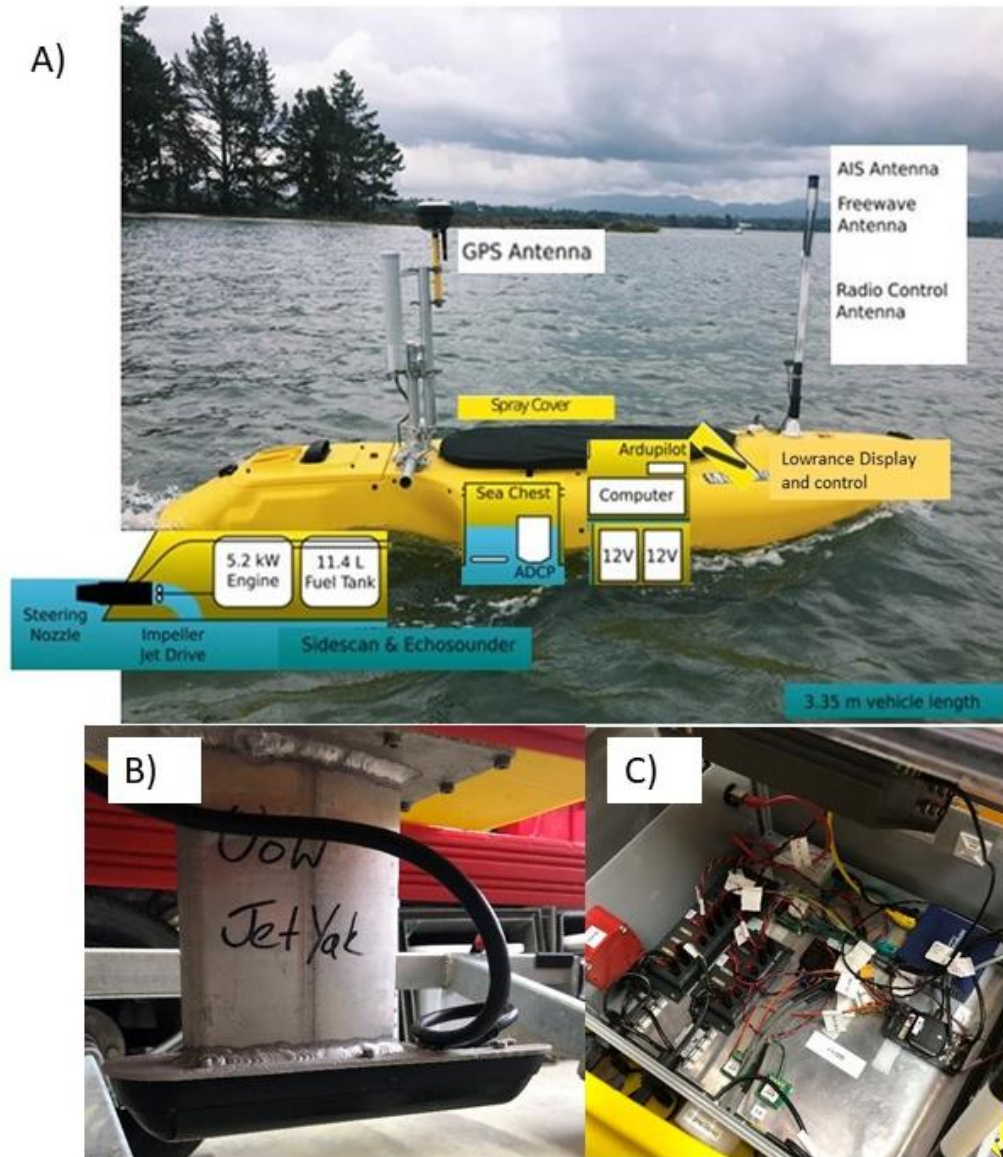


**Figure 2.1.** A) JetYak set up and configuration of instruments. Modified from Kimball *et al.* (2014). B) Side scan and echo-sounder transducer. C) Onboard computer set up.

Navigation of the JetYak is controlled by Mission Planner from ARDUPILOT, when the JetYak is switched to auto-pilot. The user interface of Mission Planner is shown in Figure 2.3. A series of way points can be loaded into a grid on top of a google earth image, where the JetYak manoeuvres between connecting latitude/longitude waypoints following a straight path. The position of the JetYak can be found using the onboard GPS co-ordinate system and can be watched in real time on the flight data screen in Mission Planner (Figure 2.3) (Dunbabin *et al.*, 2009). The speed between waypoints is controlled by PID feedback by throttle

changes and the speed of the JetYak is measured by GPS positioning. The vessel calculates the course to the next waypoint and if it deviates, the autopilot responds by correcting the heading. The autopilot also uses the result of past corrections to achieve the desired path and predicts future responses (Shojaei, 2016). The JetYak may also be split into three separate compartments for easy transportability into a large van by two adults (Kimball *et al.*, 2014). The University of Waikato JetYak however, has a modified jet ski trailer used to transport the JetYak to field sites and launch the vessel into the water.
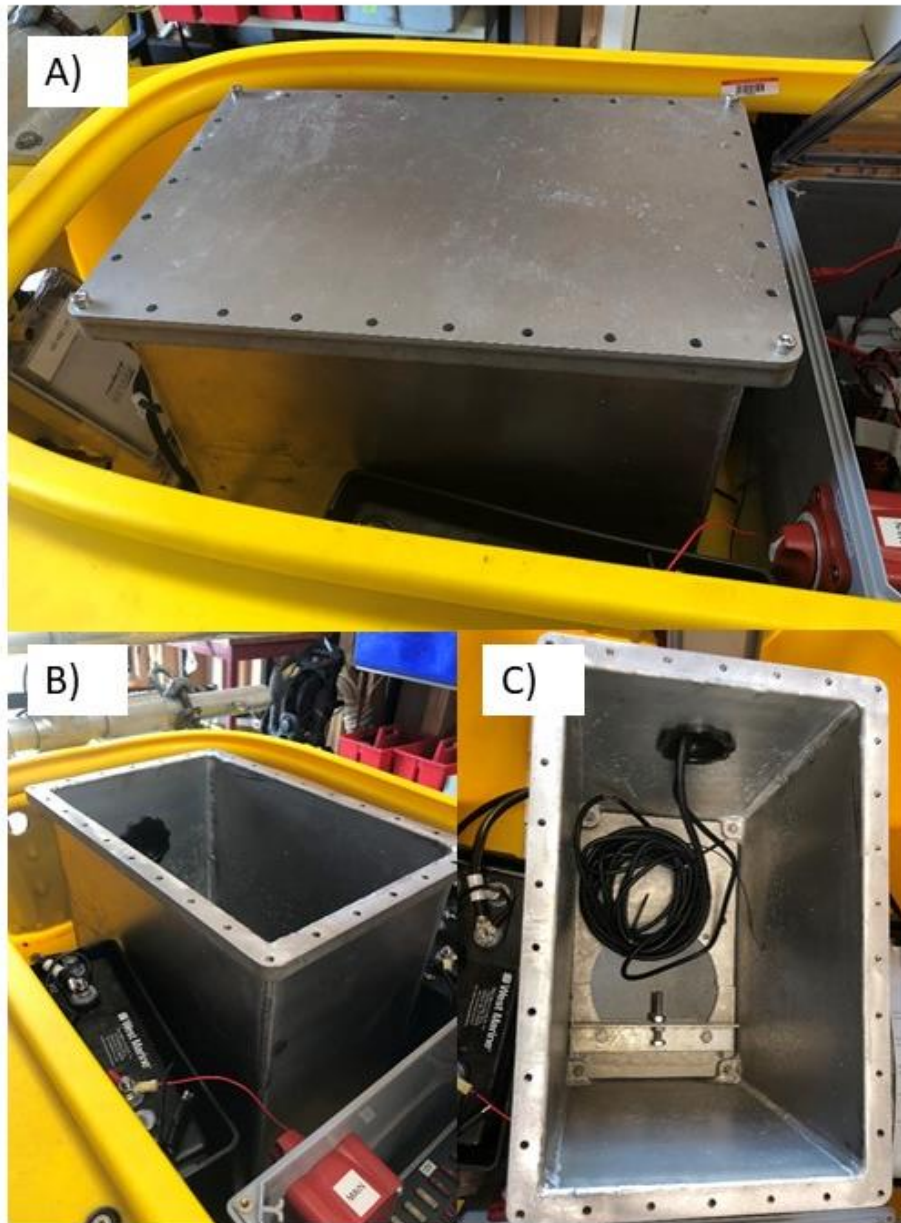


**Figure 2.2** The sea chest inside the JetYak for instruments that are required to be situated in the water. A) Side view with sea chest lid. B) Side view without sea chest lid. C) Top view inside side chest with attachments for instrumentation.
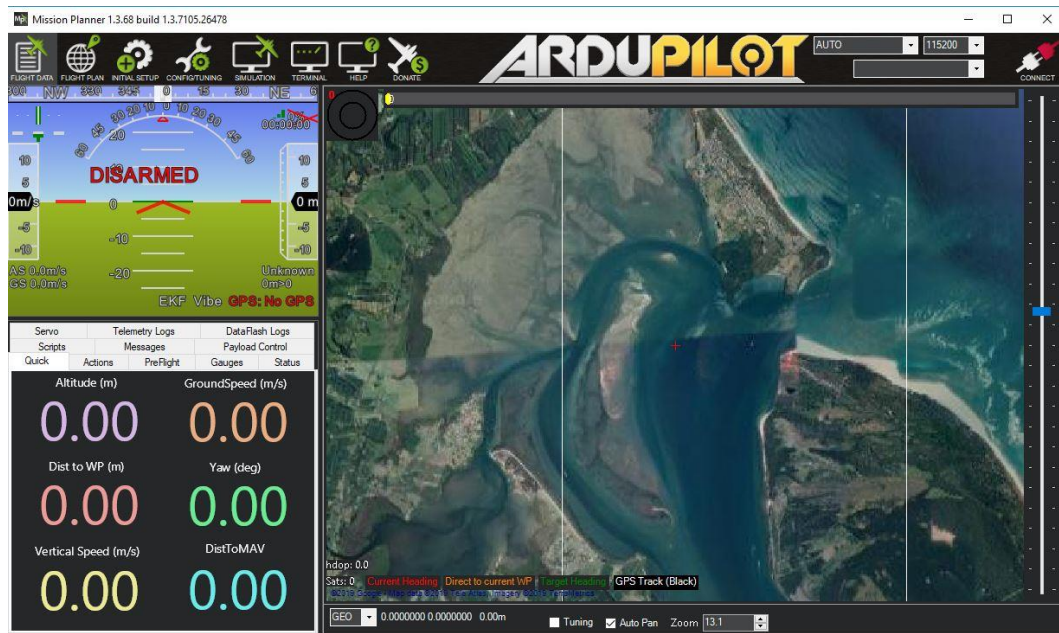
**Figure 2.3**. Mission Planner user interface flight data screen.

## 2.2 Aim

The aim of this chapter was to set-up the JetYak, develop a standard operating procedure and find the optimal steering and throttle parameters in Mission Planner to optimise the autonomous mode for the JetYak to drive a straight path from waypoint to waypoint. This capability is crucial for operating in adverse conditions (Moulton *et al.*, 2018). The JetYak was tested and set-up for use for further research examining flow over seagrass and mapping river plumes entering the coast in the Firth of Thames.

## 2.3 JetYak Set-up

### 2.3.1 Start-up Procedures

The start-up procedures and checklists are deemed one of the most important necessities for operating the JetYak and for a smooth running of the JetYak during surveying. Therefore, we developed a manual of operating procedures for the JetYak. As a starting point, we used the prototype manual developed by Integrated Coastal Solutions and developed an in-house safety case and altered the operating procedures manual to suit the University of Waikato JetYak, named 'Whaitere'. The checklist was developed over six months of trials at Lake Ngaroto, a small lake located in south of Hamilton in the Waikato, where no powered vessels are

permitted to operate, (special permission was acquired for testing the JetYak) and within the field compound at the University of Waikato.

The trials and set up of the JetYak comprised of practice of remote controlling the vessel from the shore, set up of instruments and JetYak for data collection in addition to pre-deployment checks. The first series of testing included refining and development of the checklist of procedures for pre-launching and launching and safety procedures to follow during experiments. Health and safety of individuals operating the JetYak remained the top priority as well as ensuring a smooth running of the JetYak. Therefore, we developed health and safety case, a selection of these documents are included in Appendix A.

This case included the general checklist of tasks to complete and equipment required before leaving the field compound. Tasks that needed to be completed before field deployment included notification to harbour masters, councils, MNZ or Ports and small tasks such as charging the remote controller (RC), starter battery and other electronic batteries for the set-up of base stations. The correct tools are similarly essential for transportation, set-up and deployment of the JetYak.

Software and logging equipment were also required for field deployments. This included the field laptop with Mission Planner loaded with the field site cached as well as AC-DC power supply and Icap for use of the laptop in the field to protect from the weather and sun glare (Figure 2.4). The base station for the JetYak is set up on shore with set-up of other base stations for example, an RTK GPS base station.

The Health and Safety checklist included having a fire extinguisher on hand, VHF radio, University health and safety forms completed, fuel spill kits, first aid kits as well as flashlights and personal protective equipment (PPE). A safety retrieval vessel was also required along with life jackets and paddles for the vessel, if necessary. To power the JetYak, sufficient fuel and oil were essential along with the addition of fuel stabiliser.

Before the JetYak can be deployed a few important tasks need to be completed. These tasks included establishing connection between Mission Planner and the JetYak computer, mounting of the structure scan and other data collection

equipment. Connection between JetYak and RC controller must be established by testing acceleration and left and right turning by observing propeller movement. The Lowrance echo-sounder must be set up to start logging data and the attachment of the sea chest lid as well as spray cover. Before the JetYak can be launched, the rescue vessel must be in the water, if using a powered vessel, or ready to deploy. These procedures ensure the safety of the JetYak as well as other surrounding individuals or vessels when launching in busy waters.

In preparation of the JetYak for deployment, a failsafe was added using the failsafe (FS) feature within Mission Planner for safety of the JetYak and vessels sharing the same waterways. The FS command was used to enable the JetYak to return to the home position if connection to the computer was lost for a certain period. In trial of the failsafe, it was discovered that this action was unsuitable, due to the fast speed at which the JetYak returned to the home waypoint, which was set to 2 ms$^{-1}$. In many cases, it was preferable that if connection to Mission Planner was lost during a survey, the JetYak would simply stop the survey track. The JetYak could then be piloted using the remote control.



**Figure 2.4.** JetYak base station set up with connection to field laptop inside Icap.

15

### 2.3.2  Tuning and Steering Optimisation

Before the JetYak could be deployed for data collection in the Tauranga estuary and in the Firth of Thames, the system had to be tested and set up for optimal use. A series of tests for steering parameters were conducted at Lake Ngaroto, Waikato. One key aim of these tests was to change parameters set in Mission Planner to find optimum turning angles and maximum speeds. This task also required calibration of the Pixihawk2 compass for accurate heading calculation and calibration of the on-board GPS. The tests at Lake Ngaroto also provided useful training in operating and remote controlling of the JetYak before launching in busy coastal waters such as in the Tauranga Harbour and in the Firth of Thames.

An experiment was conducted for calibration of advanced settings for automated driving for straight lines between waypoints. During the set-up of the JetYak, it was found that the JetYak would overshoot the target path. Figure 2.5 shows an initial trial run of the JetYak not achieving the desired straight path between waypoints. Each time the JetYak completed a turn, it would overshoot the target path. In order to correct this aspect and in preparation for use of the automated feature for surveying, the steering optimisation parameters were systematically adjusted to achieve a straight line between waypoints. The proportional, integral and derivative (PID) control algorithm is used in Mission Planner to is used to change the steering angles and forward velocities (Moulton *et al.*, 2018).

The PID control has five parameters, FF gain, P gain, I gain, D gain, Imax. The FF gain is changed first and is the most important control. It converts the desired rotation based on sensory output into a motor output (Moulton *et al.*, 2018). To increase the vessel's turn rate, FF gain is increased. If the vessel is overshooting the target path, FF gain is decreased to reduce the vessel's turn rate. The P gain improves short term error in turning. I gain adjusts for long term error; If the vessel never achieves the desired turn rate, I gain is increased. If the vessel oscillates over the target path, the I gain can be reduced. The D gain counters short term changes in turn rate and is generally set to zero (Huang & Liao, 2015). Another parameter which alters the path of the JetYak is the navigation period known as NAVL1_PERIOD. Small values of navigation period lead to sharper corners and more aggressive navigation, which works for smaller RC aircrafts, drones and

rovers. Large navigation period values lead to gentler turning angles suitable for larger vessels such as the JetYak.

Other important parameters include the speed the vessel travels between waypoints and P throttle for acceleration to keep a constant speed between waypoints. These parameters did not significantly affect the straightness of the path but were set to provide sufficient spatial resolution of the JetYak for surveying. There must be a compromise for covering a large area and acquiring enough survey points to make conclusions and the quality and reliability of data collected when travelling at fast speeds.
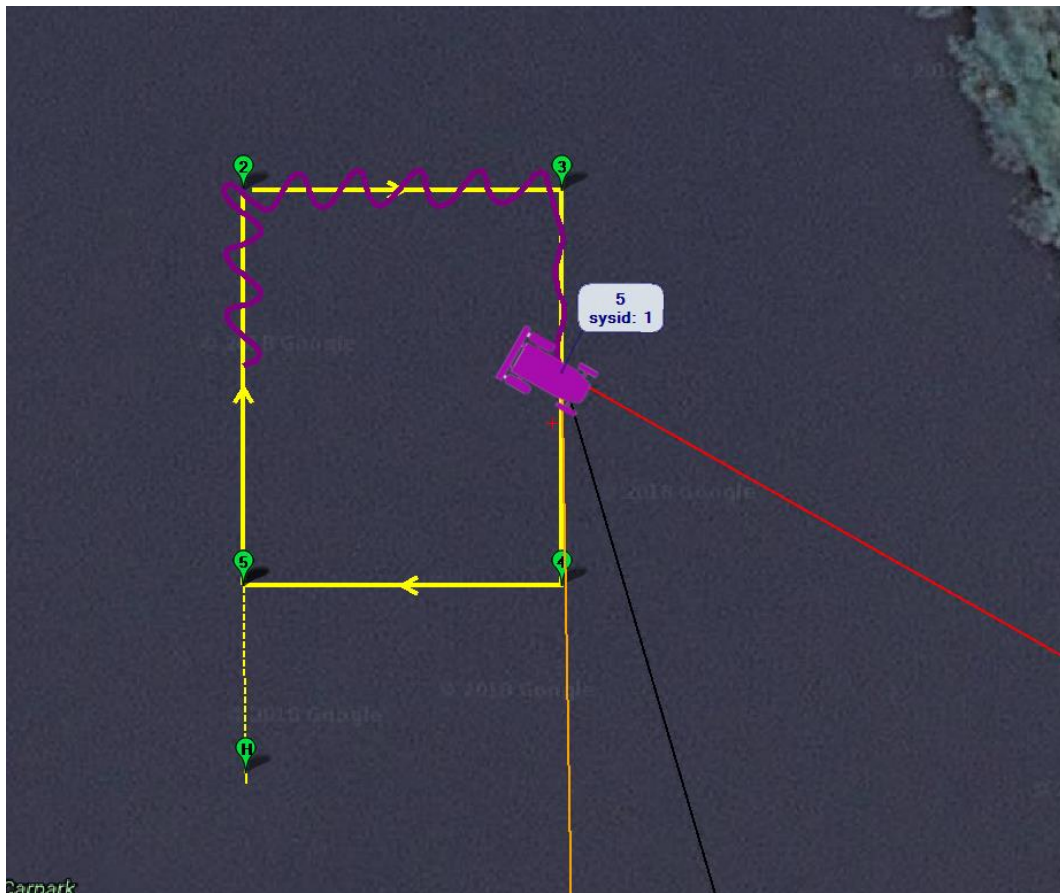


**Figure 2.5.** Mission Planner output and waypoints from initial trial run of the JetYak. The purple rover is the JetYak's position. The yellow track shows the straightest path from waypoint to waypoint. The purple line shows the track followed by the JetYak through the mission. The red line shows direction of heading of the JetYak. The black line indicates the desired turn. The H waypoint indicates the home position.

## 2.4 Methods

### 2.4.1 Instrumentation

For this research, the JetYak system was equipped with a Leica GNSS GPS for high resolution positioning data, which was measured at 1 Hz. The base station was set up on shore and is shown in Figure 2.6a. A wind sensor was set up on shore to collect wind direction and speed direction alongside the base station and measured every minute (Figure 2.6b).



**Figure 2.6.** A) Base Station set-up for RTK GPS at Lake Ngaroto. B) Wind Sensor set-up at Lake Ngaroto.

### 2.4.2 Field Experiment

On Monday 27th May 2019, a series of steering optimisation tests were performed using an RTK GPS on board the JetYak. Lake Ngaroto (Figure 2.7) was chosen as the site to do the parameterisation, as it does not allow for motor powered vessels. Special permission was acquired from the Harbour Master to test the JetYak at Lake Ngaroto. The conditions were overcast and wind speeds throughout much of the day were below 1 ms$^{-1}$ with gusts of up to 2 ms$^{-1}$ towards the end of the survey.
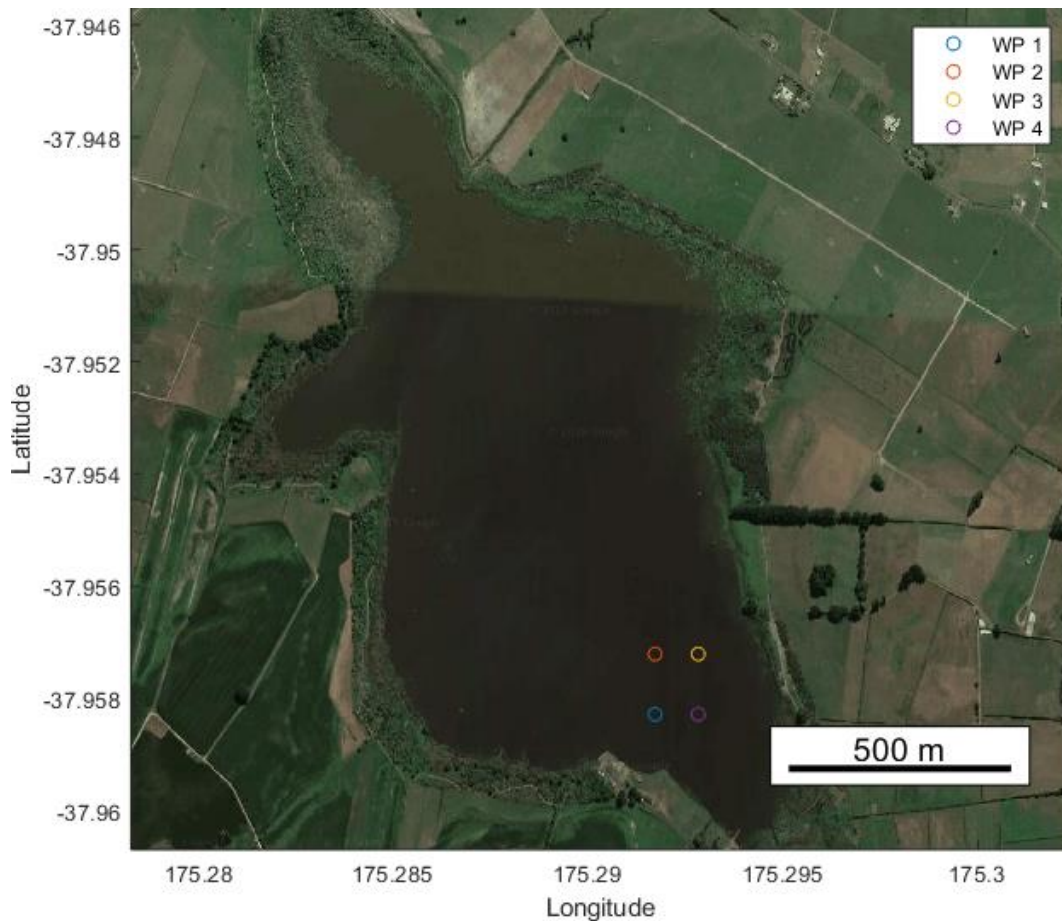
**Figure 2.7.** Lake Ngaroto in the South Waikato used for JetYak testing and optimisation of steering parameters. Waypoints 1-4 are indicated by each colour.

Waypoints were set up in Mission Planner for the JetYak to head 360 degrees North, head 90 degrees East, head 180 degrees South and head 270 degrees West, thus yielding an approximately square circuit. A wind sensor was also set up on shore to collect wind data which included wind speed and direction to determine the extent to which the wind conditions influenced the straightness of the JetYak path. The latitude/longitude positions of the waypoints were known and used to compare each run of the JetYak over the positions. It was also known that the starting conditions of the JetYak can also affect the first leg of the circuit. Therefore, the JetYak was remotely controlled to the starting 'Home' position on a heading consistent with the first leg before switching to auto-pilot.

Twenty different trial runs were completed by driving the JetYak towards home and setting it into autopilot, and only changing only one steering optimisation setting each circuit. The settings changed are shown in Table 2.1. The parameters included the FF gain, P gain, P throttle, the navigation period and waypoint speed. I gain, D

gain and Imax were kept constant as were previously found to have little effect on turning. Each of the parameters were changed while observing the JetYak from the shore and watching the onscreen path in the flight data screen in Mission Planner (Figure 2.5).

**Table 2.1.** Parameter optimisation trial runs with the values changed for each trial.

| Run Number | FF Gain | P gain | I Gain | D Gain | Imax | Waypoint speed ms$^{-1}$ | P Throttle | NAVL1_ period |
|---|---|---|---|---|---|---|---|---|
| 1 | 0.8 | 0 | 0.1 | 0.1 | 1.0 | 1.0 | 1.2 | 14 |
| 2 | 0.8 | 1.6 | 0.1 | 0.1 | 1.0 | 1.0 | 1.2 | 14 |
| 3 | 0.6 | 1.6 | 0.1 | 0.1 | 1.0 | 1.0 | 1.2 | 14 |
| 4 | 0.6 | 1.6 | 0.2 | 0.1 | 1.0 | 1.0 | 1.2 | 14 |
| 5 | 0.7 | 1.6 | 0.1 | 0.1 | 1.0 | 1.0 | 1.2 | 14 |
| 6 | 0.3 | 1.6 | 0.1 | 0.1 | 1.0 | 1.0 | 1.2 | 14 |
| 7 | 0.6 | 1.6 | 0.2 | 0.1 | 1.0 | 1.8 | 1.2 | 14 |
| 8 | 0.6 | 1.6 | 0.2 | 0.1 | 1.0 | 1.8 | 0.2 | 14 |
| 9 | 0.6 | 1.6 | 0.2 | 0.1 | 1.0 | 1.8 | 0.2 | 20 |
| 10 | 0.6 | 1.6 | 0.1 | 0.1 | 1.0 | 1.8 | 0.2 | 20 |
| 11 | 0.6 | 1.6 | 0.1 | 0.1 | 1.0 | 1.0 | 0.2 | 20 |
| 12 | 0.6 | 0.2 | 0.1 | 0.1 | 1.0 | 1.0 | 0.2 | 20 |
| 13 | 0.6 | 1.0 | 0.1 | 0.1 | 1.0 | 1.0 | 0.2 | 20 |
| 14 | 1.2 | 1.0 | 0.1 | 0.1 | 1.0 | 1.0 | 0.2 | 20 |
| 15 | 1.2 | 0.2 | 0.1 | 0.1 | 1.0 | 1.0 | 0.2 | 20 |
| 16 | 1.2 | 1.0 | 0.1 | 0.1 | 1.0 | 1.0 | 0.2 | 20 |
| 17 | 0.6 | 1.6 | 0.1 | 0.1 | 1.0 | 1.0 | 0.2 | 20 |
| 18 | 0.6 | 1.6 | 0.1 | 0.1 | 1.0 | 1.0 | 0.2 | 14 |
| 19 | 1.6 | 1.6 | 0.1 | 0.1 | 1.0 | 1.0 | 0.2 | 20 |
| 20 | 1.6 | 1.6 | 0.1 | 0.1 | 1.0 | 1.0 | 0.6 | 20 |

## 2.5 Results

During the trials, the JetYak path was observed in real time, in Mission Planner. The parameters were then changed to see if there was any difference before and after changing each parameter. The main parameters that influenced the path of the JetYak from waypoint to waypoint, were discovered to be the navigation period and FF gain with P gain contributing a small amount. P throttle and waypoint speed were also altered in the trials. D gain and Imax were kept constant in the trials.

It was found that the P throttle had no effect on the straightness of the path from waypoint to waypoint. However, when P Throttle was high, the acceleration of the

JetYak sounded loud and jerky. A smaller value of P throttle kept a constant acceleration that sounded smoother and more desirable. The waypoint speed was altered from 1.0 ms$^{-1}$ to 1.8 ms$^{-1}$ and had a small influence on the cross-track error of the JetYak.

To quantify how well the JetYak adhered to the pre-set circuit, we defined a parameter based on the variance in the track (shown in Figure 2.8). The parameter was defined as the mean of the cross-track variance from the four legs of the circuit (that is the variance in x- direction for each N-S transect and the variance in y-direction for the E-W transects, noting x and y positions were given in metres). The mean cross-track error of all transects was calculated to give the mean variance for the trial. Trial run 19 was found to have the lowest mean variance of 0.358 followed closely by trial runs 16 and 17, with mean variances of 0.366 and 0.364, respectively. The largest mean variance occurred in trial 1 and trial 12 with mean variances of 11.79 and 6.97 respectively. Figure 2.8 illustrates that the smallest cross-track error occurs when all parameters are set well, however, some parameters are shown to have a larger influence.
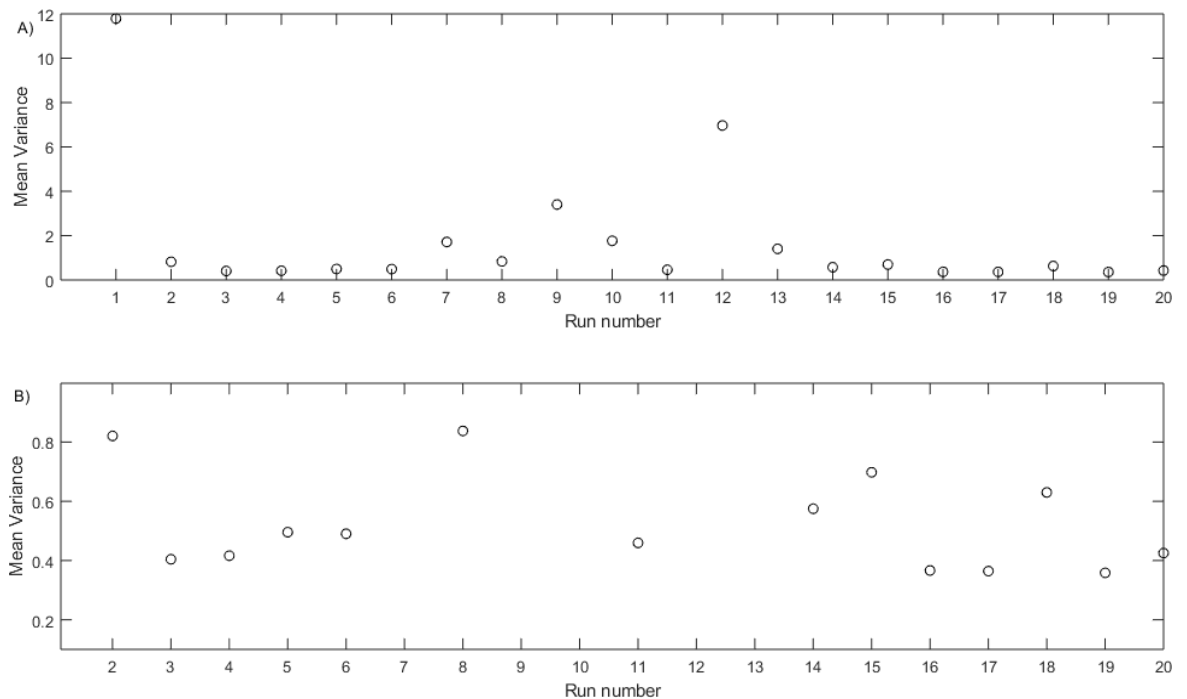


**Figure 2.8.** Comparison of mean variance for each trial run. A) All trial runs. B) Close-up of trial runs with a mean variance of less than 1.

In order to compare the effect of each parameter on the straightness of the path, each parameter was isolated by only changing the parameter of interest and keeping all other variables constant. We note that this method doesn't account for any nonlinear effects of changing multiple parameters at once; however, we assumed that such approach should provide a usable first set of parameters (and verified this assumption through the results).

The navigation period parameter was revealed in the trials to have a large influence on the straightness of the path from waypoint to waypoint. The only change in parameters between run 17 and run 18 was the increase in navigation period from 14 to 20, all other parameters were kept constant other than uncontrollable environmental conditions. This changed resulted in an increase in the mean variance by 72 %. Figure 2.9 illustrates the path and heading of the JetYak for trial runs 17 and 18 and shows the difference between the two tracks.
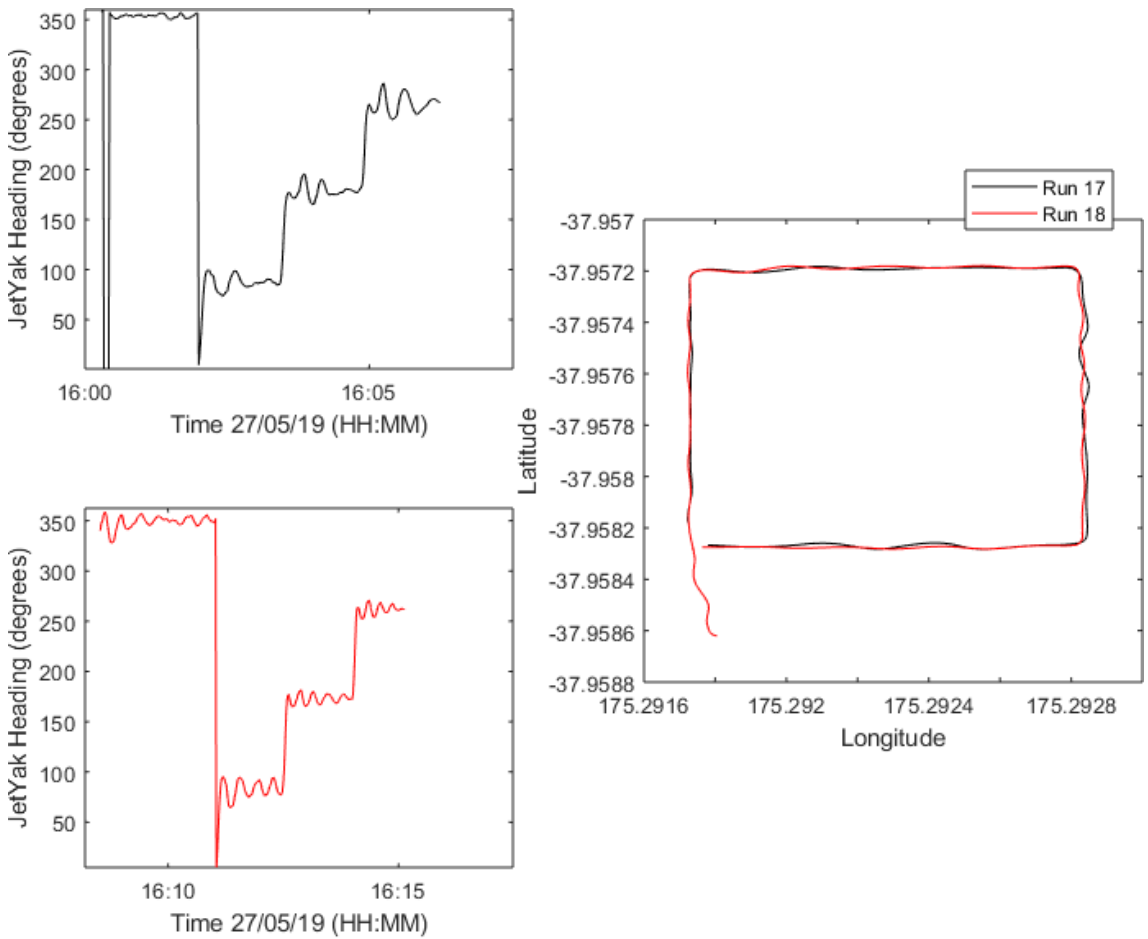


**Figure 2.9.** Comparison of run 17, navigation period of 20 and run 18, navigation period of 14. A) Run 17, JetYak heading. B) Run 18, JetYak heading. C) Run 17 and 18, latitude and longitude path.

FF gain was also deemed to have an influence on the JetYak's ability to achieve the desired straight path from waypoint to waypoint. Runs 17 and 19 can be used to compare FF gain, as all other parameters were kept constant. Run 17 had an FF gain value of 0.6 and Run 19 had an FF gain value of 1.6. Run 19 is shown in Figure 2.10 to achieve the target straight path with time after the turn to each transect whereas, run 17 comes close to reaching the target path. The influence of FF gain is shown to be small when all other parameters are set adequately. The mean variance difference between run 17 and run 19 was minimal, with only a 1.67 % increase in mean variance. Either set of parameters were deemed to be suitable for future research.
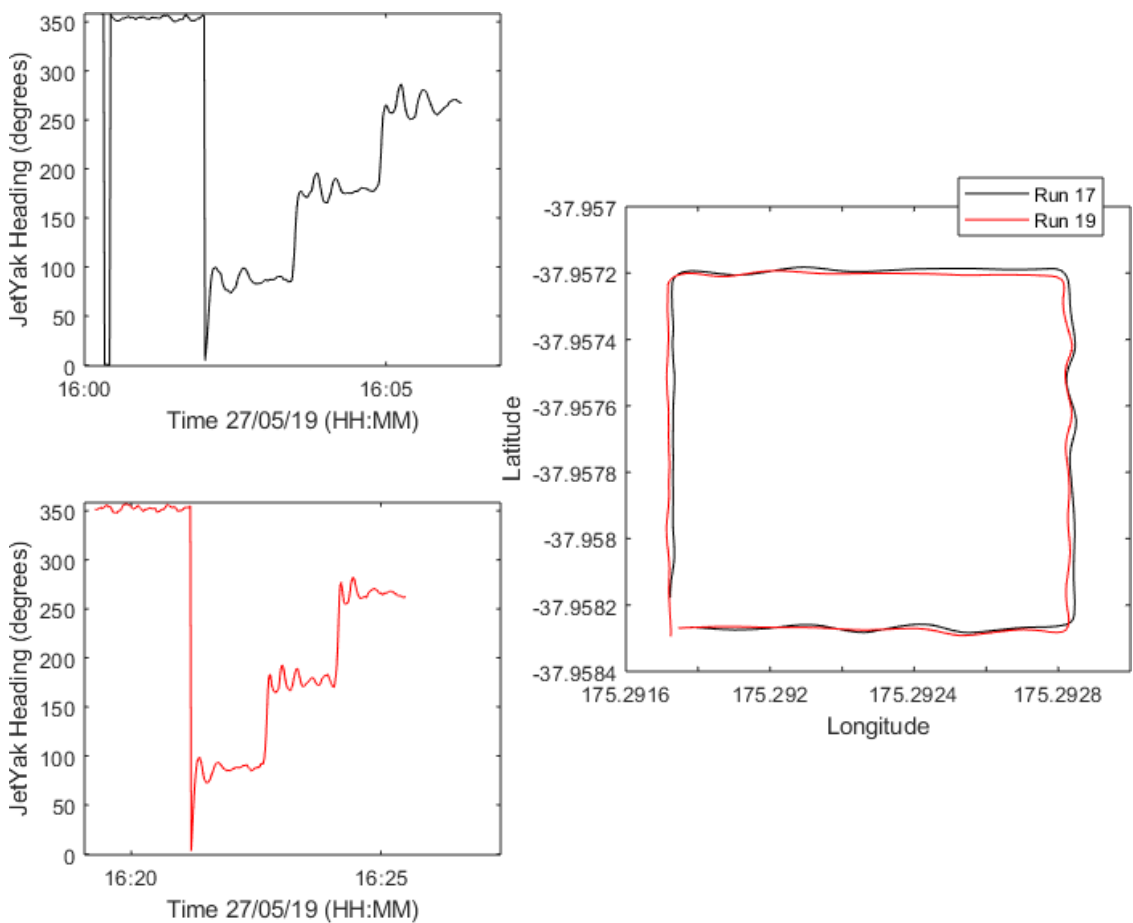


**Figure 2.10**. Comparison of run 17, FF gain 0.6, and run 19, FF gain 1.6. A) Run 17, JetYak heading. B) Run 18, JetYak heading. D) Run 17 and Run 19, latitude and longitude path.

To demonstrate the importance of controlling the steering parameters, we show results from Run one, which had the least optimal values for FF gain, P gain and navigation period parameters overall, with a mean variance of 11.79. Figure 2.11 illustrates how the JetYak performs without the optimal turning parameters. The

JetYak is shown to consistently overshoot and undershoot the target path. Throughout the entire trial run, even before the first initial turn (N-S transect), the JetYak never achieves the target path. The JetYak overshoots and undershoots the target path creating the large 'S' shape over the target path.
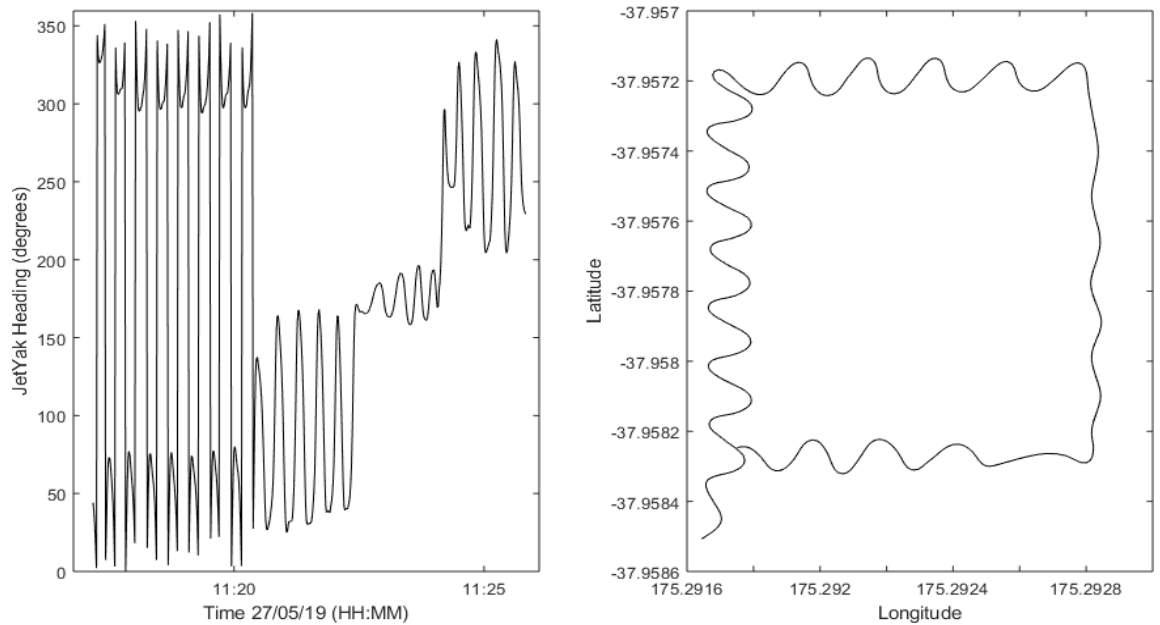


**Figure 2.11**. JetYak parameter Run one at Lake Ngaroto. A) Heading of the JetYak. B) Latitude and Longitude path.

Figure 2.12 shows the optimal parameters found from the trials. The turning parameters set in Run 19 included an FF gain of 1.6, a P gain of 1.6 and a navigation period of 20. With these parameters, the JetYak is shown to achieve the target path with time after the initial turn at each transect. The JetYak is shown to still have some cross-track error, but, is minimised with these parameters. The JetYak more often achieves the desired straight path after the first initial turn and calibration has occurred.
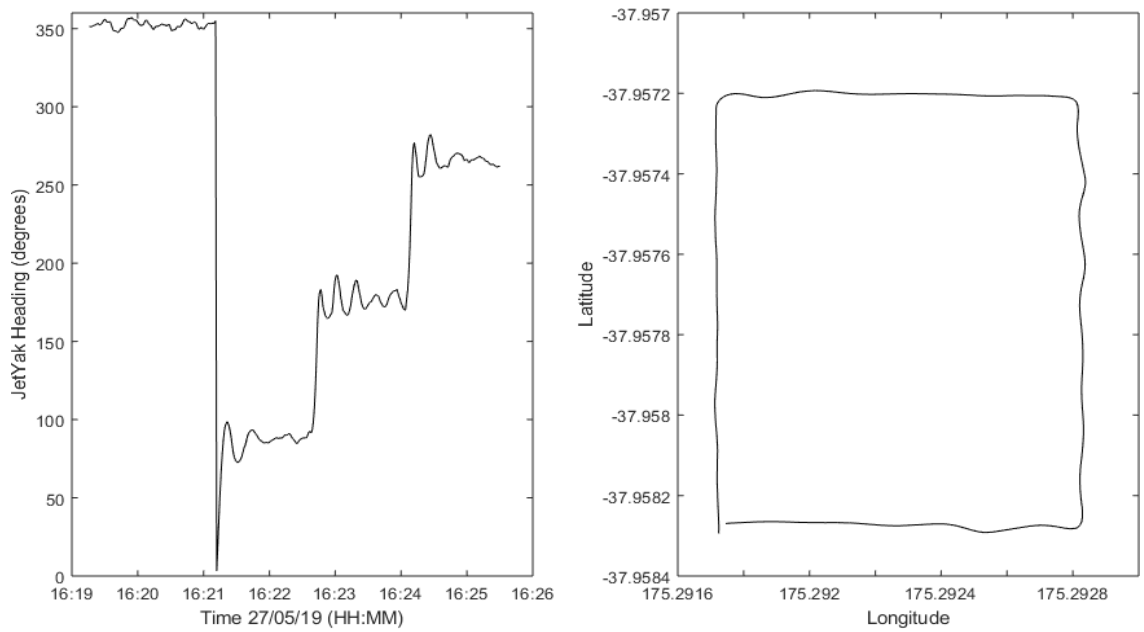
**Figure 2.12.** JetYak parameter Run 19 at Lake Ngaroto. A) Heading of the JetYak. B) Latitude and Longitude path.
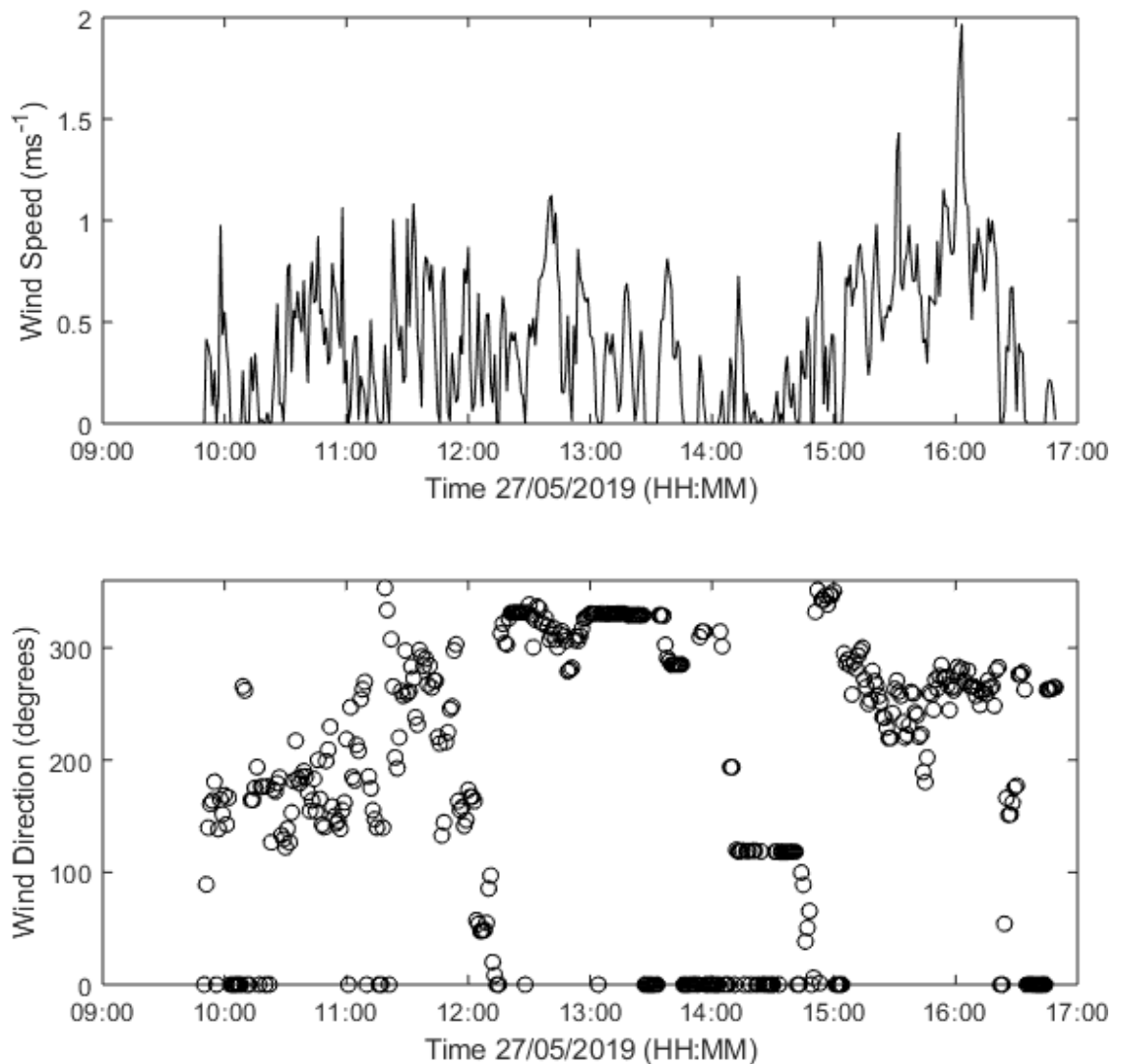


**Figure 2.13.** Wind data collected from the 27th May 2017 at Lake Ngaroto. A) Wind Speed and B) Wind Direction over the period of the 20 trials.

The wind speed and direction during a survey can impact the straightness of the JetYak path to each waypoint (Moulton *et al.*, 2018). Figure 2.13 displays the wind speeds and directions throughout the parameter optimisation trials. The fastest wind speeds recorded were 2 ms$^{-1}$ and wind speeds increased throughout the day. The fastest wind speeds recorded were North Westerlies which may have caused some of the overshooting of the target path from the JetYak. Note however that the fastest wind speeds also occurred towards the end of the trials when the optimal parameters were found.

## 2.6 Discussion

The parameter trials revealed that the JetYak needed a combination of all PID steering and throttle parameters set to adequate values before the JetYak could operate with the optimal autonomous driving settings to drive a straight path between waypoints. Trials such as run one (Figure 2.11) were shown to overshoot and undershoot the target path as all parameters were not set well. These settings created an 'S' shape as the JetYak sought to correct the problem to achieve the target path. Figure 2.12 shows the JetYak with the optimal parameters from the trials. The combination of all parameters ensured the JetYak achieved the target path after the first each initial turn towards each transect. The trials also showed that the starting position of the JetYak affected the first leg of the trial. If turning was required to reach the first waypoint, the JetYak had to correct itself and would often overshoot the target path from the start of the trial. Whereas, if the JetYak had an ideal starting position, facing the path of the first waypoint, the first leg of the trial (North) was straight as no turns had to be completed. With each trial run, even with the optimal parameters, it was established that the autonomous feature often could not achieve a tight 90 degree turn, possibly due to the watercraft shape, or environmental factors, such as strong gusts of wind (Moulton *et al.*, 2018) or due to more advanced parameters in Mission Planner that are required to be set correctly. However, the optimal parameters were shown to achieve the desired path shortly after each turn.

Mission Planner has thousands of parameters that can be altered to optimise the use of the JetYak (Huang & Liao, 2015). Due to time constraints, this trial only focused on the main PID tuning parameters as well as waypoint speed and navigation period.

However, to optimise the JetYak's ability to turn further, more settings could be examined. The main PID turning and the alteration of navigation period was perceived to have a large effect on turning as shown in the comparison between Figure 2.11 and Figure 2.12. Small scale changes in turning could be completed to further optimise the turning however, the optimal parameters established in these trials (Run 19), are satisfactory for surveying. The straight path from waypoint to waypoint is achieved and is as good or better than, survey lines achieved using a manned vessel (Weeks *et al.*, 2011; Moulton *et al.*, 2018).

The trials at Lake Ngaroto showed that the direction of the turn is affected differently by the parameters. The JetYak had different outcomes when turning from North to East compared to East to South in each trial run. This result was consistent throughout all the trials and is due to the PID parameters. There were also large differences in turning direction between trial runs. Figure 2.11 shows the small cross-track error for turn two (E-S) compared to turn one (N-E). This result demonstrates that the parameters work differently for each type of turn, although they are both 90-degree angle turns. Figure 2.12 also displays that there is a different outcome for each turn even with optimal parameters. This could be due to the large turning angle of the JetYak and not being agile for easy turning in comparison to small aircraft or rovers, previously used with Mission Planner for autonomous driving (Moulton *et al.*, 2018).

Certain values for each of the parameters decreased the amount of cross-track error. The larger navigation period of 20 (Figure 2.9) was deemed to be best for further use for surveying. The larger navigation period allowed the JetYak to turn less abruptly and therefore, decreased the overall overshooting/undershooting of the target path. For FF gain (Figure 2.10), either set of parameters would be satisfactory for surveying however, the FF gain of 0.6 had a larger mean variance than an FF gain of 1.6, therefore, an FF gain of 1.6 was chosen. Both sets of parameters could be utilised for different survey lines, depending on the turns in the survey and environmental conditions. The optimal P gain value was set to 1.6 as a smaller P gain value resulted in a slightly larger mean variance. The FF gain and navigation period were observed to have a large effect on the JetYak achieving the target path, therefore, if FF gain is set well and navigation period set to 20, the JetYak should drive the target straight path from waypoint to waypoint.

The trial runs showed that while some parameters had a larger effect on turning, such as the navigation period and FF gain, a combination of all the right parameters was needed for the JetYak to achieve the desired turn rate and achieve the target path to each waypoint. Figure 2.12 shows that with time after the first turn to each transect, the JetYak eventually achieves the straight line. Therefore, longer, straighter transects are optimal for planning of future surveying.

The wind speed and direction were determined to have little impact on the JetYak during these trials. However, we note that winds were light during the trials. The fastest wind speeds were shown to be at the end of the trial period and when the JetYak had the straightest path from waypoint to waypoint. However, small overshooting and undershooting of the target path may have been caused by the increasing wind speeds throughout the day, although it was not possible to separate this possibility from effects of changing the steering parameters in the present case, as each set of parameters was only applied for one circuit. Future tests could be undertaken to quantify and separate these effects. Increased wind speeds in this opposing direction of the JetYak heading can increase turning angles and cause the JetYak to overshoot/undershoot the target path. There were also small waves later on in the survey, which may have also affected the JetYak achieving the target path (Moulton *et al.*, 2018). Nonetheless, the increasing wind and straighter path in the later trial runs confirms that if the parameters are set well, the effect of environmental factors such as wind speeds, waves and currents within the marine environment, can be minimised for accuracy and repeatibilty of transects (Weeks *et al.*, 2011).

### 2.6.1 Optimal Parameters

For this trial, run 19 with an FF gain of 1.6, P gain of 1.6 and navigation period of 20 was deemed to be the optimal set of parameters. Parameters could be further optimised within the advanced settings in Mission Planner to decrease the amount of turning in optimal parameter run 19. The latitude/longitude track in Figure 2.12, displays the ability of the JetYak to maintain a straight path from waypoint to waypoint for accurate repeatability of transects. The observed path of the JetYak was perceived to be as straight as a man-driven vessel or straighter.

## 2.7 Conclusion

The optimal parameters and set-up of the JetYak was completed for further surveying. It was found that while some parameters had a larger effect on turning, a combination of all the PID steering and throttle parameters combined improved the JetYak's ability to achieve the target path to each waypoint. An optimal set of parameters were found however, with more time, more advanced settings within Mission Planner could be altered further for better results. The parameters found in this research are suitable for future surveying using the JetYak to repeat transects for accurate monitoring schemes (Kimball *et al.*, 2014).

# Chapter 3

# Hydrodynamics over Seagrass Beds

## 3.1 Introduction

Seagrass fields are ecosystems of great ecological and economic value (Orth *et al.*, 2006). These aquatic plants provide many ecosystem services within estuaries and can be found submerged or unsubmerged in shallow marine waters (Cullen-Unsworth & Unsworth, 2013). They are vital to the marine ecosystem as they are a source of productivity and therefore, provide food, a habitat and areas for vertebrae and invertebrate species to thrive (Orth *et al.*, 2006). Seagrasses can be sensitive to changes in water quality, and therefore, can also be used to determine the health of the coastal ecosystems (Bos *et al.*, 2007; Romero *et al.*, 2007). Seagrasses also play a vital role in stabilising the sea floor using an extensive root system to secure marine bottom sediments that are subject to wave action, strong flows and the impact of storms (Gumusay *et al.*, 2018). However, seagrass coverage is declining all over the world and in New Zealand (Duarte, 2002). The primary threats to seagrasses include changes in water quality, sedimentation and eutrophication (Matheson & Schwarz, 2007).

The hydrodynamics within an estuary control transport, erosion and deposition of sediment in the bottom boundary layer (Cheng *et al.*, 1999; He *et al.*, 2001). The presence of seagrass can strongly affect bottom roughness and hydrodynamics. Indeed, seagrasses are thought of as ecosystem engineers, as they have the ability to alter the environment they surround, including sediments and flow patterns (Bos *et al.*, 2007; Ondiviela *et al.*, 2014). Researchers have observed changes in flow patterns due to seagrass patches and as a result of fragmentation of seagrass (Fonseca *et al.*, 1982; Abadie *et al.*, 2015), which therefore, influences sediment size, types and the composition of the bottom layer (Cheng *et al.*, 1999). Seagrasses have been shown on occasion to reduce wave heights (Luhar *et al.*, 2010), provide stability of sediments and therefore, may offer coastal protection from coastal hazards such as erosion, deposition and flooding (Bos *et al.*, 2007; Ondiviela *et al.*, 2014). Such 'nature-based' protection strategies are thought to be a natural, less invasive substitute for engineering structures that can be used to combat the effects

of rising sea level and moderate coastal hazards (Ondiviela *et al.*, 2014). However, to evaluate the full efficacy of seagrasses as a coastal protection strategy, it is important to understand the effects they have on changing flow patterns (Orth *et al.*, 2006; Bos *et al.*, 2007) and to collect data to validate numerical models for accurate predictions (Ondiviela *et al.*, 2014).

## 3.2   Aim

The aim of this experiment was to determine whether the JetYak provides a suitable mechanism to resolve changes in hydrodynamics between bottom substrates populated with seagrass to bare mudflats, and therefore, could be used for further research on patterns of sediment transport patterns within seagrass in the Tauranga estuary.

We undertook the experiment in the Tauranga Harbour in the North Island of New Zealand. The seagrass that dominates the Tauranga area is known as *Zostera muelleri* which is a temperate species of seagrass found in the southern hemisphere and is the only seagrass species found in New Zealand (Matheson & Schwarz, 2007). In particular, the aims were:

> 1. to explore whether the changes in velocity in the bottom boundary layer could be resolved using the JetYak with the motion of the vessel being subtracted.
>
> 2. to examine whether there were changes in backscatter that could be used to show the changes in bottom substrate due to the seagrass.

### 3.2.1   The JetYak

The JetYak was used to drive autonomously over the seagrass and mudflat transition to survey the flows and acquire bathymetry data. The ASV was used to measure water velocities using an Acoustic Doppler Current Profiler (ADCP). The instrument was mounted into the sea chest of JetYak and therefore, moves with the JetYak. This velocity must be removed from the data to attain actual velocity data. The shallow water submerging the seagrass means traditional manned vessels are not easily used in this environment. This initial experiment was undertaken before we had completed the optimisation of steering parameters. This chapter focusses on results acquired from the JetYak from the field experiment.

## 3.3   Field experiment

### 3.3.1   Field Site Description

This research was carried out in the Tauranga harbour, located in the Bay of Plenty on the east coast of the North Island of New Zealand. It comprises of a Northern and Southern Estuary. This research was undertaken within the Northern part of the Tauranga estuary at Tanners point. The Northern part of the Tauranga estuary is enclosed by the Barrier Island, Matakana Island and Bowentown head and the entry to the estuary is approximately 1600 m wide. Tanners point is the entry to the sub-estuary enclosed by the small spit known as Tuapiro point. Seagrass species *Zostera muelleri* was found to dominate this area above Tuapiro point and was found in the higher elevation regions. The area included a deeper boating channel on the western side and an expanse of mudflats, which are populated by a dense bed of seagrass. There was a visible transition between the vegetated and non-vegetated areas. The area of interest and the area that was surveyed was between Tuapiro point and Tanners point with a latitude of between -37.481º and -37.485 º and a longitude of between 175.946 º and 175.951 º E.

The study site at Tanners point is shown in Figure 3.1 and was chosen for this study as it had a clearly visible and sharp transition between the seagrass dominated area and bare mudflat. This transition as well as some clear patches in the seagrass were mapped at low tide with a GPS prior to the experiment. This prior survey allowed for later identification of times when the JetYak crossed over the vegetated area to the non-vegetated area.
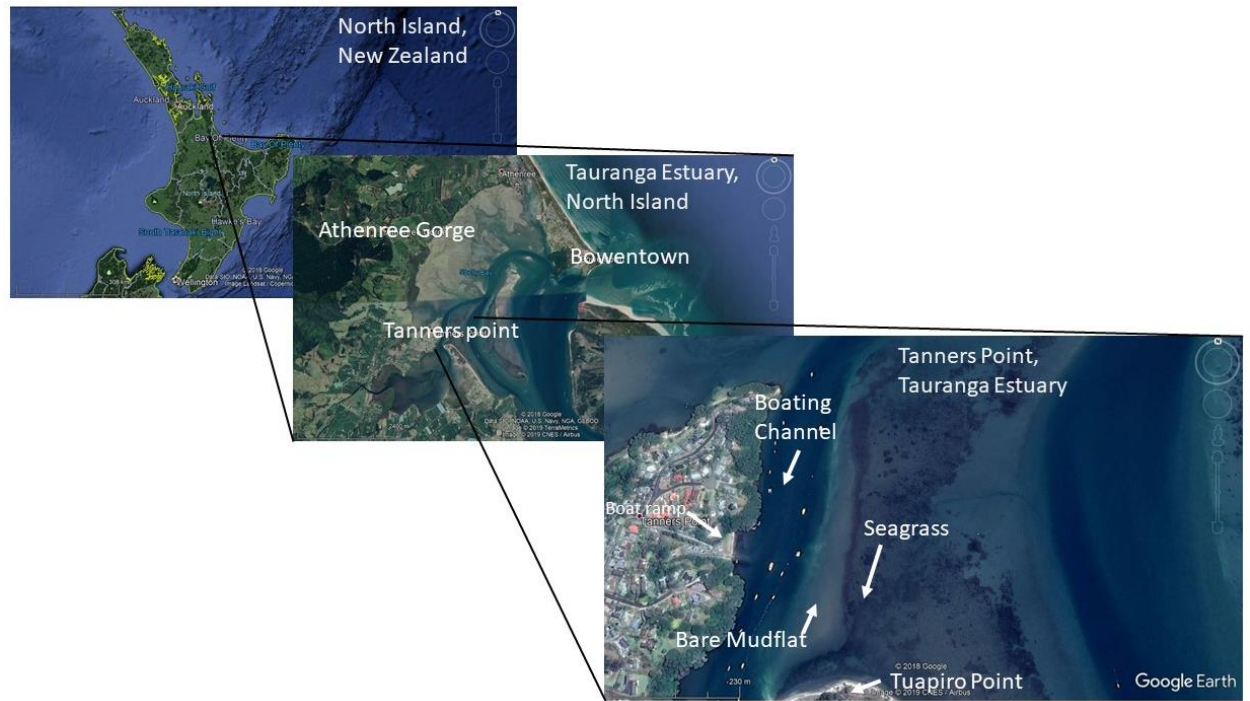
**Figure 3.1.** Survey area located in the North Island of New Zealand and in the Northern Part of the Tauranga estuary. It includes the entrance to the estuary and the entrance to the sub estuary at Tuapiro point. Seagrass species *Zostera muelleri* is shown to dominate high elevation areas. Survey area with seagrass/sandflat transition shown at Tuapiro point as well as boating channel and launching site. (Images: Google Earth).

### 3.3.2 JetYak Instrumentation

The JetYak's position, orientation, and vessel velocity information comes from an onboard GPS and compass (Kimball *et al.*, 2014). The JetYak was also equipped with an onboard Lowrance Structure Scan 3D Transducer for acoustic bottom measurements. For this study, the JetYak system was also equipped with an additional Leica GNSS GPS, for location and elevation measurements. The base station for the GPS was set-up at Tanners point alongside the base station for the JetYak (Figure 3.2).The GPS was positioned using clamps above the echo-sounder structure scan (Figure 3.3). The distance between the GPS and structure scan was 1.36 m. The Leica GS18 T GPS was set up onboard the JetYak to record the position and elevation at 1 Hz and recorded tilt and direction in real time. Therefore, the tilt of the JetYak due to wave action, did not affect the positioning data of the GPS. The GPS heading was towards the front of the boat and using differencing of x and y positioning the speed of the boat was calculated from the GPS.

**Figure 3.2.** RTK GPS Base station and JetYak laptop set-up at Tanners point.

We were also presented with an opportunity to attach a Nortek Signature1000 Acoustic Doppler Current Profiler (ADCP) to the JetYak. (Figure 3.3 a&c). For boat-mounted operations, the Signature is designed to operate with in vessel-mounted mode (VM) requiring an integrated advanced navigation GNSS GPS. However, we took the opportunity to test the capabilities of the stand-alone unit as similar ADCPs mounted on drifters have been successfully used to measure water velocities and turbulence parameters (Mullarney & Henderson, 2013). The Signature1000 ADCP was mounted downward-facing in the JetYak's sea chest for water velocity measurements (Figure 3.3 c). The height between the GPS and ADCP was 0.891 m and was positioned 0.35 m towards the front of the boat from

the GPS and structure scan. The height difference between the structure scan and the ADCP was 0.569 m. The Nortek Signature1000 ADCP was set up to measure along-beam velocities at a frequency of 8 Hz, the salinity was set to 35 and was set to measure 15 bins of 0.3 m vertical resolution. The blanking distance was 0.1 m. The ADCP was rotated with the x direction at 43 degrees to the front of the JetYak.



**Figure 3.3.** A) RTK GPS and ADCP set up on board JetYak with ADCP mounted in the sea chest. B) Side view of JetYak with RTK GPS set up. C) ADCP mounted downwards facing into sea chest.

### 3.3.3 Data collection

<u>Initial Survey</u>

On the 7th of December 2018, the experimental site was surveyed with the Leica GNSS GS18 GPS at low tide. A benchmark was set up for the GPS at Tuapiro point using a base station located at Bowentown. This benchmark was then used as a base

station to set up a benchmark at Tanners point. Elevation data was collected across the channel-mudflat-seagrass transition. In particular, the sharp transition between seagrass and mudflat dominated areas was carefully marked, in addition to the outline of two bare mudflat patches found within the seagrass area. The data collected was also used to determine the water level at high tide to see whether there would be sufficient water depth to conduct the survey in this area. The JetYak needed approximately 0.5 m of water to ensure there was enough water for the echo-sounder to function properly and avoid the JetYak hitting the bottom. The elevation data collected for this experiment and location of the mudflat/seagrass transition is shown in Figure 3.4.
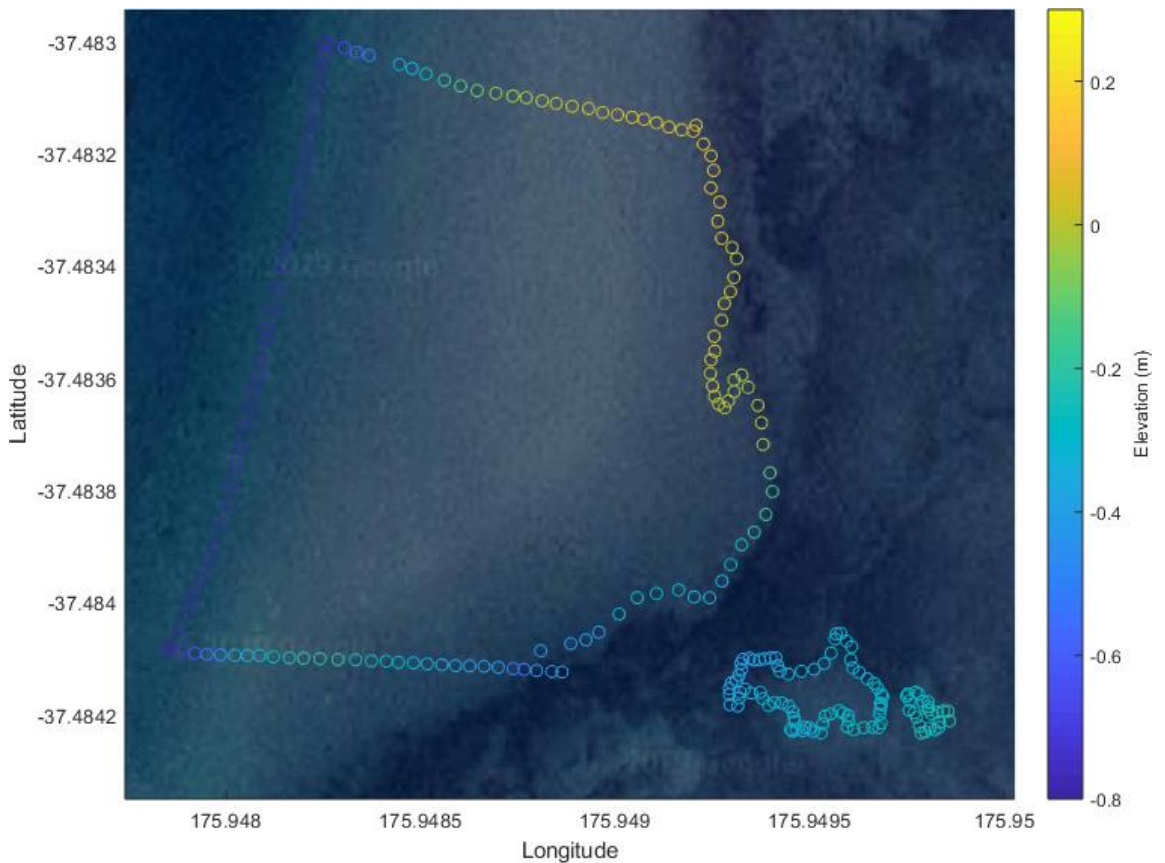


**Figure 3.4**. Initial survey elevations and transition between seagrass and mudflat and positions of two patches within the seagrass.

The second objective of the field trip was to plan the logistics of the base station set up for the GPS, safe launching of JetYak and site access to the selected area based on the tide and elevation. It was determined that the JetYak could be launched from Tanners point easily into the deep boating channel.

JetYak survey

On the 12<sup>th</sup> of December 2018 at 10.30 am, the JetYak was deployed from Tanners point, Katikati to follow a pre-programmed path using mission planner to survey the mudflat to seagrass transition mapped in the pre-survey. The weather conditions were overcast and had moderate to strong winds and therefore, there were small wind waves within the estuary. The base station for the JetYak and RTK GPS was set up on shore. The JetYak was launched from the boat ramp at Tanners point shown in Figure 3.1 and was remotely controlled to drive over the channel, the mudflat and seagrass. The JetYak was initially controlled from the rescue vessel, which was manoeuvred to follow the JetYak.

For the main surveys, the JetYak was switched into autopilot mode and the JetYak followed the pre-determined path from Mission Planner. Three smaller quadrilateral circuits and one longer circuit were completed. The small circuits consisted of two East to West oriented transects encompassing channel, sandflat and seagrass beds, and joining North to South transects (Figure 3.5 a-c). The southernmost E-W transect also crossed over the two bare patches embedded within the seagrass beds. A full circuit consisted of three East to West transects and North to South joining sections and one diagonal transect back to the starting position ( Figure 3.5 d).
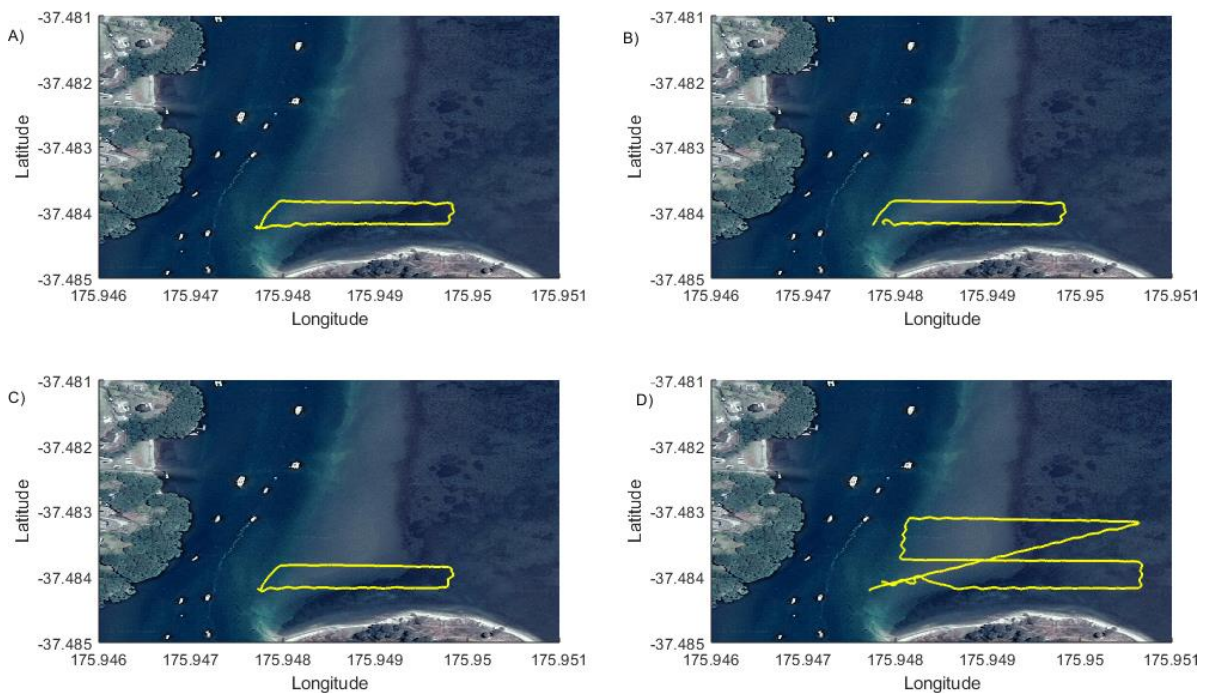


**Figure 3.5.** The four tracks driven autonomously by the JetYak passing over the seagrass

37

## 3.4 Data Processing

The data collected from each of the instruments from the field experiment undertook quality control and processing as detailed below.

### 3.4.1 RTK GPS

The GPS provided high-resolution positioning of the JetYak. Measurements of longitude (x) and latitude (y) were recorded at 1 Hz. The horizontal velocity components of the JetYak were calculated by differencing the positions in time:

$$u = \frac{\Delta x}{\Delta t} \qquad v = \frac{\Delta y}{\Delta t}$$

which were then smoothed using a 25-pt running mean. This procedure determined the horizontal velocity of the JetYak for comparison to the boat speeds calculated using from the ADCP (Mullarney & Henderson, 2013).

### 3.4.2 Signature1000 ADCP

A bottom detection algorithm was written to find the location of the seafloor from the acoustic backscatter signal. The backscatter in each beam was smoothed in time using a 5-pt running mean. The location of the bottom was identified from the vertically oriented beam five (Figure 3.11), using a varying threshold value (between 83 and 85 counts). In most cases, this technique worked well (see results); however, for a few instances, corrections were made manually. The bottom trace was then verified visually on the backscatter signal from the other four beams.

It is also important to note that there was evidence of compass interference in the original data, therefore, the compass was calibrated after the experiment by Nortek using their Ocean Contour software package and new calibration settings were applied before any other postprocessing of data. Along-beam velocities were rotated into East-North-Up (ENU) components using the pitch, roll and heading of the instrument.

Bins in which correlations in any beams were less than 50 % were removed (replaced by NaNs). Data from below the bed (as identified above) were also removed. In a frame of reference moving with the JetYak, the seafloor appears to move, so the velocity of the JetYak was then calculated as the negative of the

apparent bottom velocity. This calculation of boat speed was compared to the GPS calculation of the boat speed (Mullarney & Henderson, 2013).

The water velocity measurements acquired therefore, included the water velocity as well as the boat velocity. The measured velocities were then added to the measured boat velocities to remove the effect of the moving vessel (Figure 3.6).
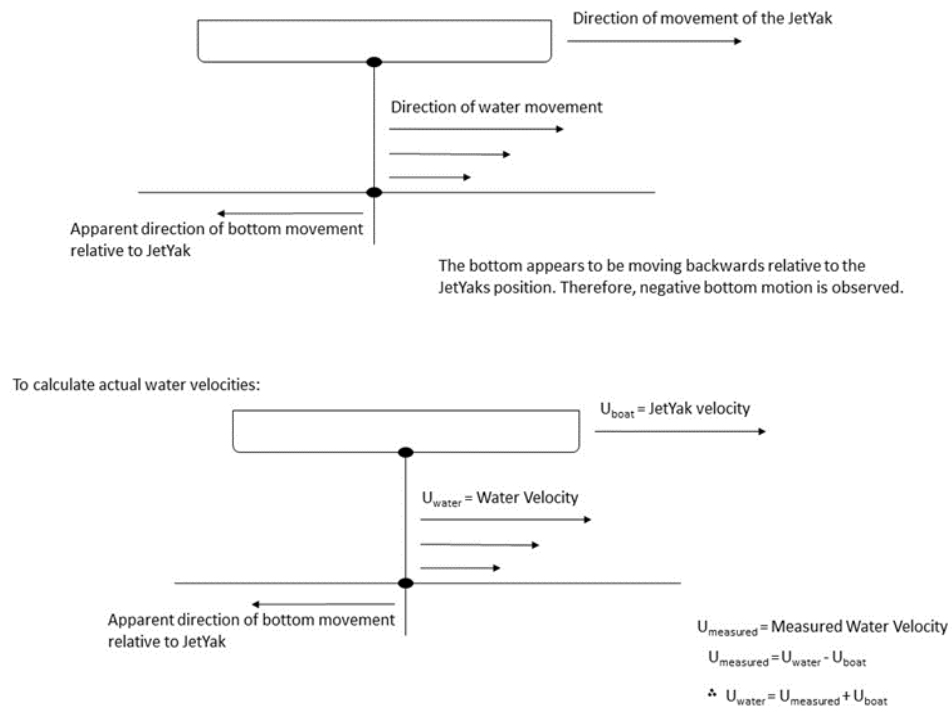


**Figure 3.6**. Calculation of actual water velocities by removing the boat speed and direction.

### 3.4.3 Echo-sounder

The echo-sounder data file was uploaded to software package ReefMaster which provides the distance to the seafloor from the transducer using maximum backscatter. The fixed distance between the water surface and transducer provides a time series of water depth for comparison with the depths estimated from the ADCP backscatter.

### 3.5 Results

The data collected gave measurements of depth from the echosounder and ADCP, which was compared to elevation data from the GPS. The ADCP also provided

'apparent bottom speeds' and the derived water column velocities. Several transects were undertaken with the JetYak going over regions of bare mudflat and regions of seagrass.

### 3.5.1 Elevation and Depth

Elevation and depth data were collected from the RTK GPS, the echo-sounder and the ADCP. The pre-survey data collected by walking around at low tide is shown in Figure 3.7. The two mudflat patches within the seagrass were mapped as well as the sharp transition between the mudflat and seagrass. The outer edge of the deeper boating channel was also mapped using the RTK GPS. The highest elevations are 0.3 m and are shown to be over the seagrass transition as well as near to the two patches of mudflat within the seagrass. The elevation decreases again going across the mudflat patches towards the East from 0.2 m at the big patch to -0.4 m. The channel was shown to be the lowest elevation at -0.6 m. Elevations varied from 0.2 m elevation to -0.4 m elevation in the N-S direction, increasing northwards over a range of 90 m.
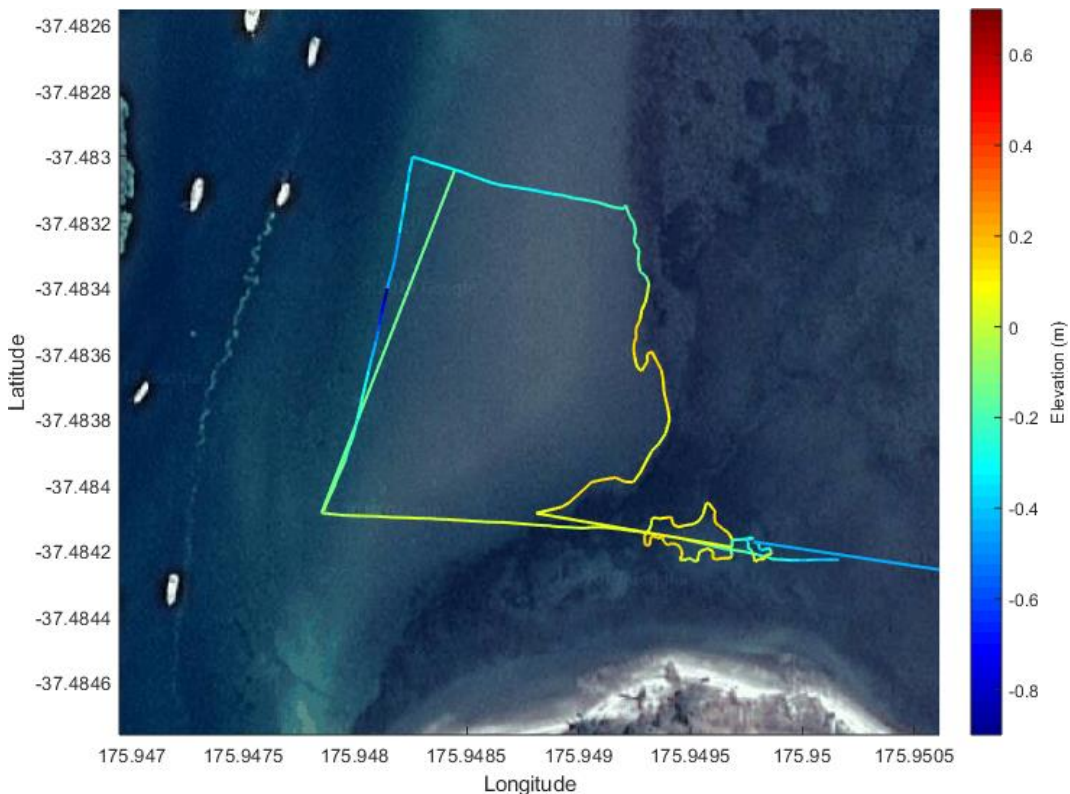


**Figure 3.7**. Elevation data collected from the pre-survey. (Datum: New Zealand Vertical Datum 2016).

Data collected from the echo-sounder was uploaded to software package ReefMaster. This software package automatically uses the method of maximum backscatter to find the seafloor (Patel *et al.*, 2019) and therefore, the distance to the bottom of the water column from the transducer. Figure 3.8 shows the raw depths calculated from the echo-sounder using ReefMaster throughout the four survey tracks. The Google Earth image shows plotted underneath Figure 3.8 shows the western boating channel as well as the bare mudflat and seagrass dominated region. The depths calculated from the echo-sounder are the distances from the transducer to the seafloor and ranged from 0 m to 2 m over the area of the survey. The deepest depths up to 4 m were observed within the boating channel and the shallowest depths are shown over the areas of high elevation over the seagrass.
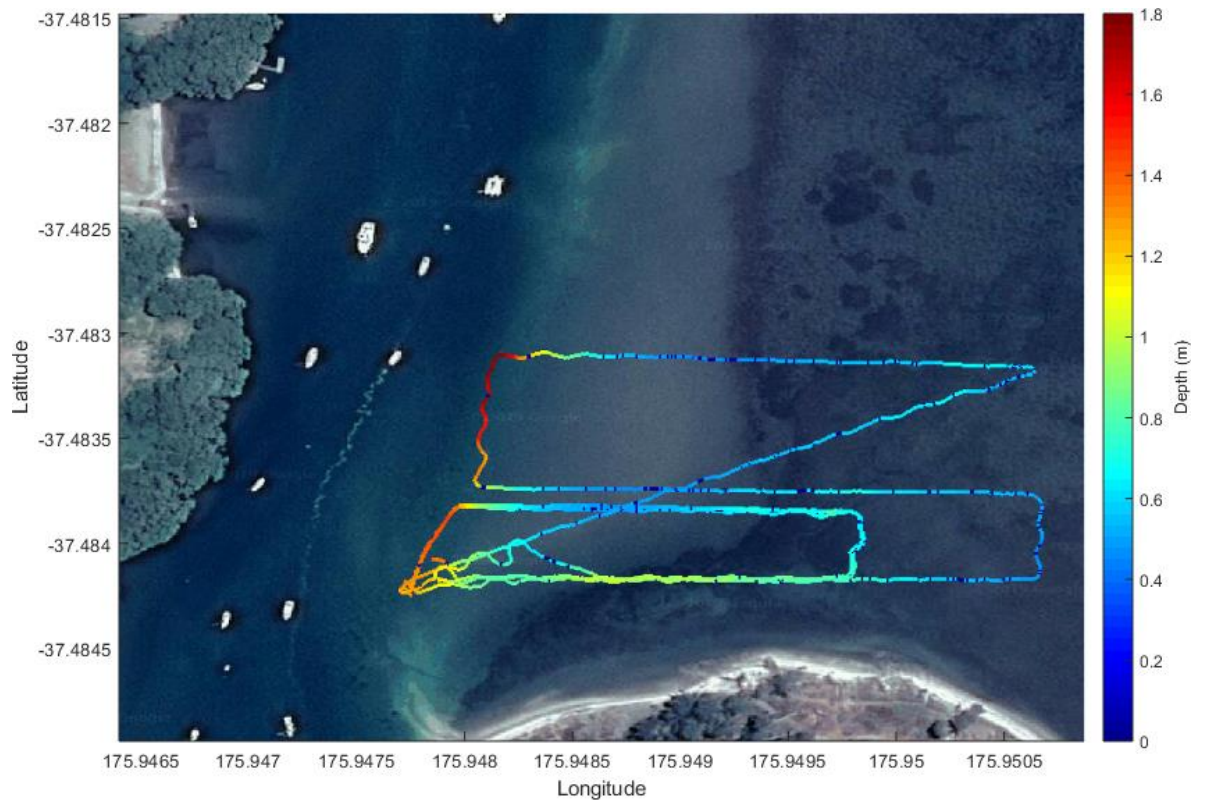


**Figure 3.8.** Raw depth data found using maximum backscatter from echosounder for the four survey tracks.

With the underlying image from Tuapiro point from google maps, the depths found from the echo-sounder match the features of the deeper boating channel on the western side and becoming shallower going from east to west over the higher elevation areas mapped with the GPS at low tide. Depths also decrease moving northwards from the bottom of the seagrass. Figure 3.8 illustrates deviations in water depth between the repeated surveys.

To eliminate the deviations between the four surveys, the elevation was found by removing the height from the RTK GPS to the echo-sounder transducer and then removing the water depth. Figure 3.9 shows the comparison of elevation from each of the four surveys for the two E-W transects. The results show the lower elevations correspond with the lower elevation areas found by the RTK GPS at low tide on the western side channel and higher elevations moving over the seagrass and decreasing again towards the eastern side. The elevations from each of the four surveys acquired by the JetYak are in good agreement. Survey four also appears to have higher elevation (Figure 3.9 b) as transect two for survey four was further north than survey one to three. The results are also consistent with the data collected from the initial survey.
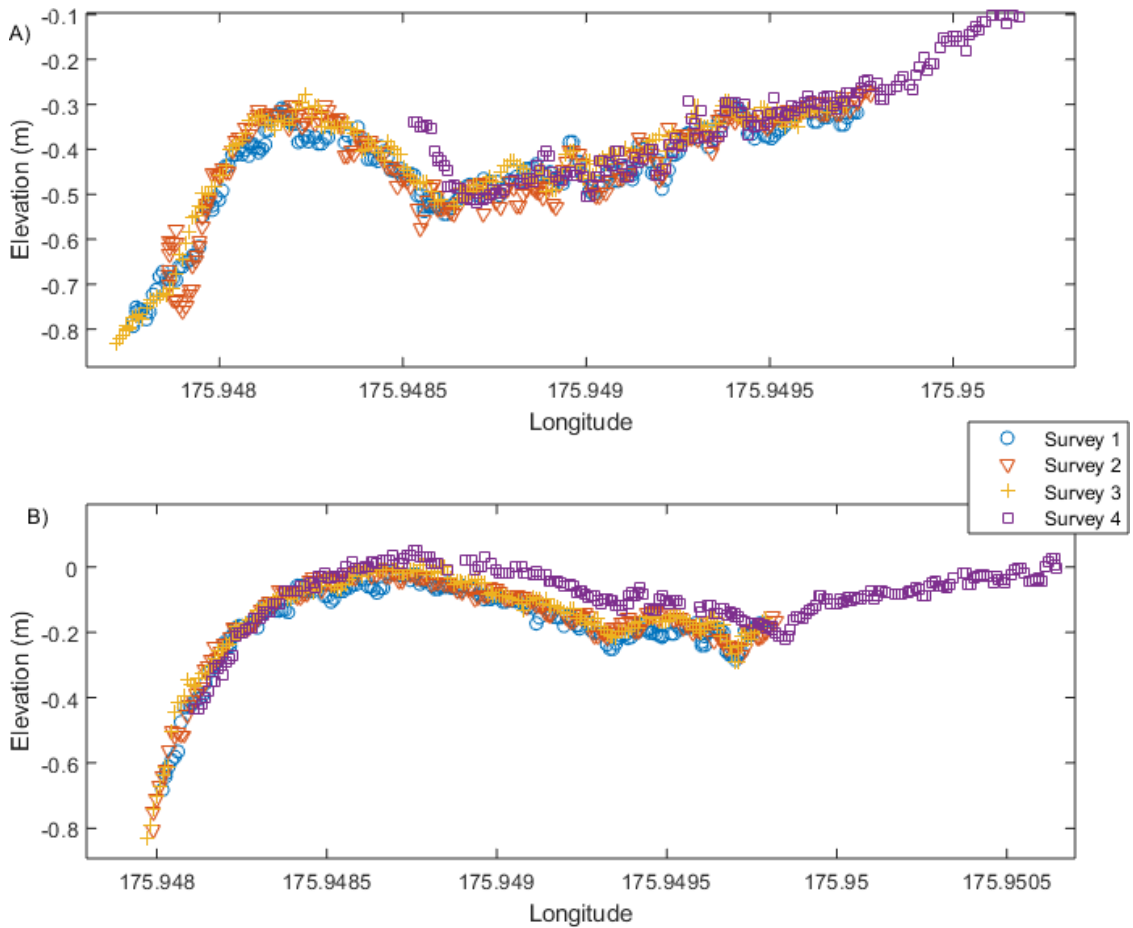


**Figure 3.9.** Comparison of elevation found by the JetYak for each of the surveys. A) E-W transect one (Southern transect). B) E-W transect two (Northern transect).

Figure 3.10 compares the elevations from the low-tide initial survey E-W transect across the seagrass (Figure 3.7) to the elevation first E-W transect attained from the first JetYak survey (Figure 3.9 a). the trend of the increasing elevation towards the seagrass from the western side channel is shown in addition to the decreasing

42

elevation towards the east followed by an increase in elevation. In general, despite being taken from slightly different locations (latitudes varied between the two sources), the elevations show reasonable agreements. The initial survey was further northwards and therefore, elevations over the seagrass were 0.1 m greater than recorded by the JetYak. This result is consistent with the elevation data collected from the presurvey, as the elevations increase northwards.
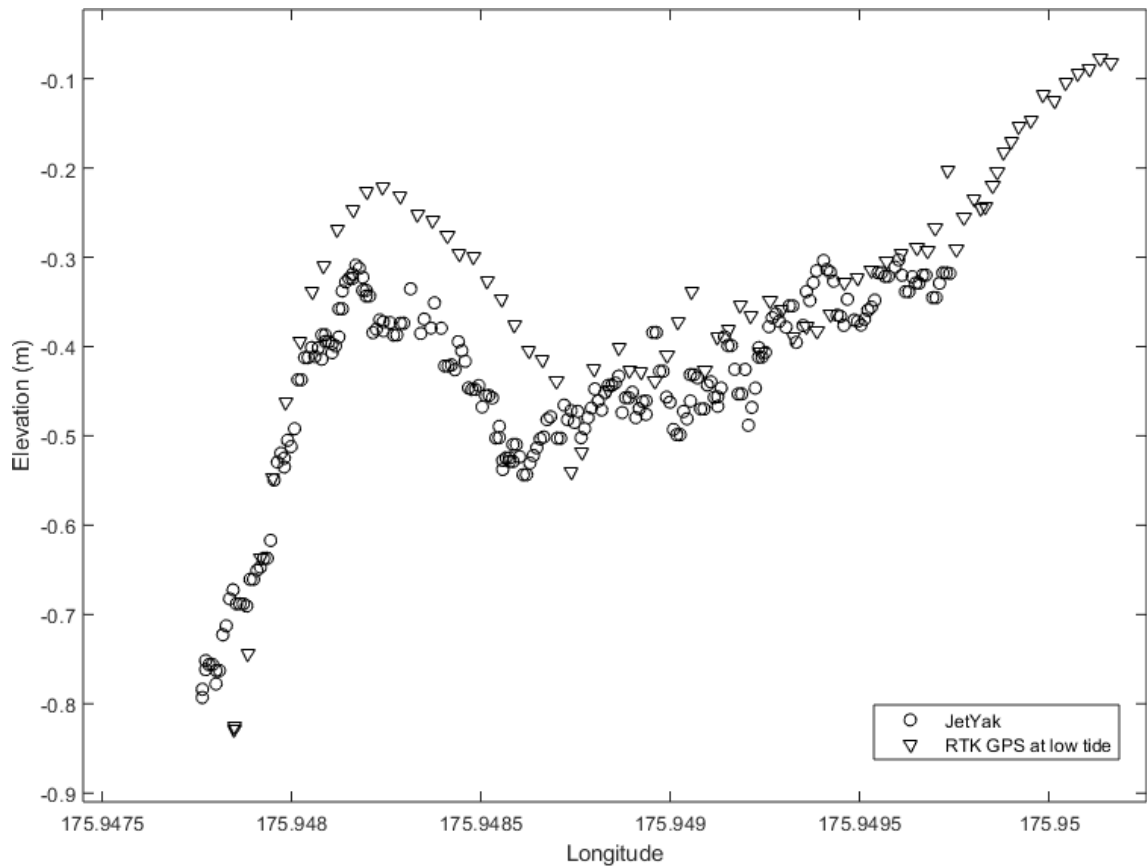


**Figure 3.10.** Comparison of elevation from E-W transect one from the first survey with the JetYak and E-W transect from the initial survey.

The ADCP was also used to find the depth of the water column using backscatter. Figure 3.11 shows the backscatter from beam five, the directly downward facing beam on the Nortek Signature1000 ADCP and the results of the algorithm used to find the seafloor (black line). This identified seafloor was then plotted against the backscatter from rest of the five beams (Figure 3.12) and appeared to match the bin with maximum backscatter for each beam, indicating that beam spread and differences caused by boat roll were minimal. Times when the distance from the transducer reached three metres matched times when the JetYak was in the boating channel and shallow depths matched times when the JetYak crossed over the

seagrass. Thus, we conclude the algorithm to identify the bottom was robust enough for this purpose.
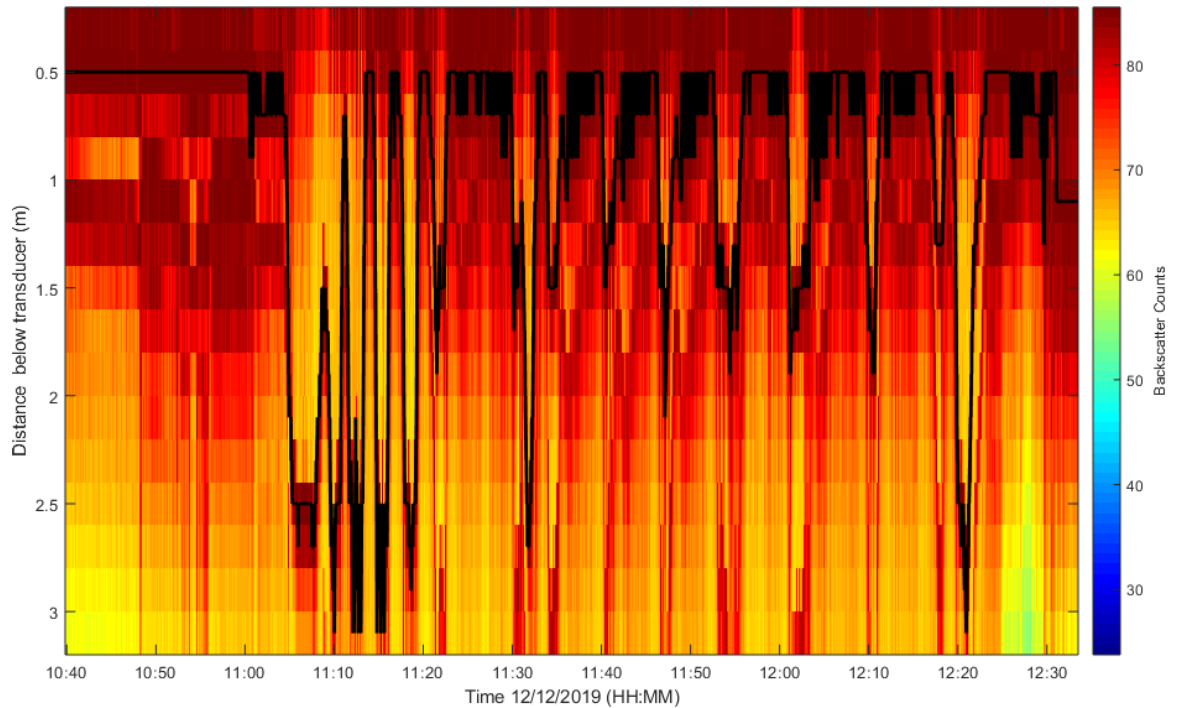


**Figure 3.11.** Backscatter from beam five used to find the maximum backscatter from the bottom upwards. The black line indicates the bin with the maximum backscatter found to be the bottom (Mullarney & Henderson, 2013).

Figure 3.12 shows the backscatter counts for each of the five beams throughout the survey. The seafloor was found from beam five (Figure 3.11) and plotted on each of the five beams. Backscatter measurements from below the bottom were removed.
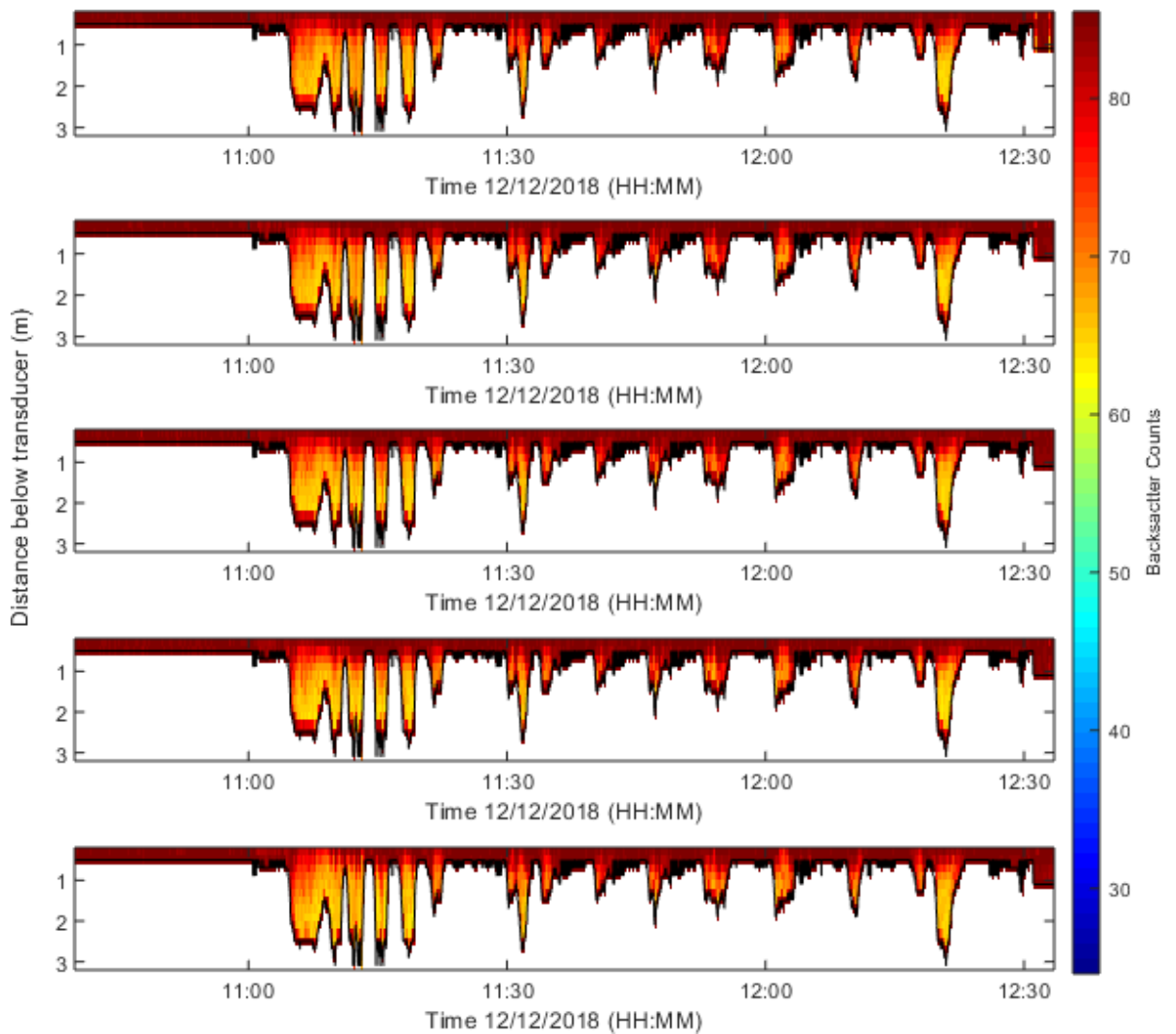
**Figure 3.12**. Backscatter counts throughout the survey with distance below the transducer for each of the five beams from the ADCP with below the seafloor data removed. A) Beam one. B) Beam 2. C) Beam 3. D) Beam 4. E) Beam 5.

Figure 3.13 compares the depths found from the echosounder and the depth found using the maximum backscatter from the ADCP and demonstrates that the two methods of finding the seafloor agreed well. The channel where the deeper depths of up to four metres are represented by both instruments as well as the smaller changes in depth over the shallow higher elevation areas covered by seagrass. The data shows the calculated bottom from the maximum backscatter correlates with the echo-sounder measurements. The echo-sounder however, had the ability to determine smaller changes in water depth, i.e. the echosounder had a much finer resolution than measurements determined by the ADCP. Depth measurements acquired by the ADCP exhibit larger discrete jumps as the bottom depth was assigned as the middle of the cell in which the bottom was detected in the backscatter. Hence the resolution was dependent on the vertical bin size.

45
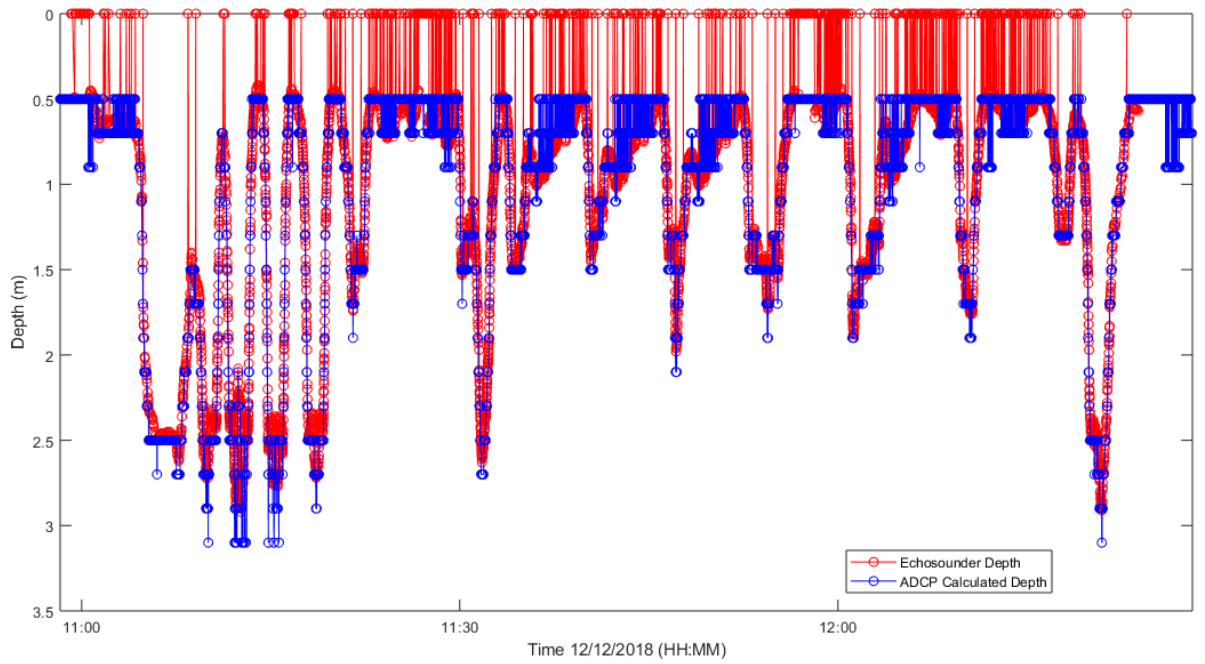
**Figure 3.13.** Comparison of depths throughout the survey from the echosounder and depths from the ADCP.

### 3.5.2   Apparent Bottom Speeds

The velocity of the JetYak was removed from the velocity data in order to accurately show the flow velocities. The boat speeds were calculated from GPS data by differencing the x and y positions (divided by the 1s time difference between measurements). These speeds were then compared to the negative of the 'apparent bottom speeds' acquired from the ADCP (i.e. the velocity components from the bin identified as the bottom) (Yorke & Oberg, 2002). Figure 3.14 shows the comparison of the two methods for finding the speeds the JetYak was travelling throughout the survey. The two methods are shown to agree well, thus providing initial confidence in the ADCP measurements.
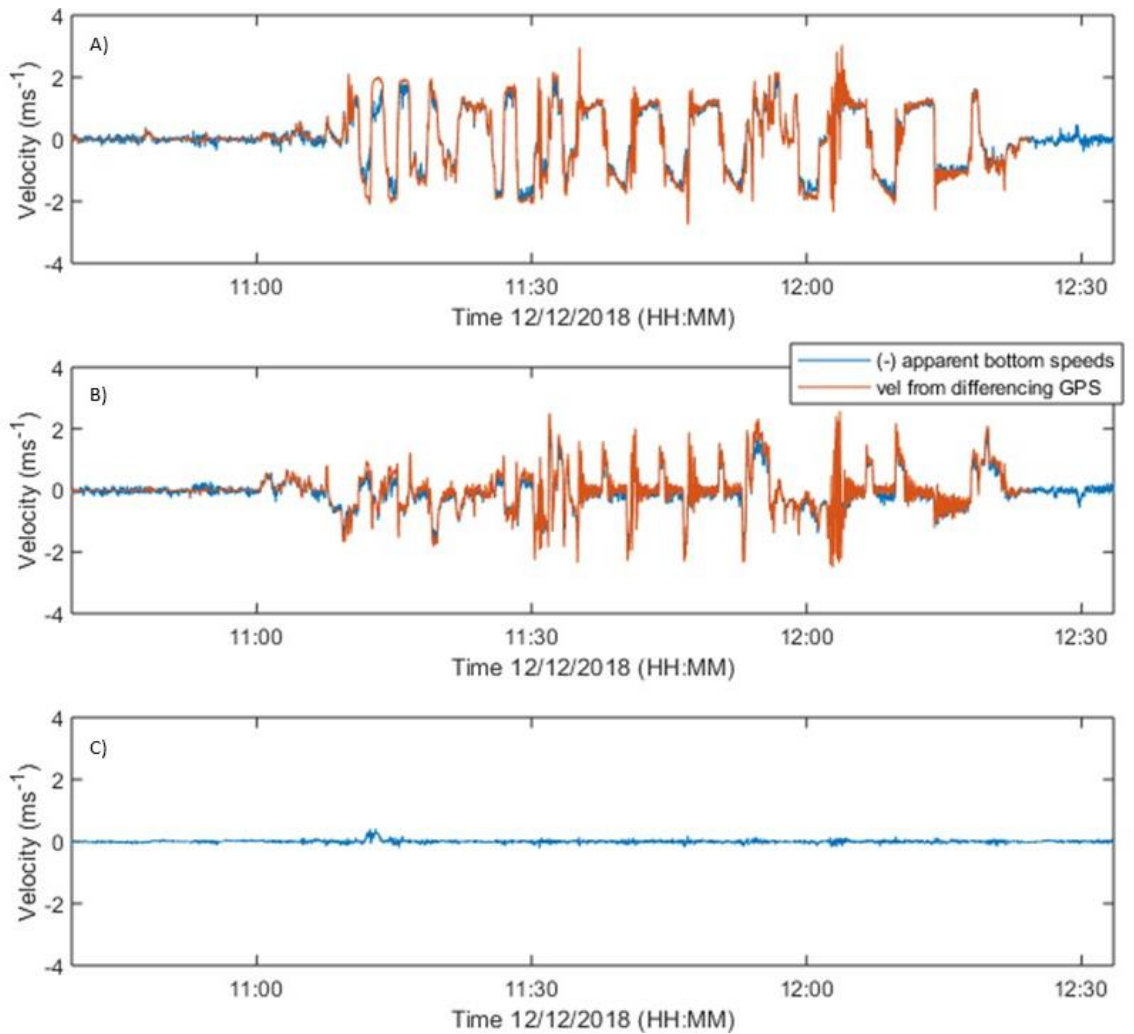
**Figure 3.14.** Comparison of apparent bottom speeds calculated from the ADCP and velocities differenced from x and y positioning of the RTK GPS. A) Eastwards velocity comparison of apparent boat speeds. B) Northwards velocity comparison of apparent boat speeds. C) Upwards velocity of apparent bottom speeds from the ADCP.

### 3.5.3 Velocities

First, the correlations from the data were plotted to show the quality of data collected (Figure 3.15). There was a band of low correlation due to the reflection of the bottom, mainly collected within the channel. The band is due to the first ping reflecting off the bottom and interfering with the second ping (Mullarney & Henderson, 2013). Other than the band of low correlation, the data was of reasonable quality. Correlations of less than 50 % were removed from the data when calculating the actual water velocities. This procedure removed the majority of the bad data points collected within the channel.
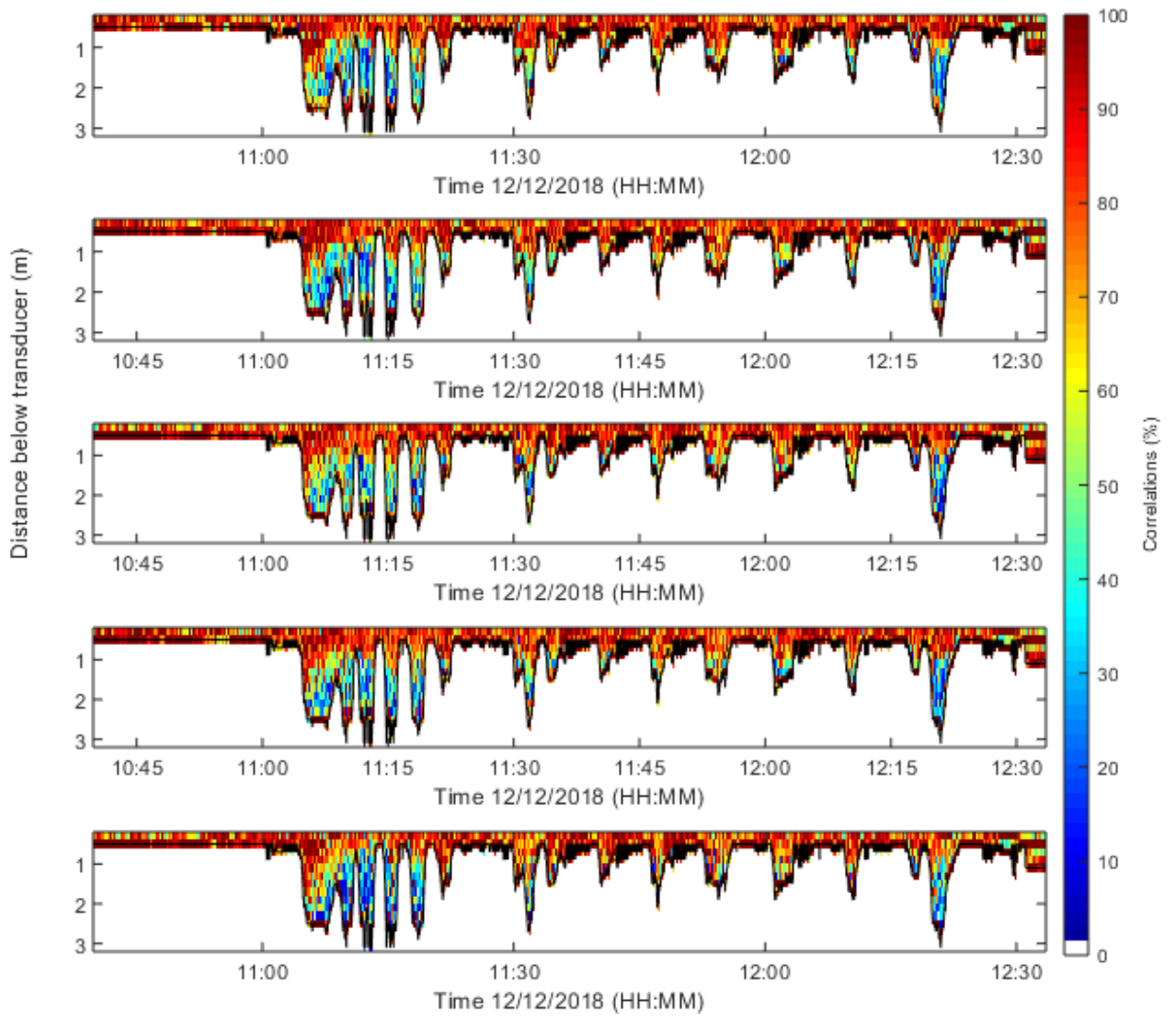
**Figure 3.15.** Correlations for each of the five beams. A) Beam one. B) Beam two. C) Beam three D) Beam four. D) Beam five.

Flow velocities around the seagrass to mudflat transition were the main interest of this research. Velocities in the water column were estimated by rotating the data into East North Up (ENU) components and removing the motion of the boat.

The speed of the boat was removed from rotated velocities in the East, North and Up (ENU) directions collected from the ADCP. Figure 3.16 shows the estimated water column flow velocities rotated into ENU components. However, the results show a distinct transition of flow directions within the channel in both the E-W and N-S directions. Such a transition would indicate a region of shear within the channel. However, such a change is in clearly unphysical: given the relatively straight channel on the flood phase of the tidal cycle, the flow should be in one consistent direction (Hernández-Dueñas & Karni, 2011). The apparent change in flow directions corresponds to the location at which the JetYak changed direction within

48

the transects. Therefore, we conclude that the velocities are still strongly influenced by the JetYak motion (into and out of the channel), and thus, are not reliable.
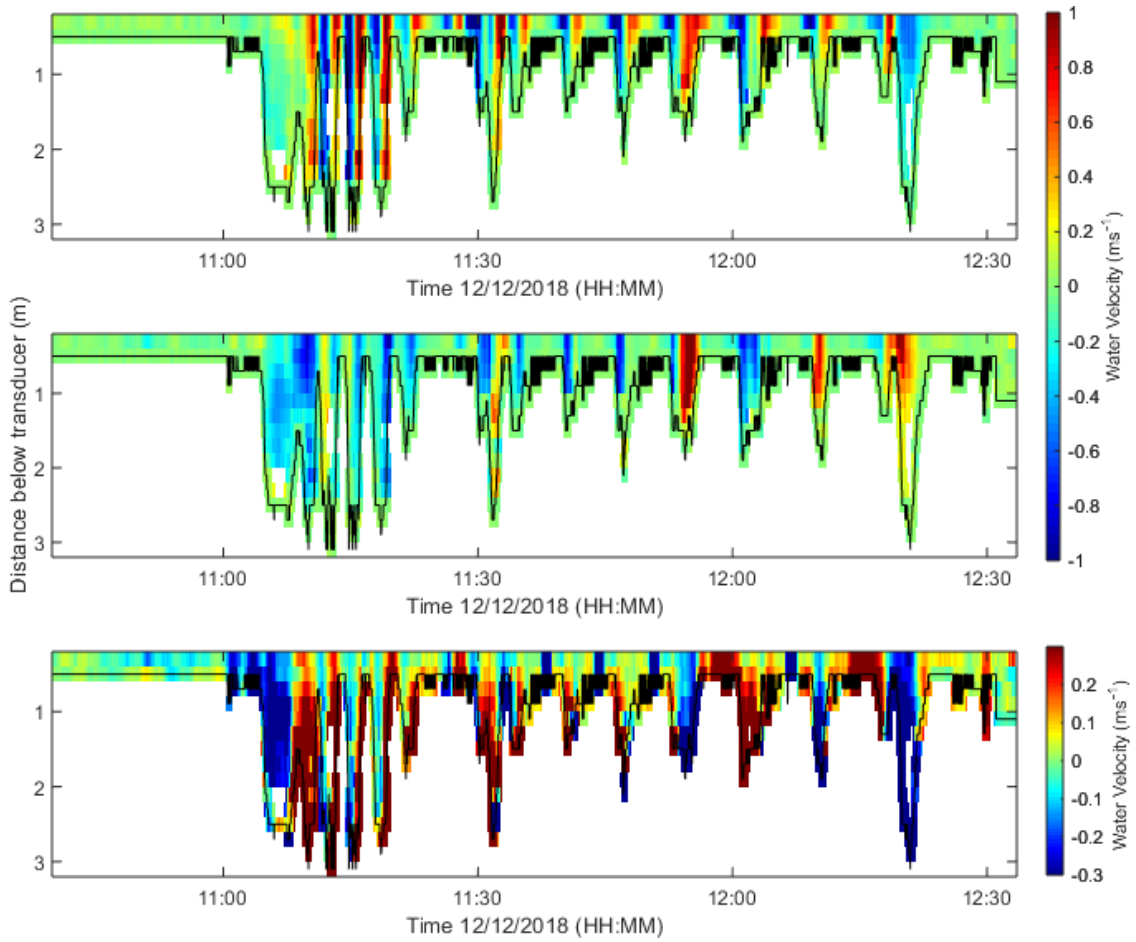


**Figure 3.16.** Water velocities throughout the survey. A) East-West velocity. B) North-South velocity. C) Vertical velocity. (Smoothed with 25-pt window).

Figure 3.17 is a close-up image of an instance of both positive and negative E-W velocities within a deeper part of the estuary in the survey. It clearly illustrates a velocity in two different directions, which is not possible, proving the results are unreliable for resolving smaller scale changes in flows at the seagrass transition.
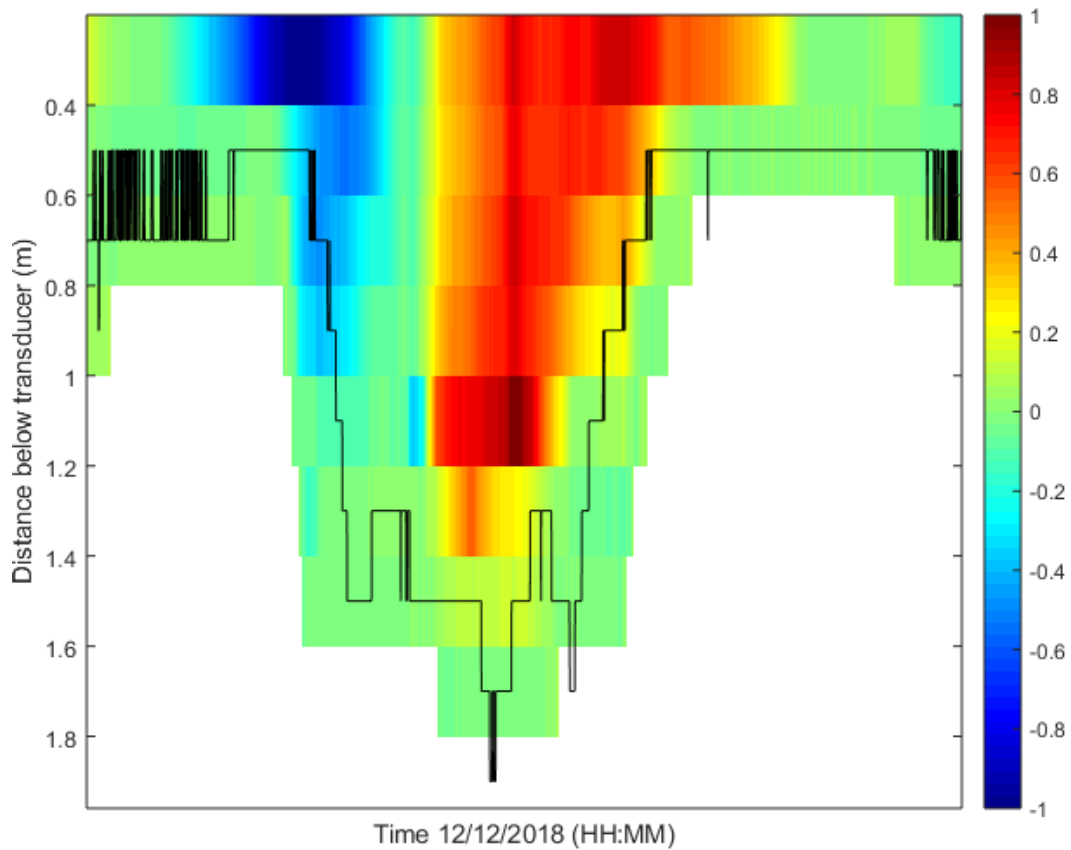
**Figure 3.17.** Close-up of example from E-W velocity of positive and negative velocities.

### 3.5.4 Backscatter

Given the velocity measurements were deemed unreliable, we instead concentrate on the backscatter reflection to explore if there were changes in the backscatter that reflect the seagrass to mudflat transition. During each of the four survey tracks, the instances the JetYak crossed the transition between mudflat and seagrass were found. These data included the occurrences the JetYak crossed over the patches within the seagrass. The changes in backscatter at the sea floor is shown in Figure 3.18.
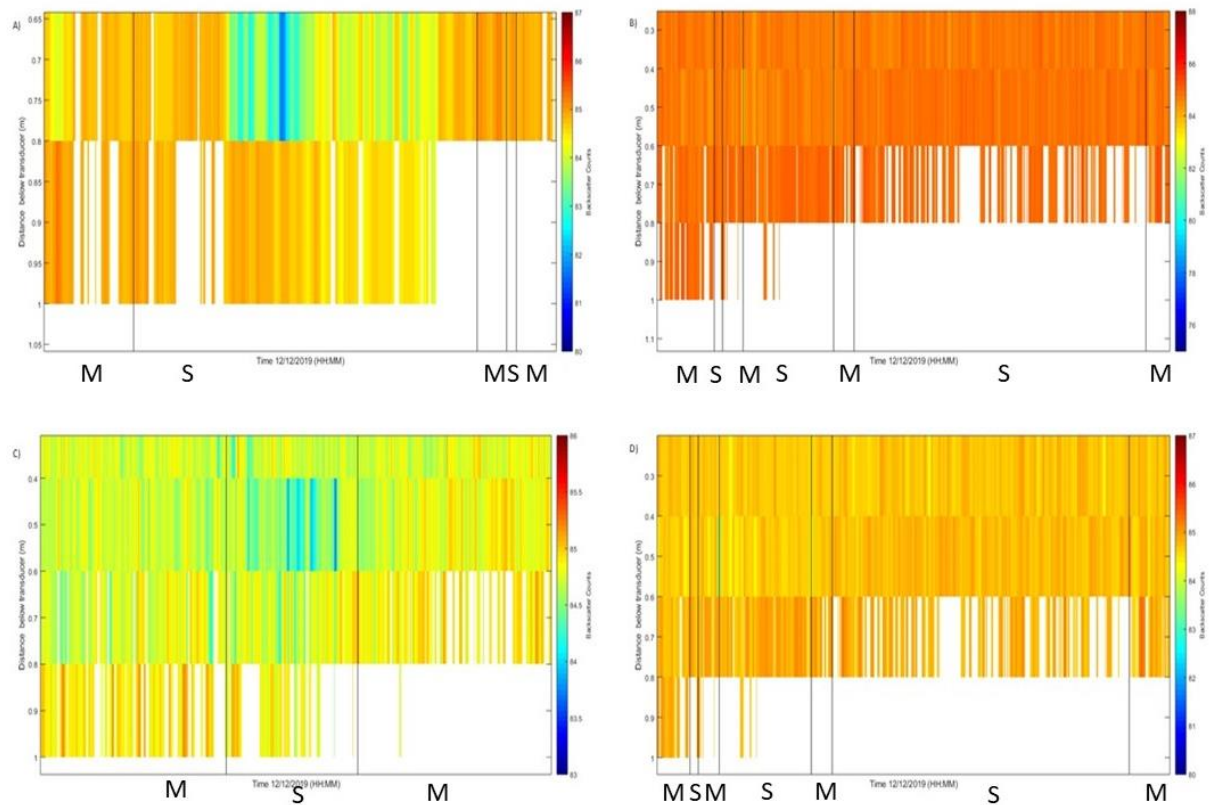
**Figure 3.18.** Backscatter from beam 5. Black line indicates time the JetYak crossed the seagrass to mudflat transition. A) Survey one. B) Survey two. C) Survey three. D) Survey four. S represents seagrass dominated areas. M represents the mudflats.

Presented in Figure 3.18 is the backscatter at the seafloor at the time the JetYak crossed the transitions between the seagrass and mudflat for each of the surveys. Throughout the four survey tracks, at the time the JetYak crossed the transition, the result in change in backscatter in the bottom bin above the seafloor was variable. In some instances, the backscatter increased or decreased, in some instances, there was no change. The occasions when the backscatter increased or decreased were also very small.

## 3.6 Discussion

The JetYak was successfully able to measure bathymetry data with the echo-sounder and ADCP. From the initial survey with the RTK GPS at low tide, to the JetYak echo-sounder and ADCP depths found using maximum backscatter, all methods agreed well. The comparison figures (Figure 3.10 & Figure 3.13) validate that all methods of attaining bathymetry data are in good agreement. The bathymetry data collected from all three methods indicate the region of low elevation and subsequently at high tide, greater depths, moving towards the channel

from the seagrass. The highest elevations were found in the middle of the seagrass bed and therefore, consisted of the lowest water depths at high tide. This result is consistent with the data collected at low tide and the known bathymetry of the estuary from photographs such as google earth images or aerial photographs. Seagrass are known to inhabit areas of high elevation (Fonseca *et al.*, 1982) as a result of increased sediment accumulation around the roots by reducing flow speeds within their canopies (Fonseca & Koehl, 2006; Luhar *et al.*, 2010). By reducing flow speeds, sedimentation increases as smaller flow speeds allow less and smaller grain sizes to be picked up in the water column (Bos *et al.*, 2007). Seagrass were found by Bos *et al.* (2007) to significantly contribute to the immobilisation of sediment and increase sedimentation within seagrass beds. This process is reflected by the increase in sediment in the seagrass beds observed at Tanners point and resulting accretion of sediment and thus, a higher elevation. Areas uninhabited by seagrass were found to have lower elevations as a result of erosion as flow speed are not moderated by seagrass (De Lima *et al.*, 2015).

The raw JetYak data also measured variations in bottom depths between surveys due to the water depth increasing with the rising tide between circuits. These variations were successfully eliminated by removing the height from the RTK GPS to the echo-sounder transducer and then removing the depth found by the echo-sounder to acquire the elevation. Elevation data from each of the transects agreed well therefore, we conclude that with the system as set up, environmental conditions during surveys can easily be removed for increased accuracy of data collected (Moulton *et al.*, 2018).

The apparent bottom speeds found by the ADCP and GPS were also in good agreement (Figure 3.14). Vessel speeds throughout the day ranged from 0 ms-1 to 4 ms-1 which was very fast for surveying (Perry & Rudnick, 2003). The cruise speed in Mission Planner was set to 2 ms$^{-1}$ for each of the surveys. However, surveys were undertaken before ideal driving parameters had been investigated. Therefore, the P throttle parameter within Mission Planner was also set too large, the JetYak accelerated and decelerated more than necessary. Faster surveying speeds have been shown to create large errors in data collected from vessels (Fischer *et al.*, 2003). Therefore, P throttle was decreased in optimisation of the parameters (Chapter 2) to achieve the desired survey speeds without large

acceleration and deceleration. The cruise speeds were also decreased for an average speed of 1 ms$^{-1}$ for further surveying using the JetYak.

The relative speeds between the JetYak and the flow were large and therefore, small changes in flow speeds over the seagrass transition were not found. The velocity data attained from the survey revealed the vessels motion was not completely removed. The positive and negative values indicated external motion rather than the actual flow velocities. Mullarney and Henderson (2013) acquired shallow water current speeds using ADCPs attached to drifters by removing instrument speeds and was shown to work well. This method of attaining current speeds successfully removed the motion of the moving instrument; however, the drifter moved with the current and therefore, moved near to the bottom speeds and relative speeds were small. In comparison, the relative speeds acquired by the JetYak going against the current were very large and therefore, speeds from the JetYak were not entirely removed from the velocity data. The large relative speeds may have been worsened by large speeds the JetYak was travelling in comparison to the smaller scale flows present. Typical surveying speeds range from up to 1.5 ms$^{-1}$ (Perry & Rudnick, 2003), whereas, the JetYak reached survey speeds of up to 4 ms$^{-1}$ in some instances, which may explain why the vessels motion was not entirely removed. This experiment was undertaken before we had completed the optimisation of steering parameters, therefore the fast JetYak speeds were a result of poor steering and throttle parameters

The backscatter was then plotted with the instances the JetYak crossed the transitions between mudflat and seagrass to observe if the change in bottom roughness could be detected. The backscatter plots showed that in some instances the backscatter changed (increased or decreased) correlated with the time the JetYak passed over the transition (Fauziyah *et al.*, 2018). Other times, there was no change in backscatter. Therefore, there was no distinct correlation with change in backscatter to show areas of seagrass transition. Again, this may have been due to the JetYak moving too fast to accurately show the change in roughness of the seafloor (Perry & Rudnick, 2003) or could perhaps be simply owing the small height of the seagrass not causing resolvable differences over the vertical bin size used in the present experiment.

### 3.6.1 The JetYak

The JetYak was the ideal instrument to collect data in these shallow water environments. The JetYak could autonomously drive and collect data in the shallow water above the seagrass and mudflats to measure the water velocities in the bottom boundary layer. Due to seagrass living in the intertidal zone, as well as seagrasses being found on high elevation areas (Chiu *et al.*, 2013), they generally cannot be surveyed using manned vessels as there is insufficient water depth (Kimball *et al.*, 2014). The shallow water of the intertidal zone that the seagrass inhabits as found by the pre-survey elevation data confirmed a manned boat was unlikely be easily operated there (assuming a larger draft and frame to mount ADCP).

The JetYak was successfully able to repeat pre-programmed transects to collect accurate elevation data as shown in Figure 3.9. For each of the four surveys, the JetYak was able to obtain correct measurements over the four surveys to increase precision of data collection. The conditions of the environment including small waves and the rising tide were removed from the data to give consistent and reliable data. The JetYak excelled in collecting bathymetry data as shown by all instruments in good agreement in addition to the comparison of elevation data between surveys. The JetYak was unsuccessful however, at resolving small-scale flows. We note that the system as set-up was not designed to be used in this fashion. In order to accurately resolve the flows, a vessel mounted system would be more appropriate. The JetYak can only achieve accurate results with the right instrumentation onboard. In future, the steering and throttle parameters will be those outlined in Chapter 2.

## 3.7 Conclusion

The JetYak was tested to resolve flows over seagrass in the Tauranga estuary. The small flows in the shallow water could not be resolved with the JetYak as the boat motion was not entirely removed. It was found that because the flows were so small, the JetYak appeared to be travelling too fast to resolve the actual velocities. For future surveying of this nature, it is advised to use purpose-built boat integrated boat-mounted systems for better results. However, the JetYak successfully collected bathymetry data for the shallow intertidal region the seagrass inhabits and could accurately repeat transects for optimal data collection.

# Chapter 4

# River Plume Monitoring

## 4.1 Introduction

River plumes are created as buoyant freshwater flows into the salty ocean water (Simpson *et al.*, 1990; Horner-Devine *et al.*, 2015). These plumes play a dynamically important role in coastal environments, as they result in strong horizontal and vertical density differences, which can drive strong flows, create regions of vigorous mixing and generate internal wave trains (Nash & Moum, 2005; Kilcher & Nash, 2010). Material supplied from inland can impact ecological health and habitat in the coastal environment (Devlin *et al.*, 2012). The impact these materials have is greatly dependent on physical processes that transport the river plume water around the coastal environment as it debouches into the deeper saltier water (Horner-Devine *et al.*, 2015). Buoyancy-driven mixing can control vertical fluxes of nutrients, transport of organisms and particles and mixing of shelf water (Geyer *et al.*, 2004). Larvae and other ecosystems rely on this dispersal to move them to hospitable environments and are crucial for their survival. The distribution of larvae has also been examined in idealised models of plumes and water dispersion to predict survival rates (Stacey *et al.*, 2000; Matheson & Schwarz, 2007). The shape and character of the plume are predominantly set by the two physical processes of advection and dispersion (Horner-Devine *et al.*, 2015). Advection sets the direction of the plume out of the river mouth and dispersion sets the lateral and vertical movement of the plume (Matheson & Schwarz, 2007).

Freshwater rivers are also the principal mechanism by which terrestrial sediment is delivered to the coastal environment (Geyer *et al.*, 2004; Walsh & Nittrouer, 2009). Moreover, rivers are a dominant source of coastal pollutants (Devlin *et al.*, 2012). Pollutants are increasing due to overharvesting of marine and land resources, and contaminants in river run off. The area affected by pollutants depends on the surface plume water which can be affected by the size of the catchment, peak flow events and prevailing winds and currents. Terrigenous material carrying pollutants can also be deposited and again entrained into the water column during periods of large winds and waves (Devlin *et al.*, 2012).

Monitoring of river plumes forms the basis for describing ecological impacts and whether effects are chronic long-term impacts adversely effecting water quality or short-term effects changing with changing sediment and nutrient loads in the river system (Warrick *et al.*, 2007; Devlin *et al.*, 2012). Excessive fresh water from flood plumes can cause adverse effects to ecosystem health decreasing light availability and smothering marine organisms from high sedimentation loads (Devlin *et al.*, 2012). There is also uncertainty in the amount of sediment transported in river systems as a result of land use changes that is essential to be monitored (Geyer *et al.*, 2004).

Every individual river plume system comprises of dynamically distinct areas which range over large spatial and temporal scales (Horner-Devine *et al.*, 2015; Osadchiev & Zavialov, 2019). The structure of a river plume depends on discharge, ocean currents and properties, tidal amplitudes, bathymetry and geometry of the coastline, wind, and Coriolis, the effect of the earth's rotation (Horner-Devine *et al.*, 2015). For each system, freshwater discharge can vary substantially throughout an annual cycle and between storm events (Fong & Geyer, 2002). Additionally, the forcing and geometries can vary greatly from system to system. Capturing the full range of temporal and spatial scales for each system is therefore challenging (Horner-Devine *et al.*, 2015). It is often difficult to encompass a large area for monitoring as vessel sampling is often limited as a result of cost and time constraints as well as adverse weather conditions (Devlin *et al.*, 2012).

### 4.1.1   The JetYak

We tested the use of the JetYak as a tool to map the location and boundaries of the Waihou and Piako River plumes, in the Firth of Thames, New Zealand. Due to the size, large area and shallow intertidal region, the river plumes are difficult to map without using remote sensing data collection methods such as satellite imagery and aerial photographs. However, reliable field data is still needed to validate and calibrate remotely sensed measurements (Klemas & Victor, 2009). For this experiment, the JetYak was taken into the semi-enclosed sea and therefore, was subject to the impact of waves. The JetYak was equipped with a dorade box to prevent water from waves or salt spray from getting into the engine. The addition

of a dorade increases temperatures of the motor compartment therefore, temperatures inside the engine compartment were also recorded.

## 4.2 Aim

The aim of this field experiment was to resolve the boundaries of the two river plumes in the Firth of Thames using the JetYak. The JetYak was operated to increase efficiency of data sampling alongside a research vessel. The data from the manned vessel was compared the output of the JetYak measurements of conductivity, temperature and turbidity across the Waihou River plume and Piako River plume.

## 4.3 Methods

### 4.3.1 Site Description

The Firth of Thames is an estuarine embayment located in the Hauraki Gulf, in the North Island of New Zealand (Lovelock *et al.*, 2010) and is shown in Figure 4.1. The Firth of Thames has also been described as a modern flat fronted deltaic system and a semi-enclosed sea within a structural graben (Healy, 2002). The system is meso-tidal, with a spring tidal range of 2.8 metres and a neap tidal range of 2 metres (Eisma, 1998). The Waihou River is situated at the eastern border of the Firth of Thames. The main stem of the river is 186 km in length and the river passes through pasture and forest (Lovelock *et al.*, 2010). The Waihou River is a 1966 km$^2$ catchment (Swales *et al.*, 2007), which consists of a mixture of flat to gently undulating areas to steep topography and the annual rainfall averages 1400 mm/year (Lovelock *et al.*, 2010). The Firth of Thames also receives run off from the Piako River with a catchment size of 1476 km$^2$ for a total of 3600 km$^2$ catchment that delivers into the Firth of Thames (Swales *et al.*, 2007; Lovelock *et al.*, 2010). The Waihou River debouches into the Firth of Thames with high sediment loads as a result of modifications to the land over the past 150 years such as mining, deforestation and drainage of freshwater wetlands in the region (Swales *et al.*, 2007; Lovelock *et al.*, 2010; Pritchard *et al.*, 2015). These sediments being delivered to the Firth of Thames are trapped and deposited as a result of estuarine circulation and tidal currents (Healy, 2002). This deposition has built up to 70 km$^2$ of intertidal mud flats and created a shallow bed slope of 0.03°. The southern end of the Firth of

Thames was a sandy tidal flat in the 1950's as shown by aerial photographs (Lovelock *et al.*, 2010), and by 2007, a 1000 metre wide, and growing, mangrove forest surrounds the firth and the river banks in the muddy intertidal region (Healy, 2002). The mangrove species is *Avicennia marina* and occupies the intertidal region from 1 metre above mean sea level at the seaward limit to 2 metres above mean sea level at the landward edge. A stop-bank was constructed to prevent flooding of the farmland and prevent freshwater loss to the mangrove forest (Lovelock *et al.*, 2010). At ebb tide, the shallow tidal flats of the Firth of Thames are left exposed (Deppe, 2000). These shallow estuarine waters include expanse areas of mudflat, shell banks, grass flats, mangrove forest, salt marsh and freshwater swamp margins. Areas such as these and the expanding mangrove forest, are internationally important for feeding areas for wader and waterfowl and provide habitat for birds and nursery areas for fish (Deppe, 2000).



**Figure 4.1.** Firth of Thames located in the Hauraki Gulf in the North Island of New Zealand. Featured is the Waihou River and Piako River. (Images: Google Earth)

### 4.3.2 Instrumentation

Two research vessels were used to survey the Waihou River plume (Figure 4.2). The JetYak was equipped with an echosounder, to measure water depth. Location data was provided by the GPS linked to the echosounder and the inbuilt Pixihawk navigation system. An RBR Concerto was mounted on the port side to measure

conductivity, temperature and turbidity. These properties were recorded at 6 Hz. The motor compartment was also equipped with a HOBO temperature logger, set to record every minute to examine the temperature changes with the addition and removal of the dorade box. The research vessel, Taitimu was equipped with a CEE-LINE dual frequency echo-sounder measured at 200 kHz, along with an RTK GPS (positioned directly 2.31 m above the echosounder transducer) which both recorded every second. The vessel also had conductivity, temperature and turbidity sensors cabled to a Campbell Scientific Data Logger to measure conductivity, temperature and turbidity every three seconds. Data from the vessel-mounted the GPS instruments were displayed in real time on an onboard ship computer. Set up included setting the base station up on board the research vessel. During the survey, we took sporadic CTD (conductivity-temperature-depth) profiles using a Seabird Scientific SBE 19plus V2 SeaCAT CTD profiler. The positions of profiles were recorded using a hand-held GPS.



**Figure 4.2.** JetYak and Research vessel instrument and dorade set-up.

### 4.3.3  Field Experiment

On Friday the 14th June, a survey was conducted to obtain simultaneous measurements from the JetYak and research vessel 'Taitimu'. The vessels were navigated across the intertidal mudflats at the southern end of the Firth of Thames, and the Piako and Waihou River mouths. Four transects were undertaken, two

across-Firth and two along the Waihou River (Figure 4.3). The JetYak was piloted by the remote control from on board the research vessel (Figure 4.4) for the two along-river transects. However, for transects across the river mouths, the JetYak was switched to autopilot. During these across-Firth transects, the research vessel was simultaneously piloted along approximately parallel transects, thus allowing a larger area of the plumes to be surveyed. The JetYak surveyed further seaward than the research vessel for transect two and further inland for transect three. The survey tried to encompass both Waihou and Piako river mouths with the aim of measuring any interaction between the two plumes. The across-Firth transects were surveyed using the autopilot function of the JetYak with the optimised steering and throttle parameters (see Chapter 2).
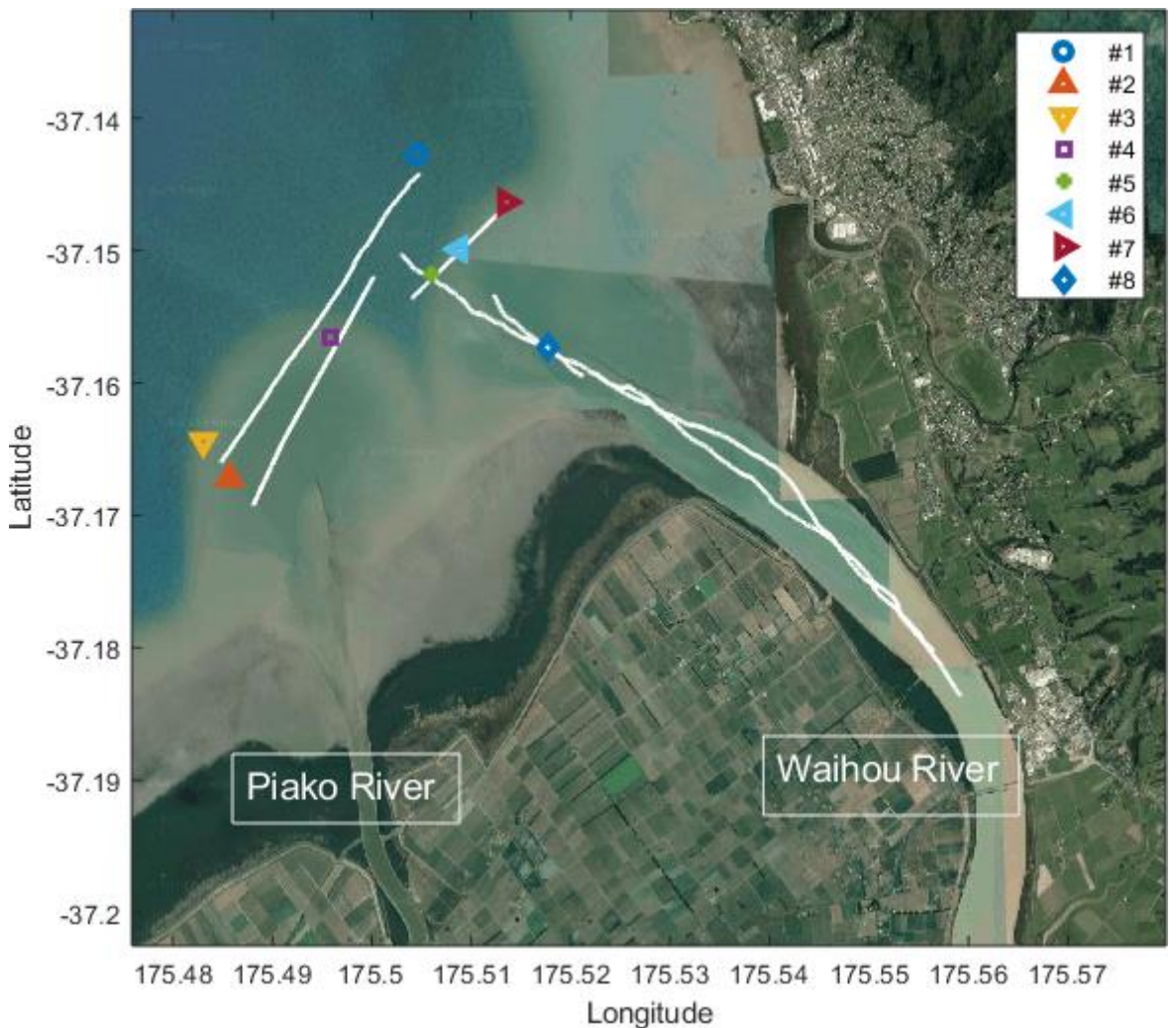


**Figure 4.3.** Survey tracks from the Firth of Thames from the JetYak and locations of CTD casts. Legend indicates the number of CTD cast.

**Figure 4.4.** JetYak being remote controlled during the survey from research vessel through the Waihou River in the Firth of Thames.

## 4.4   Data Processing

### 4.4.1   GPS

GPS positioning was recorded using the two onboard GPSs on the JetYak and RTK GPS on board the research vessel. Log files were downloaded from the onboard JetYak GPS through Mission Planner. The echo-sounder onboard the JetYak stopped logging before all the transects were undertaken therefore, Mission Planner log positioning used in the data processing. However, positions from overlapping times were compared and there was excellent agreement. The speed of the research vessel and JetYak was calculated using x and y position differencing and smoothed with a 25-pt running mean.

### 4.4.2   Conductivity, Temperature, Turbidity

Both the research vessel and JetYak were both set up with conductivity, temperature and turbidity sensors. The temperature measurements from the vessel were much

higher than anticipated, possibly indicating a sensor malfunction. However, the variability over the survey appeared roughly consistent with the RBR measurements. Therefore, we report the results here to provide an indication of the spatial and temporal trends, but note that the absolute values are not likely to be correct. Data of turbidity measurements from the JetYak sometimes gave physically unrealistic values of 0 NTU. These values were possibly affected by air bubbles around the sensor so are neglected in the interpretation of plume behaviour. Given time constraints and the aim of the experiment was to act as a trial survey to show spatial patterns in the vicinity of the plume, a full laboratory calibration of turbidity to obtain suspended sediment concentrations was not undertaken.

### 4.4.3 CTD casts

Conductivity was converted to salinity and then density was calculated using the Thermodynamic Equation Of Seawater - 2010 (TEOS-10) Matlab toolboxes (McDougall & Barker, 2011). The CTD was held at the surface for several minutes to allow the pump to flush the sampling volume with water. Therefore, measurements from near surface depths (generally <0.8m, but <0.86 m for a one profile) were removed. Similarly, we removed measurements from the bottom of the profile with unstable stratifications as there were errors in the data. These errors were likely owing to the sensors having penetrated the muddy seafloor. Only the downcast measurements of salinity, temperature and density were used.

## 4.5 Results

The data collected gave measurements of salinity, temperature and turbidity from the RBR onboard the JetYak and from sensors onboard research vessel. This data was used to map the movement of the river plume with the tide at full ebb to high tide. Depth and elevation measurements were also recorded although, the study was not intended to be nor designed as an accurate bathymetry survey. Another key variable of interest was the temperature recorded inside the engine compartment with a dorade box fitted on, to keep water from reaching the engine.

Four transects were undertaken two along the river and two across the Firth. The JetYak and research vessel traversed parallel approximately 100 metres apart for the across Firth transects with the JetYak completing the transects slower than the

research vessel. For the along river transects the JetYak was piloted near to the vessel.

## 4.5.1 Salinity, Temperature, Turbidity

Figure 4.5 displays the temperature, salinity and turbidity measurements from the first transect along the Waihou River. Measurements from transect one were taken at full ebb and the direction of both vessels was out of the river towards the open estuary. Measurements of salinity from the JetYak and research vessel are very similar, which is unsurprising given the proximity of the vessels. Salinity remains constant at 18 throughout the transect until a sharp increase from 18 to 24 (Figure 4.5 a). However, temperature measurements from the vessel are observed to gradually increase from 14°C to 18°C. Whereas, the JetYak recorded measurements of 12°C to 14°C with no sharp transition (Figure 4.5 b). Turbidity measurements from the JetYak were recorded to be greater than 500 NTU for the full period of the transect suggesting the edge of the plume was not reached in the transect and was further out in the Firth. Turbidity measurements from the research vessel showed no consistent trend; however, there is a region of transition from 200 NTU to 500 NTU (Figure 4.5 c).which occurs at the same position as the sharp transition in salinity.

.
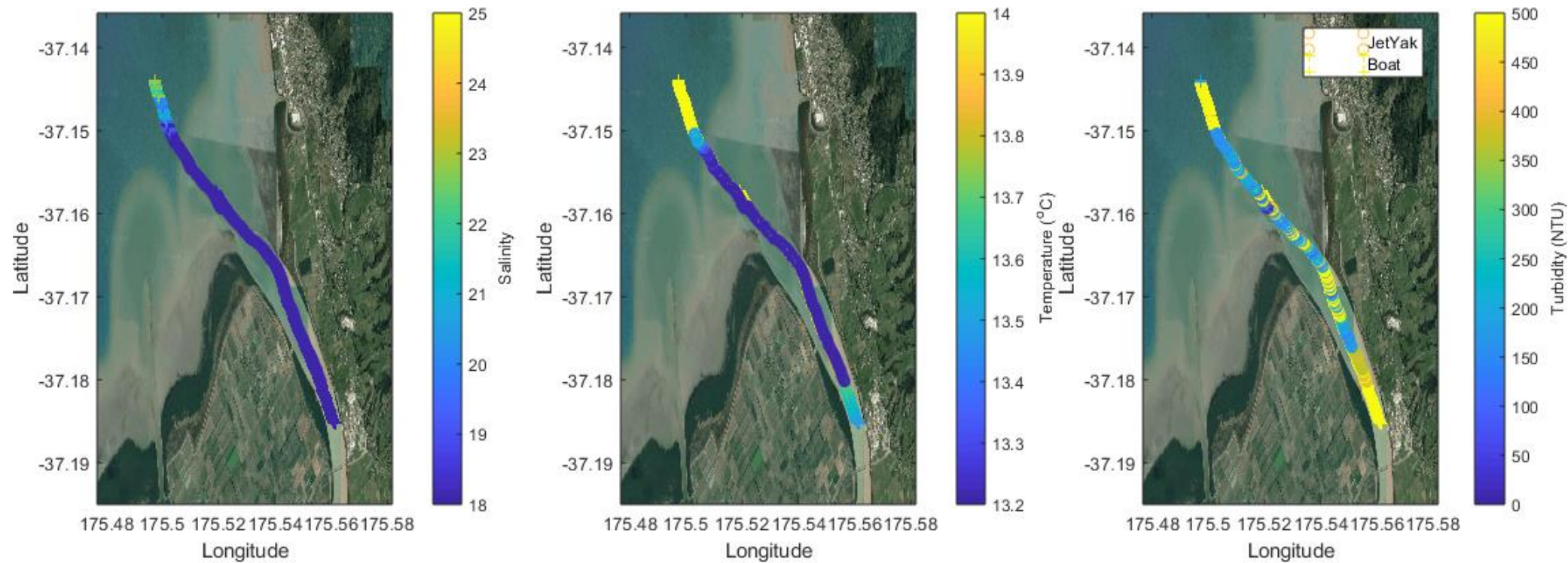
**Figure 4.5.** Transect one along the Waihou River. Comparison of JetYak (represented by o) and research vessel (represented by +) measurements of A) salinity, B) temperature and C) turbidity.

Figure 4.6 displays transect two, the first across-Firth transect. The direction of both vessels was towards the South-West. Both the research vessel and the JetYak displayed a decrease in salinity from 30 to 18 in the centre of the transect depicting a region of freshwater and then gradual increase again to between 26 and 28 for the remainder of the transect (Figure 4.6 a). The change to fresh water in the centre was first observed by the research vessel and then by the JetYak showing the freshwater movement towards the North-West. The JetYak and research vessel again differ in measurements of temperature and turbidity. The research vessel recorded temperatures ranging from 17°C to 19°C, whereas the JetYak recorded temperatures of 14°C throughout the transect with a region of slightly warmer water (14.3°C) in the before the transition in salinity (Figure 4.6 b). Turbidity measurements recorded by the vessel range from 150 NTU to 500 NTU in the centre of the transect (Figure 4.6 c). This positioning of high turbidity also does not completely the region of the recorded low salinity. Turbidity measurements from the JetYak were recorded to be 0 NTU, which is not plausible.
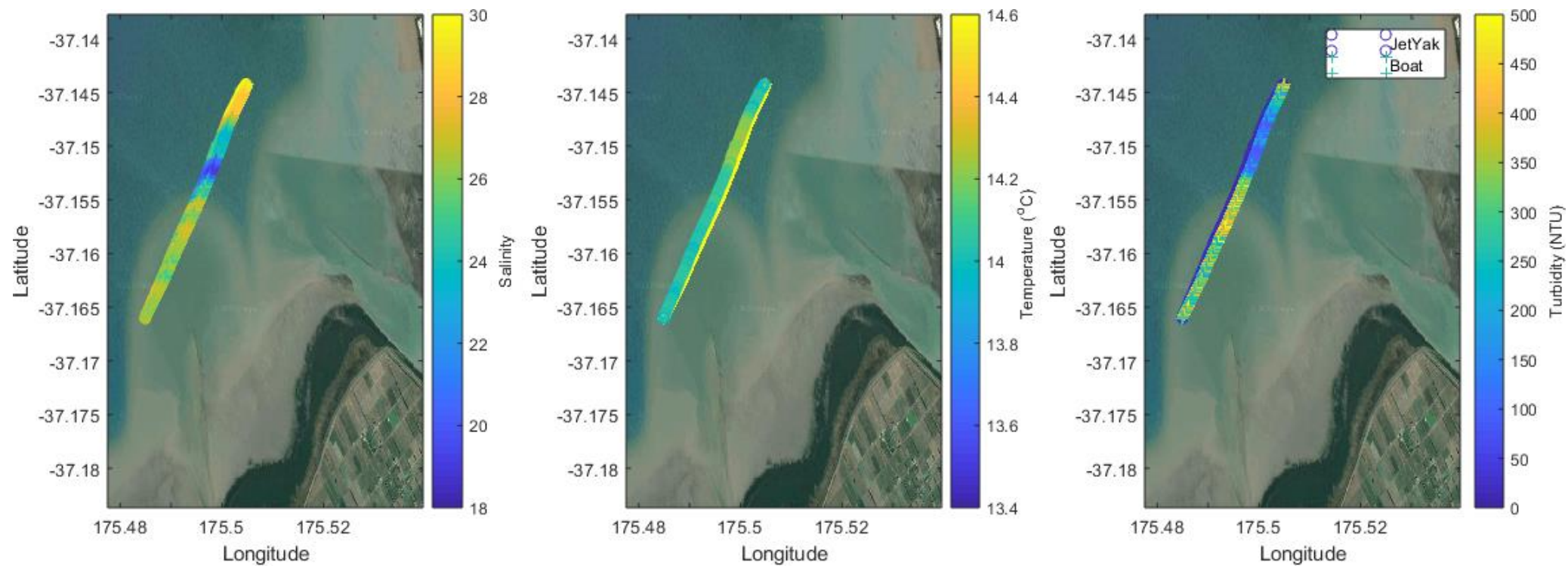
**Figure 4.6.** Transect two across the Firth of Thames. Comparison of the JetYak (represented by o) and research vessel (represented by +) measurements of A) salinity, B) temperature and C) turbidity.

Transect three across the Firth is shown in Figure 4.7. The direction of the vessel and JetYak was opposite to transect two, towards the North-East. The transect from the JetYak was split into two sections as the JetYak stalled during this transect. The salinity figure (Figure 4.7 a) shows a region of reduced salinity of 28 at the at the start of the transect with a transition to a salinity of 30 for the rest of the transect. Both the JetYak and research vessel display this transition at around the same location. The temperatures recorded from the JetYak were around 15$^{\mathrm{o}}$C throughout the transect, whereas, the vessel recorded temperatures of 19$^{\mathrm{o}}$C throughout the transect (Figure 4.7 b). The turbidity measurements between the JetYak and vessel also differ, measurements from the research vessel range between 250 NTU and 500 NTU with the higher turbidity measurements taken at the start of the transect (Figure 4.7 c). Turbidity measurements from the JetYak were again recorded to be 0 NTU.
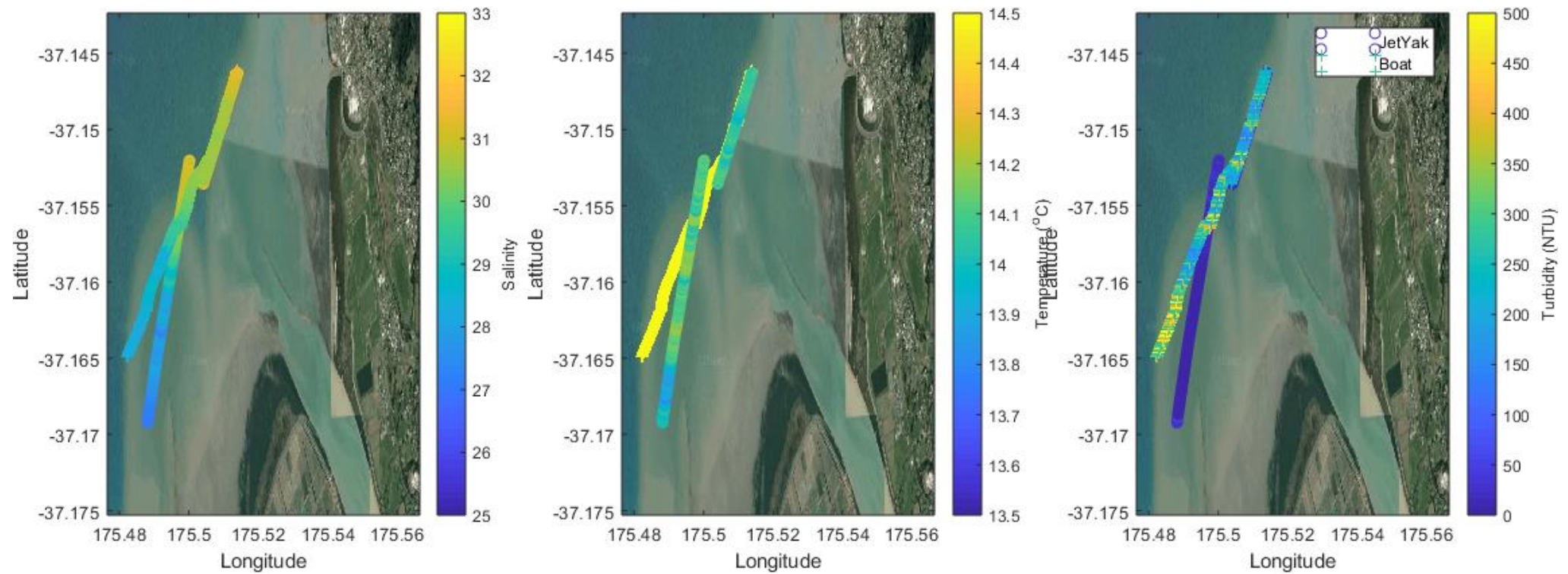
**Figure 4.7.** Transect three across the Firth of Thames. Comparison of the JetYak (represented by o) and research vessel (represented by +) measurements of A) salinity, B) temperature and C) turbidity.

Figure 4.8 shows the returning along-river transect. The direction of the vessels for transect four was southward or heading upstream along the river. Figure 4.8a shows a sharp transition in salinity at the river mouth from 30 to 20. This transition is followed by a gradual increase in salinity to 26. Temperatures recorded by the vessel were 18$^{o}$C and the JetYak recorded temperatures of between 13.5$^{o}$C and 13.6$^{o}$C (Figure 4.8 b). The turbidity figure (Figure 4.8 c) illustrates the vessel and JetYak recorded a transition from 250 NTU to 0 NTU. A sharp decrease in salinity coincides with a sharp decrease in turbidity, followed by an increase in turbidity for the remainder of the transect.
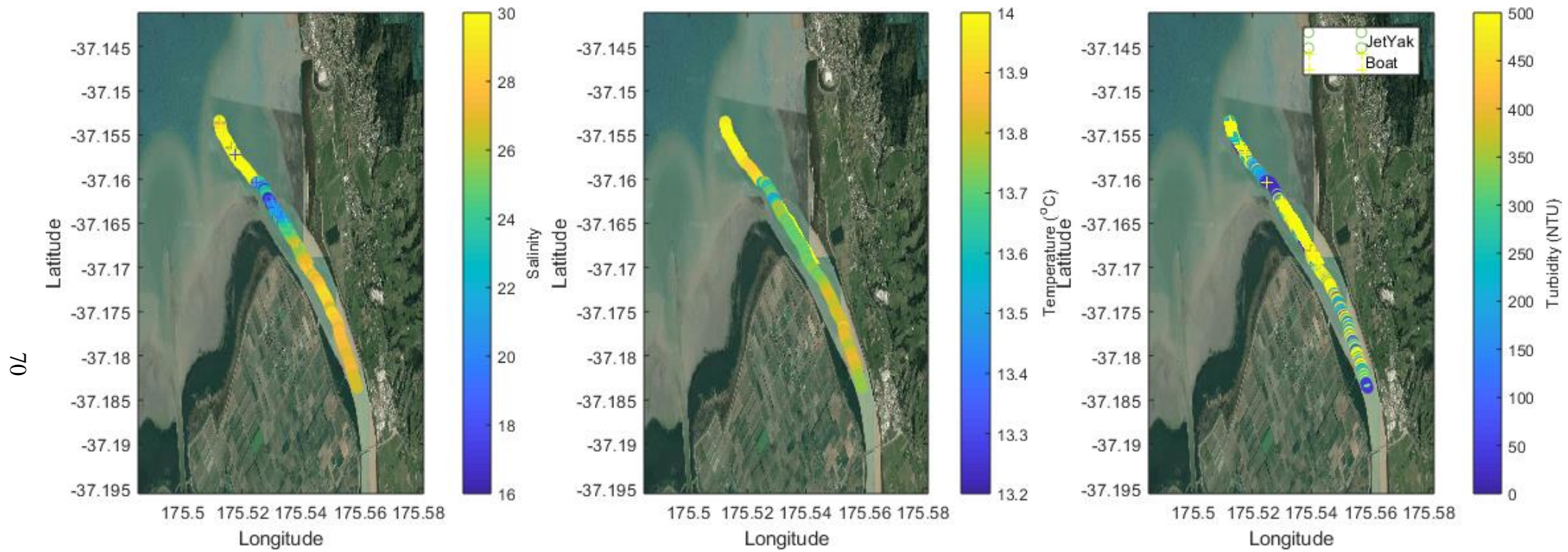
**Figure 4.8.** Transect four along the Waihou River. Comparison of JetYak (represented by o) and research vessel (represented by +) measurements of A) salinity, B) temperature and C) turbidity.

The temperature salinity diagram from the JetYak and research vessel is shown in Figure 4.9. The figure displays an increase in temperature from 12.5°C to 14.5°C with an increase in salinity from 2 to 34 throughout the entire survey recorded by the JetYak. The research vessel recorded temperatures of 13°C to 18.7°C with an increase in salinity from 2 to 31. There is an approximately linear relationship between temperature and salinity for both vessels with the two end points corresponding to warmer salty sea water and fresh cold river water, and the intermediate regions corresponding to mixing zones. The general trend of the increasing temperature with salinity is shown by both vessels, noting that the absolute values of temperature are incorrect from the vessel.
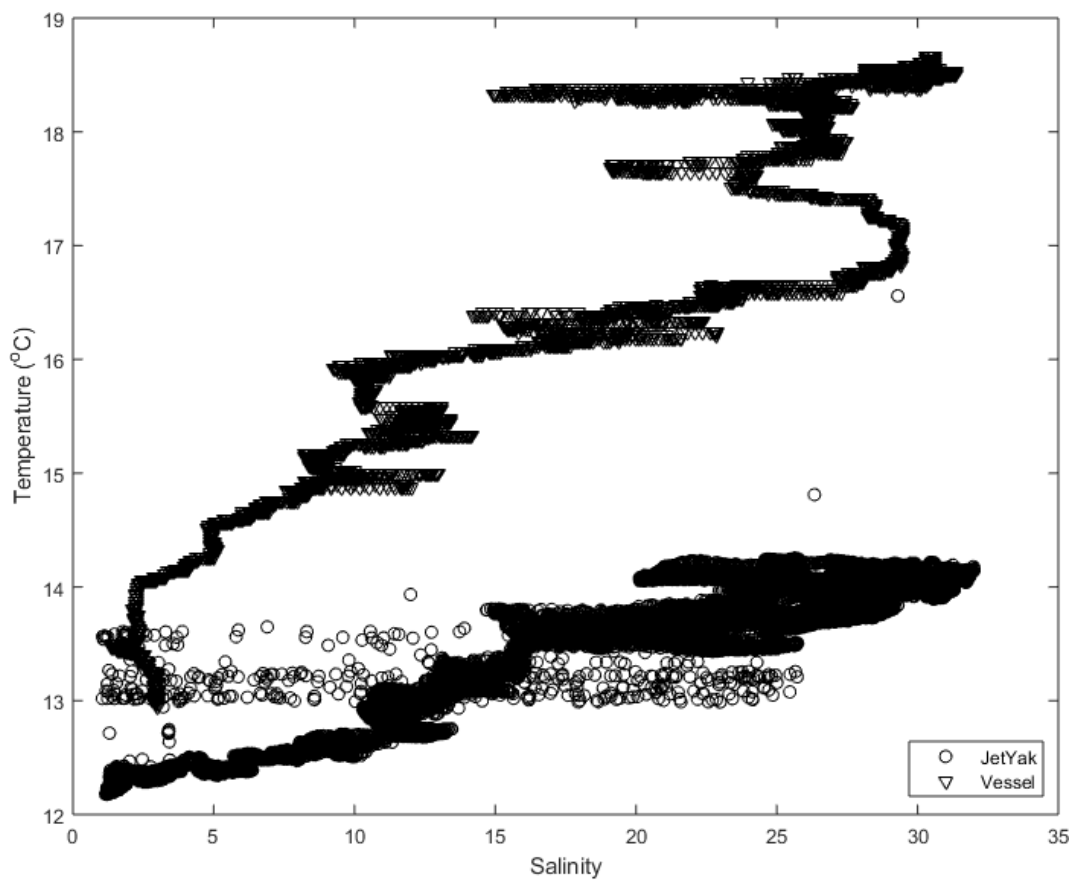


**Figure 4.9.** Temperature and Salinity recorded from the JetYak (represented by o) and vessel (represented by ▽).

## 4.5.2 Depth and Elevation

This survey was not intended to be an accurate bathymetry survey; however, bathymetry data was collected from the echo-sounder onboard the JetYak and elevation and depth were recorded onboard the research vessel from the RTK GPS

and echo-sounder. The elevation data was collected over the tidal cycle, therefore, changed with the tide.

The JetYak recorded depth for the first transect, transect one. Figure 4.10 shows the depth from beneath the echo-sounder throughout the survey ranging from 0 m to 5.6 m. The deepest depths were shown at the edge of the river mouth and decreased moving seaward with regions of deeper water at the start of the transect and shallower within the centre of the transect in the Waihou River. Precise depths cannot be obtained as the JetYak was not equipped with a GPS that recorded vertical elevations at sufficiently high resolution.
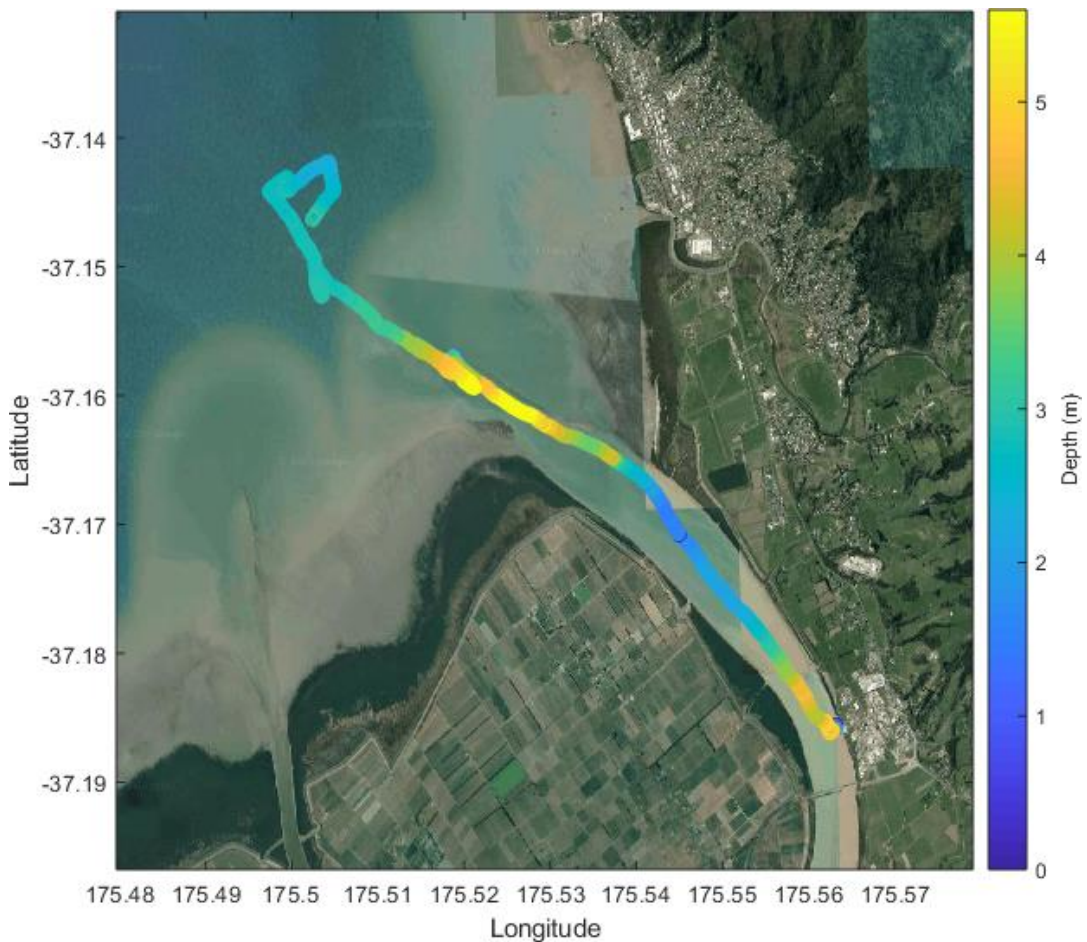


**Figure 4.10.** Raw depth measurements (depth below echosounder transducer) from JetYak transect one.

Elevation data from the vessel was obtained from the depth data from the research vessel, by subtracting the depth data obtained by the echo-sounder, and the vertical distance from the echo-sounder transducer to the GPS (2.31 m) from the elevation data acquired from the RTK GPS. The elevation data in Figure 4.11. The elevation ranges from 0 m to -7 m in reference to the New Zealand Vertical Datum (2016).

The Land Information New Zealand (LINZ) elevation chart is shown in Figure 4.12. The elevation and depth data agree with the LINZ data updated on the 5th of July 2019. Both vessels show the trends in decrease in elevation (increase in depth) within the Waihou River, depicting the deeper channel at the river mouth, followed by an increase in elevation (decrease in depth) within the estuary.
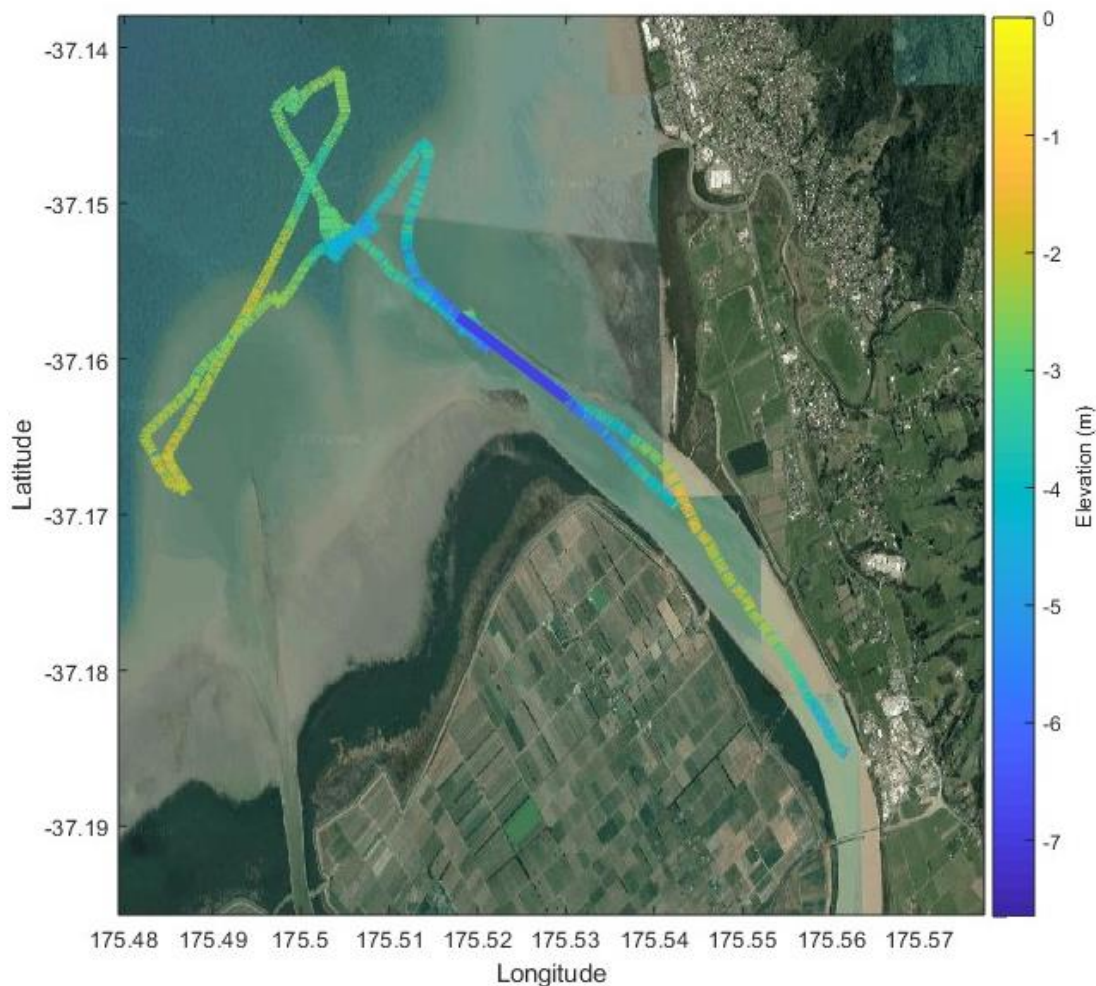


**Figure 4.11.** Elevation data from the research vessel. (Datum: New Zealand Vertical Datum 2016).

**Figure 4.12**. Land Information New Zealand (LINZ) elevation chart for the Firth of Thames (Land Information New Zealand, 2019).

### 4.5.3 CTD casts

CTD casts were taken throughout the experiment in perceived areas of interest. The locations of each of these CTD casts are shown in Figure 4.3. The CTD profiles are shown in Figure 4.13. The salinity profiles are all depth uniform except for one cast, cast 8, which was taken in transect 4 and was noted that it could be inside the plume. Similarly, the temperature profiles are all depth uniform except cast number 5 and 8. The plume may not have been captured by each of the CTD casts, as the plume sits on the water surface as more buoyant water than the estuarine water. However, cast 8 shows some indication of the fresh water plume at the surface.
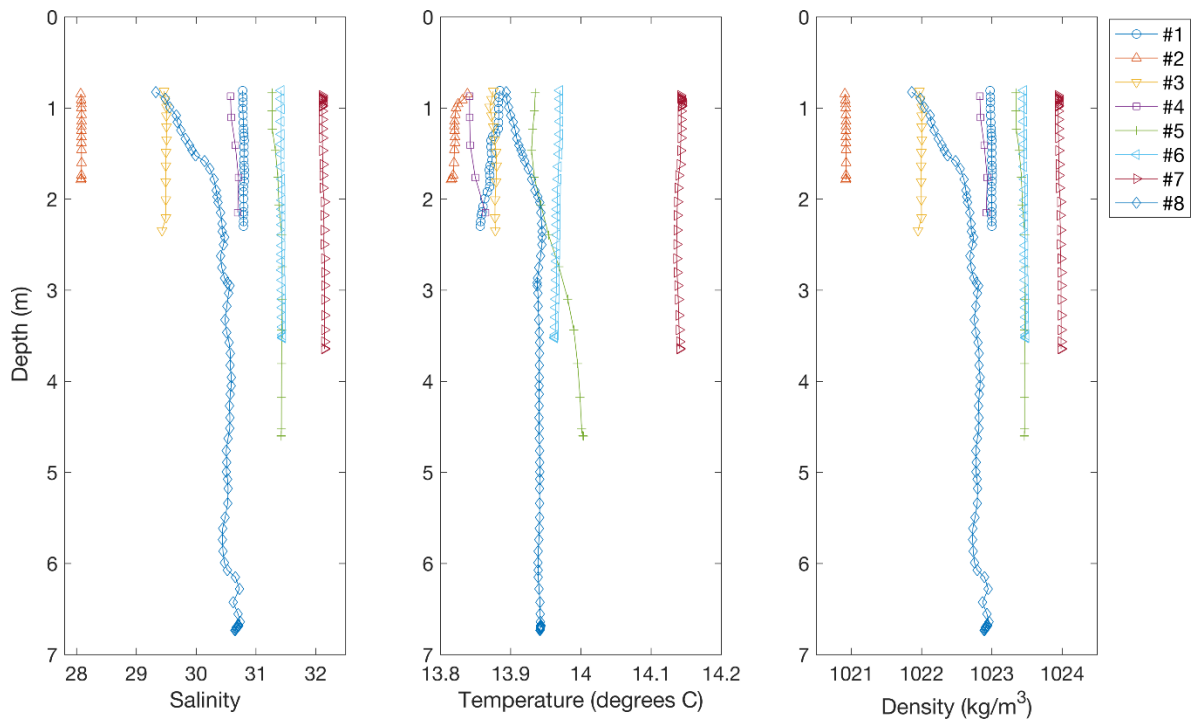
**Figure 4.13.** CTD casts throughout the survey. Legend indicates the number of CTD cast correlating with the location shown in Figure 4.3.

The maximum differences in salinity, temperature, density and depth for each of the CTD casts over each profile were small as shown in Table 4.1. Differences in temperature were less than 1°C, which explains the small differences in temperature recorded by the JetYak. The salinity differences for all profiles were less than 1 except for the last profile which showed a difference of 1.4 indicating there may have been fresh water at the top of the water column indicating the plume that had been mixed with estuarine water. The depth differences show the distance from the top to the bottom of CTD profile which were all very small owing to the shallow waters in much of the Firth as shown in the depth in elevation data (Figure 4.10 & Figure 4.11). The largest depth difference was also cast 8 with the depth of the profile being 5.9080 m.

**Table 4.1.** Maximum difference in salinity, temperature, density and depth for each of the CTD casts

|  | Cast 1 | Cast 2 | Cast 3 | Cast 4 | Cast 5 | Cast 6 | Cast 7 | Cast 8 |
|---|---|---|---|---|---|---|---|---|
| **Salinity** | 0.0309 | 0.0161 | 0.0757 | 0.1333 | 0.1705 | 0.0266 | 0.0433 | 1.4136 |
| **Temperature (°C)** | 0.0278 | 0.0235 | 0.0098 | 0.0226 | 0.0739 | 0.0075 | 0.0071 | 0.0513 |
| **Density (Kgm³)** | 0.0307 | 0.0183 | 0.0538 | 0.1047 | 0.1316 | 0.0335 | 0.0436 | 1.1007 |
| **Depth (m)** | 1.4870 | 0.9450 | 1.5310 | 1.2780 | 3.7700 | 2.7160 | 2.7850 | 5.9080 |

### 4.5.4   Temperatures inside the Engine Compartment

The temperature inside the engine compartment was recorded using a HOBO temperature logger. In order to survey in adverse weather conditions, a dorade box is required to keep out water and salt spray. A dorade was designed and tested during the experiment to investigate if the addition of the dorade over the engine compartment significantly increased engine temperatures. In previous experiments without the dorade, the JetYak's engine got very hot when surveying. Therefore, with the addition of the dorade box, it was examined whether the heat was further trapped inside this compartment.

During the experiment, the times when the dorade box was attached and removed were recorded. Figure 4.14 reveals the temperature inside the engine compartment during the survey. At 12.26 pm the dorade box was taken off, this resulted in a dramatic decrease from almost 80ºC to 30ºC inside the engine compartment. The JetYak stalled as a result of water getting into the engine compartment so was therefore, positioned on again at 12.48 pm and resulted in the temperature rising again to approximately 80ºC. A gradual increase in temperature is shown with the start of transect two line across the Firth. At 2.26 pm the JetYak reached the end of the survey line therefore, the motor turned off and cooled down. Autopilot was again switched on at 2.49 pm and resulted in a gradual increase in temperature. At 3.25 pm the JetYak stalled during the survey and the temperature dropped to around 65ºC. The JetYak was then turned back on and resulted in a gradual increase to the highest temperature inside the engine compartment of 85ºC. At 5.01 pm the dorade box was again taken off and the JetYak was remote controlled slowly back to shore which resulted in a sharp decrease in temperature until the JetYak was turned off at 5.43 pm and was allowed to cool down completely.
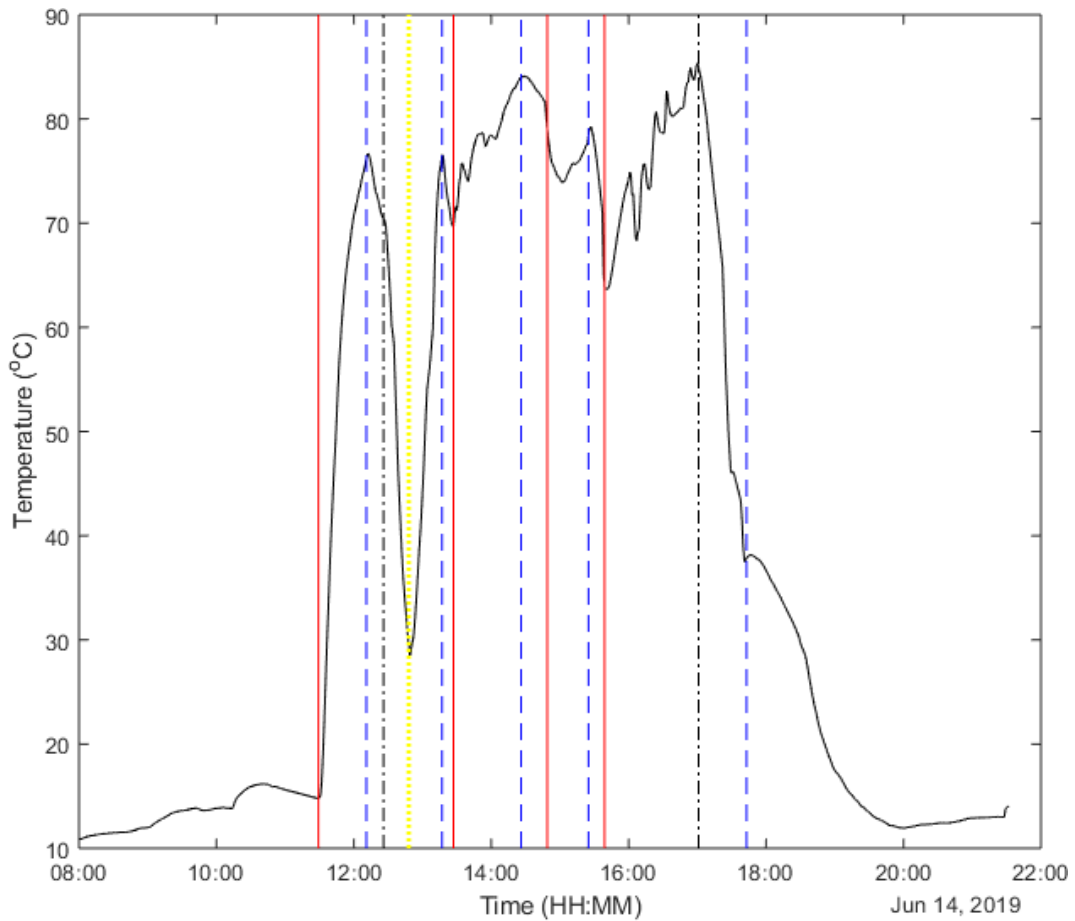
**Figure 4.14.** Temperature recorded throughout the Firth of Thames experiment inside the engine compartment. Dashed lines indicate times of interest. Red line JetYak turned on. Blue line JetYak turned off. Black line dorade taken off. Yellow line dorade put on.

## 4.6 Discussion

The measurements of salinity, temperature and turbidity within and adjacent to the Waihou River plume were variable throughout the tidal cycle. From the measurements, there was little indication of the position of the Piako River plume. Just after low tide, the main plume entered the Firth and appeared jet-like, propagating in a relatively straight direction, similar to the orientation of the river channel at the mouth (roughly north-westerly). The width of the plume was approximately 1000 metres (similar to the width of the river mouth of 850 metres) indicating that the plume was likely inertia-dominated and buoyancy-driven spreading was minimal. However, the plume was forced towards the west and then towards the mangroves at the southern end of the Firth of Thames by the incoming tide (in the later flood stages of the tidal cycle).

### 4.6.1 Salinity

Salinity measurements are deemed to be the most important plume tracer (Warrick *et al.*, 2007). This statement was shown to be true as salinity recorded throughout the survey was crucial for mapping the plume as measurements from both the JetYak and vessel agreed well. The first transect along the Waihou River (Figure 4.5 a) displayed that the plume was forced out from the Waihou River mouth towards the North of the Firth of Thames, with no indication of salty water until the end of the transect, perhaps marking the edge of the plume. The first transect along the river occurred at full ebb tide when the plume was perceived to be at its maximum. The edge of the plume is shown by the sharp increase in salinity. The transition between the salty estuarine water and fresh plume water is shown by the change in salinity at the edge of the plume.

The second transect across the Firth Transect two across the Firth shows a distinct region of freshwater within the salty estuarine water. Figure 4.6a indicates that the plume is forced to the North-West as depicted by the decrease in salinity across the transect recorded by the JetYak and the vessel.

Transect three (Figure 4.7 a) across the firth in the opposing direction confirms some mixing has occurred as the plume is forced towards the mangroves with the incoming tide. The salinity measurements from both the vessel and JetYak show that the water is predominantly seawater (salinities of around 30). However, less salty water is recorded at the southern end of the transect. Although the measurements of salinity from the JetYak and research vessel appear to diverge (Figure 4.7a), as the vessels cross the deeper channel, this small difference (28 relative to 32) are consistent as the JetYak crossed this section approximately 17 minutes later than the manned vessel, during which time the tide was strongly incoming. The plume appeared to have been forced towards South-West as indicated by the region of less salty water at the beginning of the transect.

Figure 4.8a shows evidence of a transition between the salty estuarine water and suggests the plume is pushed into the mangroves. The edge of the plume is depicted by the salinity gradient near to the river mouth and suggests the plume is pushed towards the east with the incoming tide and infills the intertidal region with the incoming tide. Estuarine water is shown to force the plume into the mangroves at

the southern end. Our visual observations from the boat noted multiple foam and scum lines on the surface at this time. These lines are typically associated with surface convergences, downwelling and fronts between two water masses (Mullarney & Henderson, 2011). CTD cast 8 was taken at this point in transect 4 and shows there may have been plume water at the surface as shown by the decreased salinity at 1 m water depth followed by an increase in salinity at the surface. This difference in salinity was very small but, may have been caused by mixing of the estuarine water and fresh river water giving some indication of the plume at the surface.

### 4.6.2 Temperature

The temperature profiles attained from the vessel and JetYak contrast significantly. The JetYak recorded temperatures were much less than those attained by the vessel. The temperature measurements from the vessel are shown to gradually increase throughout the survey from 14$^\circ$C to 19$^\circ$C. It is highly unlikely that water temperatures on this day were so high, given the survey was completed in the middle of Winter. We therefore conclude, that the absolute temperature values measurements recorded by the vessel are incorrect. The trend however, of increasing in temperature travelling out of the river and then decreasing travelling back into the river is expected. The CTD casts show the temperatures were depth uniform therefore, it was difficult to distinguish the plume water and fresh water from the temperature alone.

Transect one along the Waihou River (Figure 4.5 b) displayed an increase in temperature towards the end of the transect as a result of crossing the plume boundary into estuarine waters. This transition location is consistent with change in salinity from 18 to 22. Transect two in the across-Firth direction (Figure 4.6 b) shows warmer temperatures of 14.2$^\circ$C in the centre of the transect just before the change in salinity indicating a region of estuarine water to a decrease in temperature to 14$^\circ$C. This temperature change is minimal and does not clearly illustrate the plumes movement. The opposing transect, transect three, displays a region of cooler water at the start of the transect and temperatures increasing by 0.2$^\circ$C, but, there is no clear indication of the plume or estuarine waters (Figure 4.7 b). Temperatures recorded in transect four (Figure 4.8 b) give no real indication of the movement of

the plume. Changes in temperature were very small (in the order of 0.2ºC) so therefore, could not be used to determine whether the water was the plume or not. This result may have been due to the weather conditions on the day and the season of the experiment not showing a clear indication of change in temperature to differentiate river water and estuarine water. Typical temperatures in the Waihou River have been shown to have winter minimums of 12.7°C and summer maximums of 15.7°C (Cox & Rutherford, 2000) therefore, there is little contrast between the two water masses.

### 4.6.3 Turbidity

The turbidity measurements collected were interrupted by the speed of the vessel and JetYak and therefore, measurements logged were highly variable throughout the survey. For transect one (Figure 4.5 c), the JetYak measured high turbidity throughout the entire transect with no transition to estuarine water as recorded by the salinity and temperature. The Waihou river contains high suspended sediment loads, therefore, these recorded high turbidity measurements are possible. Sedimentation rates within the Firth of Thames have increased since the 1950's as a result of deforestation and change in land use (Swales *et al.*, 2007) increasing sediment loads in the Waihou River resulting in the high turbidity measurements recorded. These high turbidity measurements may have been due to the speed the vessel was travelling throughout the transect, as it was piloted using the remote controller and therefore, was not set at a constant waypoint speed. The resulting large turbidity measurements may have due to air bubbles around the sensor measuring the high turbidity. The vessel recorded a decrease in turbidity from the river mouth into the estuary and no indication of a transition to less turbid estuarine water. Figure 4.6 c depicts the increase in turbidity towards the centre of the transect recorded by the vessel, which matches the salinity measurements of the plume getting forced towards the West. The turbidity measurements for transect three (Figure 4.7 c) shows the plume at the southern end of the Firth, and less turbid water, representing the estuarine water forcing the plume towards the mangroves and intertidal area. The JetYak measured turbidity measurements of 0 NTU for transects two and three indicating some error in the data collected, as this is implausible. Transect four (Figure 4.8 c). displays a strong turbidity gradient that corresponds

with the salinity gradient, illustrating the same feature of the plume to be forced towards the East into the mangroves with the incoming tide.

It was concluded that the speed the JetYak was travelling affected the turbidity measurements. Air bubbles may have been created when the JetYak was travelling at high speeds causing large turbidity measurements to be recorded (Burlingame *et al.*, 1998). In addition, slow JetYak speeds caused the turbidity sensor to not be fully immersed in the water, recording turbidity measurements of 0 NTU. Turbidity measurements of 0 NTU or 500 NTU throughout entire transects are deemed unlikely, therefore, it is likely the speeds affected the results. However, for the final transect (Figure 4.8 c) the speed was neither too fast, nor too slow and some accurate measurements of turbidity were recorded by the JetYak.

### 4.6.4  Plume Dynamics

The overall movement of the plume as it debouches into the Firth of Thames is illustrated in Figure 4.15. Figure 4.15 shows the direction of the plume with the outgoing tide to the direction of the plume with the incoming tide. The edge of the plume is marked by a sharp marked sharp frontal region where density differences are large (Garvine, 1982).The combination of the temperature and salinity defines the density of the water. Less dense water will such as fresh water from rivers will flow above more dense salty water such as the estuarine water. The river water spreads out over the more dense sea water creating a stratified system, this movement is known as estuarine circulation (Schumann *et al.*, 1999). The direction of plume movement is straight out from the Waihou River at low tide and towards the North of the Firth. High velocities of water out from the river mouth causes fast initial advection of the plume. This advection causes the plume to reach far into North of the estuary with little lateral movement as a result of the buoyancy of the fresh water in comparison to the salty estuarine water (Warrick *et al.*, 2007). With the change of the tide, initial velocities forcing the plume out of the river mouth are slowed and the plume is forced out towards the North-West. As the tide progressed further, the plume is forced towards the South-West. At high tide, the plume water was shown to infill the intertidal region inhabited by mangroves at the southern end of the Firth. The input of fresh water into the estuary creates horizontal gradients as a result of density differences and drives circulation within the estuary. The more

dense sea water flows towards the land at the bottom with the incoming tide as the less dense river plume moves seaward at the surface (Simpson *et al.*, 1990). The results show the plume is highly variable with clear evidence of mixing and patches of the plume. It is also possible that the plume is steered by bathymetric features; however, a more comprehensive study would be required to identify if any bathymetric steering was occurring in the Waihou plume.

Wind patterns are often the dominant control on the dispersal of river plumes (Warrick *et al.*, 2007). Wind patterns throughout the experiment may have caused the Waihou River plume to be forced towards the Western side of the Firth and then further towards the southern end. Other factors that can influence the plume advection as it emerges into the estuary include river inertia, buoyancy-related currents, tidal currents and non-wind generated subtidal currents (Warrick *et al.*, 2007). These processes can also cause mixing of the plume water and estuarine water. There are large density differences at the edge of the plume as shown by the sharp decrease in salinity. This region is where turbulent exchange occurs which can result in the generation of strong currents which drives mixing of the fresh water and estuarine water (Garvine, 1982).

The data collected showed no evidence of the Piako River plume or plume interaction. This may have been due to the time the second plume was perceived to be crossed it may have already been forced towards the West with the incoming tide comparable to the Waihou River plume. In order to map the interaction between the two-plume interface in future studies, transects should be longer and closer to the mangrove forest fringe and across to the Western side of the Firth.

**Figure 4.15.** Movement of the Waihou River plume from low tide to high tide on the 14th June 2019 (Direction of plume indicated by black arrow). A) Plume direction at low tide (10.35 am). B) Plume direction between tides (12.30 pm). C) Plume direction close to low tide (2.30 pm). D) Plume direction at low tide (4.52 pm). (Images: Google Earth).

We propose the Waihou River plume was forced out of the river and into the western side of the estuary and forced into the mangroves with the incoming tide. Sediment and pollution from the Waihou are then being trapped within the intertidal area and in the mangrove fringe as velocities decrease. This pattern of sediment dispersal is consistent sedimentation patterns in the region creating the muddy intertidal region in the southern end of the Firth of Thames and a slightly raised elevation just inside the forest fringe (Horstman *et al.*, 2018). Recent research suggests the change in land use since the 1950's, has increased the sedimentation of the Waihou River and therefore, increased deposition in the Firth of Thames creating the muddy banks inhabited by mangroves (Swales *et al.*, 2015). The deposited sediment from the plume appears to have created a shallow intertidal slope of 0.03° as a result of the human-induced increased sedimentation (Lovelock *et al.*, 2010).

### 4.6.5 Dorade Evaluation

The use of the dorade box significantly increased temperatures inside the engine compartment (Figure 4.14). The dorade box was revealed to considerably increase temperatures inside the engine compartment and was believed to be the cause of the

JetYak to stall during one of the across-Firth transects. However, without the addition of the dorade, water got into the engine and also caused the JetYak to stall. The addition of the dorade box significantly increased temperatures and removal of the dorade box decreased temperatures inside the engine compartment. Overheating of the engine may cause substantial damage. In order to reduce the damage to the engine, increased air inlets for fresh air and outlets for exhausting air outside of the engine compartment are required (Abdeljawad, 2006). Therefore, for future use of the JetYak, the design of the dorade was modified to increase the number of vents to allow cool air to flow through the engine and the ability of warm air to escape through the vents. The additional vents were positioned facing the bow for increased air flow when the JetYak is completing surveys. Thus, in future, temperatures inside the engine compartment should be cooler, even with the dorade fitted. If further cooling is required, a pump to enhance air circulation through the vents should be considered.

### 4.6.6  The JetYak

The JetYak worked well as the research vessels companion to span large areas to collect data. The river plume covers a large area, therefore, the JetYak worked well in addition to the research vessel to collect data from large spatial scales as well as temporal scales as the plume changes throughout the tidal cycle. Such an approach increases efficiency and keep costs low. Therefore, due to the cost-effective nature of the JetYak (Moulton *et al.*, 2018) it can be used to increase productivity with sensors and equipment on both vessels to collect data. The approach of using the vessel and JetYak also meant the vessel was able to pick up the JetYak in case of a malfunction such as when the JetYak stalled in transect three.

For future studies of this nature, the JetYak and research vessel should survey a further distance of greater than 100 metres, to capture a range of data over larger spatial scales to further understand the extent of the plume and how it varies throughout a tidal cycle. This research was the first time the JetYak was launched into the semi-enclosed estuary without sheltering from large winds, waves and currents. Therefore, the JetYak was kept at a close distance to the vessel for safety measures. However, with the success of the research and the JetYak being operated in this region, in future the JetYak can be sent much further away from the vessel.

The addition of cameras on board the JetYak could also allow the JetYak to further even further away from the vessel to capture the extent of the plume over the tidal cycle.

## 4.7   Conclusion

The primary aim of this experiment was to assess the ability of the JetYak to map the movement of the Waihou River plume over a tidal cycle. The plume was revealed to be forced to the West with the incoming tide and then forced into the intertidal region inhabited by mangroves at high tide. The JetYak served as a handy tool alongside the research vessel to increase surveying speeds and increase spatial resolution of the movement of the plume throughout the tidal cycle. In future surveys of the plume, it would be beneficial to increase the distance between vessels for further spatial resolution and show the interaction between the two-plume interface. River plumes are important to monitor to show amounts of terrestrial pollution and nutrients. A good understanding of the processes that occur in river plumes are required to inform water quality and ecological implications (Warrick *et al.*, 2007).

# Chapter 5

# Conclusions

## 5.1  Research Conclusions

Here, we summarise the main conclusions from this thesis and provide suggestions for future research using the JetYak.

### 5.1.1  Hydrodynamics over Seagrass Beds

The research in the Tauranga estuary examining the hydrodynamics over seagrass beds revealed minor problems with the JetYak for surveying. While we took an opportunity to test use of a specific ADCP with the JetYak, the setup of the instrument was not appropriate for this usage and this meant flows were not resolved as the boat motion was not removed from the data. Fast surveying speeds also meant the flows were not resolved and survey speeds were required to be slower to accurately resolve the flows (Perry & Rudnick, 2003). Moreover, the vertical bin size was too large to resolve changes in the vertical; to address the specific research question outlined in this experiment would require use of an ADCP set to operate in high-resolution mode (such as a Nortek pulse-coherent Aquadopp (i.e. Mullarney and Henderson (2013)) or indeed the Nortek Signature with the high-resolution firmware implemented.

The large survey speeds were a result of poor steering and throttle parameters set in Mission Planner, noting that this initial experiment was undertaken before we had completed the optimisation of steering parameters. The JetYak was a reliable tool however, for mapping bathymetry and collecting data in very shallow waters, in which a large majority of manned vessels would not be able to operate (when considering vessel draft and instrument mounting constraints). The JetYak allowed for easy repetition of transects for accurate data collection when operating the autonomous feature (Kimball *et al.*, 2014). In future studies, the JetYak's steering and throttle parameters will be those outlined in Chapter 2 and use of purpose-built boat integrated boat-mounted systems for achieving better results.

### 5.1.2 River Plume Monitoring

For the research in the Firth of Thames, we conclude that the JetYak worked well as a companion to the larger manned vessel. While the JetYak can repeatably conduct pre-programmed surveys, as it requires no interaction, the manned boat can conduct interactive operations such as CTD casts and secchi disk casts and can be used to launch and recover the JetYak. The JetYak could also be controlled manually from the vessel and watched on by crew members (Kimball *et al.*, 2014). The vessel could also be used to collect the JetYak if it malfunctioned. The JetYak allowed for increased data collection over spatial and temporal scales without significantly increasing costs of surveying and proving to be time-efficient. The JetYak was used to show the movement of the Waihou River plume throughout the tidal cycle. The plume was revealed to be forced towards the West with the incoming tide and then towards the southern end mangrove forest at high tide.

## 5.2 JetYak Capabilities

We tested use of the JetYak in two different coastal environments. The JetYak could navigate through very shallow waterways to measure flows in seagrass canopies in the Tauranga estuary and was capable of collecting conductivity, temperature and turbidity measurements from the river plume in deeper regions such as in the Firth of Thames.

The JetYak was tested to answer these questions:
1. How can the JetYak be used for future coastal research and used at maximum potential?
2. What are the limitations surrounding use of the JetYak and the data it can collect?

The JetYak offers long-surveying times, cost and energy efficiency, ease of operation after training and has capabilities of navigating extended marine areas including both shallow and deep waters (Weeks *et al.*, 2011). However, both experiments showed the speed of surveying was very important for collecting reliable data. In comparison to human piloted vessels, the JetYak is better at executing straight survey track lines and does not have constraints of human fatigue (Kimball *et al.*, 2014). Therefore, durations of surveys can increase, for a greater

data collection for reliable results. The automated feature allows increased accuracy and repeatability of transects for optimal data collection and repetition of the planned route continuously to remove errors in the data (Weeks *et al.*, 2011). In general, small manned vessels have more difficulties in driving a straight line between waypoints. Errors can be from up to 20 metres to 50 metres in strong cross currents, which is an order of magnitude worse than the JetYak (Kimball *et al.*, 2014). The JetYak also proved to be easier launching, cleaning and set-up than the research vessel, Taitimu, used in the Firth of Thames experiment. Radio communications allow the JetYak to be controlled up to 20 km away therefore, with the attachment of a small camera or other video equipment, the JetYak could be controlled far away to remote survey locations or far from the vessel to increase the resolution of spatial scales. In comparison to Jet skis used for research, the JetYak is much larger and has more space for scientific instruments for a variety of data collection (Kimball *et al.*, 2014). With an operating height of under two metres, it is also possible for the JetYak to survey beneath hazardous areas such as bridges, tunnels, caves and trees (Kimball *et al.*, 2014). Significant advances in the JetYak can allow for data collection of any kind with the right instruments installed (Perry & Rudnick, 2003). The sea chest also allows scientific instruments to be easily immersed in the water.

There are nonetheless limitations surrounding the data the JetYak can collect. Some constraints include the JetYak only being able to operate at the surface and the air-cooled engine, which must not get wet. Therefore, a dorade box that prevents rain, spray and sea wash from getting in, was created to increase usability of the JetYak. The dorade box design also dramatically increased temperatures inside the engine compartment which may have caused the motor to overheat and consequently, stall during one of the transects in the Firth of Thames. A new dorade was therefore designed with extra cooling vents facing the bow of the JetYak. The new dorade design should allow for sufficient air through the motor to cool the engine so the motor does not overheat and shut down during surveys.

The JetYak can also not perform in large breaking waves (Kimball *et al.*, 2014). The JetYak is less tested in marine environments and can be more complex to control and set-up without appropriate training. Many problems with the JetYak were solved in the first couple of months of testing; however, issues can still arise

that need to be corrected before it can be put into widespread use (Kimball *et al.*, 2014). The open design of the JetYak allows for addition of parts and special equipment, to increase efficiency and surveying capabilities such as cameras or winches. The JetYak does not allow interactive activities to be performed and is not able to sense danger or navigate around moving vessels on its own without supervision. However, there is the possibility to upgrade the JetYak with sensors, therefore, could be possible in future upgrades. Depending on instrumentation used, the JetYak is less suited to waters deeper than 10 metres as it produces lower-resolution surveys of the seafloor as the depth of the water increases (Kimball *et al.*, 2014). Autonomous vessels also need small, low power sensors to measure variables such as temperature, velocity, salinity and turbidity as measured in this research. The JetYak, and instruments on board the JetYak, must be set-up correctly to acquire the desired output. Researchers must be trained in operating procedures as well as knowledge of data processing skills for quasi-Lagrangian methods of attaining field data. The JetYak is however, open design, therefore it can be developed further and scientific instruments added to aid in scientific research dependant on motivations (Kimball *et al.*, 2014).

## 5.3 Further Research

The JetYak has great potential for further coastal monitoring and research. The ability to attain high quality monitoring data, which could be used in development of coastal management strategies means. The JetYak could be used to benefit the wider community as well as the scientific community (Lovett *et al.*, 2007). The capabilities of the JetYak for future studies could be provide more ability to study areas that too dangerous or shallow for scientists to take traditional vessels through. The JetYak can also be used to build standardised long-term data sets to assess environmental conditions to show the response to human impacts (Ellis *et al.*, 2012).

The JetYak's ability to repeat pre-programmed transects allows for repeatibilty for reliable results for large spatial scale mapping in the order of tens of kilometres if required (Nicholson *et al.*, 2018). There is also the possibility to repeat transects for data collection in the scale of months to years. There could also be the possibility for biologically controlled variables such as fluoresce and transmission for a greater understanding of ecosystem health (Perry & Rudnick, 2003). Overcoming these

challenges requires the development and implementation of new sensing approaches. There is an increasing need for reliability of data and endurance at lower cost which the JetYak provides (Perry & Rudnick, 2003). The JetYak could also be operated to further explore biological, chemical and ecosystem properties for a more detailed view of the ocean and a greater understanding of the processes and dynamics relating to ecological health and response to anthropogenic impacts (Perry & Rudnick, 2003).

With the optimal steering and throttle parameters, the JetYak can be used to benefit further studies of marine and fresh water in New Zealand. Research could include the effects on the sediment transport due to seagrass patches in the Tauranga Harbour and further mapping of the Waihou River Plume and Piako River plume in the Firth of Thames to validate idealised models and monitoring of sediment loads and ecosystem health as a result of anthropogenic impacts.

The JetYak can be used to assist in further research examining the effect of fragmentation of seagrass patches in the Tauranga estuary. Using the optimum JetYak parameters and vessel-mounted ADCPs, the JetYak could be used to show the changes in near bed velocities due to seagrass. Velocities could be attained to examine whether seagrass meadows affect flow velocities and subsequently, sedimentation patterns caused by seagrass. This information could be used to show the impacts of declining seagrass rates and fragmentation of seagrass meadows on near-bed hydrodynamics and sediment transport. The JetYak could also be used to resolve current velocity profiles around seagrass patches (Weeks *et al.*, 2011). With this data, validation of numerical modelling can occur to inspect the use of seagrass as natural coastal defence strategies (Ondiviela *et al.*, 2014).

There is also the ability for the JetYak to be used in further surveying in the Firth of Thames. The JetYak could be operated to repeat surveys conducted in the Firth of Thames over a tidal cycle to resolve tidal effects of the river plume and show the sedimentation dispersal patterns. The JetYak could be used to illustrate the changes of pollution for land run off and the effect of wind and wave conditions and forcing of the plume. Velocity and composition profiles could be used to analyse the plume dynamics. Numerical models need basic inputs to calibrate the data to give accurate results (Schumann *et al.*, 1999).The JetYak's ability to accurately repeat transects

allows surveys to be repeated multiple times for data collection, to survey larger spatial and temporal scales to show the plume dynamics. The JetYak could be used to show the effect of the processes involved in sediment deposition and erosion to aid in validating idealised numerical models for accurate predictions of the part mangroves play in sediment patterns. The land owners in the region (i.e. the Te Whangai Trust) are interested in quantifying whether their efforts to decrease pollution are in fact, effective or not. The JetYak could be used over time to collect data from the same location to build a long-time series over the period of months to years to show whether pollution is decreasing.

# References

Abadie, A., Gobert, S., Bonacorsi, M., Lejeune, P., Pergent, G., & Pergent-Martini, C. (2015). Marine space ecology and seagrasses. Does patch type matter in Posidonia oceanica seascapes? *Ecological Indicators, 57*, 435-446.

Abdeljawad, A. A. (Compiler) (2006). *System for aiding in prevention of engine overheating in a vehicle*: Google Patents.

Beck, M. W., Heck, K. L., Able, K. W., Childers, D. L., Eggleston, D. B., Gillanders, B. M., Halpern, B., Hays, C. G., Hoshino, K., Minello, T. J., Orth, R. J., Sheridan, P. F., & Weinstein, M. P. (2001). The Identification, Conservation, and Management of Estuarine and Marine Nurseries for Fish and Invertebrates. *BioScience, 51*(8), 633.

Blum, W., & Ferri, R. B. (2009). Mathematical modelling: Can it be taught and learnt? *Journal of mathematical modelling and application, 1*(1), 45-58.

Boesch, D. F., & Turner, R. E. (1984). Dependence of Fishery Species on Salt Marshes: The Role of Food and Refuge. *Estuaries, 7*(4), 460.

Bos, A. R., Bouma, T. J., de Kort, G. L. J., & van Katwijk, M. M. (2007). Ecosystem engineering by annual intertidal seagrass beds: Sediment accretion and modification. *Estuarine, Coastal and Shelf Science, 74*(1), 344-348.

Burlingame, G. A., Pickel, M. J., & Roman, J. T. (1998). Practical applications of turbidity monitoring. *American Water Works Association. Journal, 90*(8), 57-69.

Cajaraville, M. P., Bebianno, M. J., Blasco, J., Porte, C., Sarasquete, C., & Viarengo, A. (2000). The use of biomarkers to assess the impact of pollution in coastal environments of the Iberian Peninsula: a practical approach. *Science of The Total Environment, 247*(2), 295-311.

Cameron, W., & Pritchard, D. (1963). Estuaries, The Sea. *John Wiley & Sons, 2*, 306-324.

Cheng, R. T., Ling, C.-H., Gartner, J. W., & Wang, P. F. (1999). Estimates of bottom roughness length and bottom shear stress in San Francisco Bay, California. *Journal of Geophysical Research: Oceans, 104*(C4), 7715-7728.

Chiu, S.-H., Huang, Y.-H., & Lin, H.-J. (2013). Carbon budget of leaves of the tropical intertidal seagrass *Thalassia hemprichii*. *Estuarine, Coastal and Shelf Science, 125*, 27-35.

Claudet, J., & Fraschetti, S. (2010). Human-driven impacts on marine habitats: A regional meta-analysis in the Mediterranean Sea. *Biological Conservation, 143*(9), 2195-2206.

Cox, T. J., & Rutherford, J. C. (2000). Thermal tolerances of two stream invertebrates exposed to diurnally varying temperature. *New Zealand Journal of Marine and Freshwater Research, 34*(2), 203-208.

Cullen-Unsworth, L., & Unsworth, R. (2013). Seagrass meadows, ecosystem services, and sustainability. *Environment: Science and policy for sustainable development, 55*(3), 14-28.

Davis, R. E. (1994). Lagrangian and Eulerian measurements of ocean transport processes. In *Ocean Processes in climate dynamics: Global and Mediterranean examples* (pp. 29-60). Springer.

De Lima, P. H., Janzen, J. G., & Nepf, H. M. (2015). Flow patterns around two neighboring patches of emergent vegetation and possible implications for deposition and vegetation growth. *Environmental Fluid Mechanics, 15*(4), 881-898.

Department of Conservation. (2010). NZ coastal policy statement 2010. *Wellington: Department of Conservation*.

Deppe, F. (2000). Intertidal mudflats worldwide. *Common Wadden Sea Secretariat (CWSS), Wilhelmshaven, 100*.

Devlin, M. J., McKinna, L. W., Álvarez-Romero, J. G., Petus, C., Abott, B., Harkness, P., & Brodie, J. (2012). Mapping the pollutants in surface riverine flood plume waters in the Great Barrier Reef, Australia. *Marine Pollution Bulletin, 65*(4), 224-235.

Doney, S. C., Ruckelshaus, M., Duffy, J. E., Barry, J. P., Chan, F., English, C. A., Galindo, H. M., Grebmeier, J. M., Hollowed, A. B., & Knowlton, N. (2011). Climate change impacts on marine ecosystems. *Annual Review of Marine Science, 4*(1), 11-37.

Duarte, C. M. (2002). The future of seagrass meadows. *Environmental conservation, 29*(2), 192-206.

Dunbabin, M., Grinham, A., & Udy, J. (2009). An autonomous surface vehicle for water quality monitoring. In *Australasian conference on robotics and automation (ACRA)* (pp. 2-4).

Eisma, D. (1998). *Intertidal deposits: river mouths, tidal flats, and coastal lagoons*. (Vol. 16). CRC Press.

Ellis, J., Barter, P., & Cornelisen, C. (2012). *Coastal monitoring using moored instrumentation: Regional to National considerations. Prepared for Hawke's Bay Regional Council.* Report 2199.

Falter, J. L., Lowe, R. J., Atkinson, M. J., Monismith, S. G., & Schar, D. W. (2008). Continuous measurements of net production over a shallow reef community using a modified Eulerian approach. *Journal of Geophysical Research: Oceans, 113*(C7).

Fauziyah, Priatna, A., Prakoso, W. F., Hidayat, T., Surbakti, H., & Nurjuliasti, E. (2018). Measurement and analysis of acoustic backscattering strength for

characteristics of seafloor sediment in Indian Ocean WPP 572-573. *IOP Conference Series: Earth and Environmental Science, 162*.

Fischer, J., Brandt, P., Dengler, M., Müller, M., & Symonds, D. (2003). Surveying the upper ocean with the Ocean Surveyor: a new phased array Doppler current profiler. *Journal of Atmospheric and Oceanic Technology, 20*(5), 742-751.

Fong, D. A., & Geyer, W. R. (2002). The Alongshore Transport of Freshwater in a Surface-Trapped River Plume. *Journal of Physical Oceanography, 32*(3), 957-972.

Fonseca, M. S., Fisher, J. S., Zieman, J. C., & Thayer, G. W. (1982). Influence of the seagrass, *Zostera marina* L., on current flow. *Estuarine, Coastal and Shelf Science, 15*(4), 351-364.

Fonseca, M. S., & Koehl, M. A. R. (2006). Flow in seagrass canopies: The influence of patch width. *Estuarine, Coastal and Shelf Science, 67*(1-2), 1-9.

Garvine, R. W. (1982). A steady state model for buoyant surface plume hydrodynamics in coastal waters. *Tellus, 34*(3), 293-306.

Geeraerts, J., Troch, P., De Rouck, J., Verhaeghe, H., & Bouma, J. J. (2007). Wave overtopping at coastal structures: prediction tools and related hazard analysis. *Journal of Cleaner Production, 15*(16), 1514-1521.

Geyer, W. R., Hill, P. S., & Kineke, G. C. (2004). The transport, transformation and dispersal of sediment by buoyant coastal flows. *Continental Shelf Research, 24*(7), 927-949.

Gornitz, V. (1991). Global coastal hazards from future sea level rise. *Global and Planetary Change, 3*(4), 379-398.

Gumusay, M. U., Bakirman, T., Tuney Kizilkaya, I., & Aykut, N. O. (2018). A review of seagrass detection, mapping and monitoring applications using acoustic systems. *European Journal of Remote Sensing, 52*(1), 1-29.

Halpern, B. S., Kappel, C. V., Selkoe, K. A., Micheli, F., Ebert, C. M., Kontgis, C., Crain, C. M., Martone, R. G., Shearer, C., & Teck, S. J. (2009). Mapping cumulative human impacts to California Current marine ecosystems. *Conservation Letters, 2*(3), 138-148.

Harley, M. D., Turner, I. L., Short, A. D., & Ranasinghe, R. (2011). Assessment and integration of conventional, RTK-GPS and image-derived beach survey methods for daily to decadal coastal monitoring. *Coastal Engineering, 58*(2), 194-205.

He, Q., Li, J., Li, Y., Jin, X., & Che, Y. (2001). Field measurements of bottom boundary layer processes and sediment resuspension in the Changjiang Estuary. *Science in China Series B: Chemistry, 44*(1), 80-86.

Healy, T. (2002). Muddy coasts of mid-latitude oceanic islands on an active plate margin—New Zealand. In T. Healy, Y. Wang & J.-A. Healy (Eds.), *Proceedings in Marine Science* (Chapter 14, pp. 347-374). Elsevier.

Hernández-Dueñas, G., & Karni, S. (2011). Shallow Water Flows in Channels. *Journal of Scientific Computing, 48*(1-3), 190-208.

Horner-Devine, A. R., Hetland, R. D., & MacDonald, D. G. (2015). Mixing and transport in coastal river plumes. *Annual Review of Fluid Mechanics, 47*, 569-594.

Horstman, E. M., Lundquist, C. J., Bryan, K. R., Bulmer, R. H., Mullarney, J. C., & Stokes, D. J. (2018). The dynamics of expanding mangroves in New Zealand. In *Threats to Mangrove Forests* (pp. 23-51). Springer.

Huang, C., & Liao, Y. (2015). Gui pid self-tuning system for quadcopters. In *13th International Conference on Control, Automation, Robotics and Vision* (Vol. 24, pp. 103-108).

Kilcher, L. F., & Nash, J. D. (2010). Structure and dynamics of the Columbia River tidal plume front. *Journal of Geophysical Research: Oceans, 115*(C5).

Kimball, P., Bailey, J., Das, S., Geyer, R., Harrison, T., Kunz, C., Manganini, K., Mankoff, K., Samuelson, K., & Sayre-McCord, T. (2014). The whoi jetyak: An autonomous surface vehicle for oceanographic research in shallow or dangerous waters. In *2014 IEEE/OES Autonomous Underwater Vehicles (AUV)* (pp. 1-7): IEEE.

Klein, R. J., & Nicholls, R. J. (1999). Assessment of coastal vulnerability to climate change. *Ambio*, 182-187.

Klemas, P., & Victor, V. (2009). Remote sensing of coastal resources and environment. *Environmental Research, Engineering and Management, 48*(2), 11-18.

Land Information New Zealand. (2019). Chart NZ 533 Firth of Thames. *LINZ data service*.

Lathrop, R., & Lillesand, T. M. (1989). Monitoring water quality and river plume transport in Green Bay, Lake Michigan with SPOT-1 imagery. *Photogrammetric Engineering & Remote Sensing, 55*(3), 349-354.

Lathrop, R. G., Vande Castle, J. R., & Lillesand, T. M. (1990). Monitoring River Plume Transport and Mesoscale Circulation in Green Bay, Lake Michigan, Through Satellite Remote Sensing. *Journal of Great Lakes Research, 16*(3), 471-484.

Lovelock, C. E., Sorrell, B. K., Hancock, N., Hua, Q., & Swales, A. (2010). Mangrove forest and soil development on a rapidly accreting shore in New Zealand. *Ecosystems, 13*(3), 437-451.

Lovett, G. M., Burns, D. A., Driscoll, C. T., Jenkins, J. C., Mitchell, M. J., Rustad, L., Shanley, J. B., Likens, G. E., & Haeuber, R. (2007). Who needs

environmental monitoring? *Frontiers in Ecology and the Environment, 5*(5), 253-260.

Ludvigsen, M., Berge, J., Geoffroy, M., Cohen, J. H., Pedro, R., Nornes, S. M., Singh, H., Sørensen, A. J., Daase, M., & Johnsen, G. (2018). Use of an Autonomous Surface Vehicle reveals small-scale diel vertical migrations of zooplankton and susceptibility to light pollution under low solar irradiance. *Science advances, 4*(1), 1-8.

Luhar, M., Coutu, S., Infantes, E., Fox, S., & Nepf, H. (2010). Wave induced velocities inside a model seagrass bed. *Journal of Geophysical Research: Oceans, 115*(C12).

Matheson, F. E., & Schwarz, A. M. (2007). Growth responses of *Zostera capricorni* to estuarine sediment conditions. *Aquatic Botany, 87*(4), 299-306.

McDougall, T. J., & Barker, P. M. (2011). Getting started with TEOS-10 and the Gibbs Seawater (GSW) oceanographic toolbox. *SCOR/IAPSO WG, 127*, 1-28.

Memon, P. A., & Gleeson, B. (1995). Towards a new planning paradigm? Reflections on New Zealand's resource management act. *Environment and Planning B: Planning and Design, 22*(1), 109-124.

Milliman, J. D., & Syvitski, J. P. (1992). Geomorphic/tectonic control of sediment discharge to the ocean: the importance of small mountainous rivers. *The journal of Geology, 100*(5), 525-544.

Moulton, J., Karapetyan, N., Bukhsbaum, S., McKinney, C., Malebary, S., Sophocleous, G., Li, A. Q., & Rekleitis, I. (2018). An Autonomous Surface Vehicle for Long Term Operations. In: IEEE.

Mullarney, J. C., & de Lange, W. P. (2018). Hydrodynamic modelling of proposed expansion of the Port of Tauranga shipping channels and wharves. *Environmental Research Institute Report No. 119., Client report prepared for the Port of Tauranga. Environmental Research Institute, Faculty of Science and Engineering, The University of Waikato, Hamilton.*, 30 pp.

Mullarney, J. C., & de Lange, W. P. (2019). Impacts on sediment transport of proposed expansion of the Port of Tauranga shipping channels and wharves. *Environmental Research Institute Report No. 123., Client report prepared for the Port of Tauranga. Environmental Research Institute, Faculty of Science and Engineering, The University of Waikato, Hamilton* 11 pp.

Mullarney, J. C., & Henderson, S. M. (2011). Hydraulically controlled front trapping on a tidal flat. *Journal of Geophysical Research: Oceans, 116*(C4).

Mullarney, J. C., & Henderson, S. M. (2013). A novel drifter designed for use with a mounted Acoustic Doppler Current Profiler in shallow environments. *Limnology and Oceanography: Methods, 11*(8), 438-449.

Nash, J. D., & Moum, J. N. (2005). River plumes as a source of large-amplitude internal waves in the coastal ocean. *Nature, 437*(7057), 400.

Nedwell, D., Jickells, T., Trimmer, M., & Sanders, R. (1999). Nutrients in estuaries. *Advances in Ecological Research, 29*, 43-92.

Nicholls, R., & Hoozemans, F. (1996). The Mediterranean: vulnerability to coastal implications of climate change. *Ocean & Coastal Management, 31*(2-3), 105-132.

Nicholls, R. J., & Small, C. (2002). Improved estimates of coastal population and exposure to hazards released. *Eos, Transactions American Geophysical Union, 83*(28), 301.

Nicholson, D. P., Michel, A. P., Wankel, S. D., Manganini, K., Sugrue, R. A., Sandwith, Z. O., & Monk, S. A. (2018). Rapid mapping of dissolved methane and carbon dioxide in coastal ecosystems using the ChemYak autonomous surface vehicle. *Environmental science & technology, 52*(22), 13314-13324.

Nittrouer, C. A., Kuehl, S. A., Sternberg, R. W., Figueiredo, A. G., & Faria, L. E. C. (1995). An introduction to the geological significance of sediment transport and accumulation on the Amazon continental shelf. *Marine Geology, 125*(3), 177-192.

Ondiviela, B., Losada, I. J., Lara, J. L., Maza, M., Galván, C., Bouma, T. J., & van Belzen, J. (2014). The role of seagrasses in coastal protection in a changing climate. *Coastal Engineering, 87*, 158-168.

Orth, R. J., Carruthers, T. J. B., Dennison, W. C., Duarte, C. M., Fourqurean, J. W., Heck, K. L., Hughes, A. R., Kendrick, G. A., Kenworthy, W. J., Olyarnik, S., Short, F. T., Waycott, M., & Williams, S. L. (2006). A Global Crisis for Seagrass Ecosystems. *BioScience, 56*(12), 987.

Osadchiev, A., & Zavialov, P. (2019). Structure and Dynamics of Plumes Generated by Small Rivers. In *Estuaries and Coastal Zones-Dynamics and Response to Environmental Changes*. IntechOpen.

Patel, M., Jernigan, S., Richardson, R., Ferguson, S., & Buckner, G. (2019). Autonomous Robotics for Identification and Management of Invasive Aquatic Plant Species. *Applied Sciences, 9*(12), 2410.

Perry, M. J., & Rudnick, D. L. (2003). Observing the ocean with autonomous and Lagrangian platforms and sensors (ALPS): The role of ALPS in sustained ocean observing systems. *Oceanography, 16*(4).

Pritchard, M., Swales, A., & Green, M. (2015). Influence of buoyancy-and wind-coupling on sediment dispersal and deposition in the Firth of Thames, New Zealand. In *Australasian Coasts & Ports Conference 2015: 22nd Australasian Coastal and Ocean Engineering Conference and the 15th Australasian Port and Harbour Conference* (pp. 733): Engineers Australia and IPENZ.

Resio, D. T., Irish, J., & Cialone, M. (2009). A surge response function approach to coastal hazard assessment – part 1: basic concepts. *Natural Hazards, 51*(1), 163-182.

Riser, S. C., & Rossby, T. H. (1983). Quasi-Lagrangian structure and variability of the subtropical western North Atlantic circulation. *Journal of Marine Research, 41*(1), 127-162.

Romero, J., Martínez-Crego, B., Alcoverro, T., & Pérez, M. (2007). A multivariate index based on the seagrass *Posidonia oceanica* (POMI) to assess ecological status of coastal waters under the water framework directive (WFD). *Marine Pollution Bulletin, 55*(1-6), 196-204.

Schumann, E., Largier, J., & Slinger, J. (Compiler) (1999). *Estuarine hydrodynamics*: Cambridge University Press Cambridge.

Sea Change Stakeholder Working Group. (2017). Sea Change: Tai Timu Tai Pari/Hauraki Gulf Marine Spatial Plan.

Shand, T., Reinen-Hamill, R., Kench, P., Ivamy, M., Knook, P., & Howse, B. (2015). Methods for Probabilistic Coastal Erosion Hazard Assessment. *Australasian Coasts & Ports Conference 2015*, 1-7.

She, J., Berg, P., & Berg, J. (2007). Bathymetry impacts on water exchange modelling through the Danish Straits. *Journal of Marine Systems, 65*(1), 450-459.

Shojaei, K. (2016). Observer-based neural adaptive formation control of autonomous surface vessels with limited torque. *Robotics and Autonomous Systems, 78*, 83-96.

Simpson, J., Brown, J., Matthews, J., & Allen, G. (1990). Tidal Straining, Density Currents, and Stirring in the Control of Estuarine Stratification. *Estuaries, 13*, 125-132.

Small, C., & Nicholls, R. J. (2003). A global analysis of human settlement in coastal zones. *Journal of coastal research, 19(3)*, 584-599.

Stacey, M. T., Cowen, E. A., Powell, T. M., Dobbins, E., Monismith, S. G., & Koseff, J. R. (2000). Plume dispersion in a stratified, near-coastal flow: measurements and modeling. *Continental Shelf Research, 20*(6), 637-663.

Swales, A., Bentley, S. J., Lovelock, C., & Bell, R. G. (2007). Sediment processes and mangrove-habitat expansion on a rapidly-prograding muddy coast, New Zealand. In *Coastal Sediments' 07* (pp. 1441-1454).

Swales, A., Bentley Sr, S. J., & Lovelock, C. E. (2015). Mangrove‐forest evolution in a sediment‐rich estuarine system: opportunists or agents of geomorphic change? *Earth Surface Processes and Landforms, 40*(12), 1672-1687.

Tsai, C.-M., Lai, Y.-H., Perng, J.-W., Tsui, I.-F., & Chung, Y.-J. (2019). Design and Application of an Autonomous Surface Vehicle with an AI-Based

Sensing Capability. In *2019 IEEE Underwater Technology (UT)* (pp. 1-4): IEEE.

Valada, A., Velagapudi, P., Kannan, B., Tomaszewski, C., Kantor, G., & Scerri, P. (2014). Development of a low cost multi-robot autonomous marine surface platform. In *Field and service robotics* (pp. 643-658): Springer.

Vickery, P. J., Masters, F. J., Powell, M. D., & Wadhera, D. (2009). Hurricane hazard modeling: The past, present, and future. *Journal of Wind Engineering and Industrial Aerodynamics, 97*(7), 392-405.

Wainwright, D. J., Ranasinghe, R., Callaghan, D. P., Woodroffe, C. D., Jongejan, R., Dougherty, A. J., Rogers, K., & Cowell, P. (2015). Moving from deterministic towards probabilistic coastal hazard and risk assessment: Development of a modelling framework and application to Narrabeen Beach, New South Wales, Australia. *Coastal engineering, 96*, 92-99.

Walsh, J., & Nittrouer, C. (2009). Understanding fine-grained river-sediment dispersal on continental margins. *Marine Geology, 263*(1-4), 34-45.

Wang, W., Engelaar, R., Chen, X., & Chase, J. (2009). The state-of-art of underwater vehicles-theories and applications. In *Mobile Robots-State of the Art in Land, Sea, Air, and Collaborative Missions* (pp. 129-152). IntechOpen.

Warrick, J. A., DiGiacomo, P. M., Weisberg, S. B., Nezlin, N. P., Mengel, M., Jones, B. H., Ohlmann, J. C., Washburn, L., Terrill, E. J., & Farnsworth, K. L. (2007). River plume patterns and dynamics within the Southern California Bight. *Continental Shelf Research, 27*(19), 2427-2448.

Weeks, E., Li, C., Roberts, H., Shaw, R. F., & Walker, N. (2011). A comparison of an unmanned survey vessel to manned vessels for nearshore tidal current and transport measurements. *Marine Technology Society Journal, 45*(5), 71-77.

Wolfe, D., Champ, M., Flemer, D., & Mearns, A. (1987). Long-term biological data sets: their role in research, monitoring, and management of estuarine and coastal marine systems. *Estuaries, 10*(3), 181.

Wu, H.-Y., Rubinstein, M., Shih, E., Guttag, J., Durand, F., & Freeman, W. (2012). Eulerian video magnification for revealing subtle changes in the world. *ACM Transactions on Graphics, 31(4)*, 1-8.

Yorke, T. H., & Oberg, K. A. (2002). Measuring river velocity and discharge with acoustic Doppler profilers. *Flow Measurement and Instrumentation, 13*(5-6), 191-195.

# Appendices

**Appendix A.** JetYak Safety Case Plan

**SCHOOL OF SCIENCE**
Faculty of Science & Engineering
*Te Mātauranga Pūtaioao me te Pūkaha*
The University of Waikato
Private Bag 3105
Hamilton, New Zealand

# Safety Case Plan

## University of Waikato Autonomous Surface Vessel (USV)

Vessel Name: Whaitere
Maritime New Zealand Number: MNZ136791
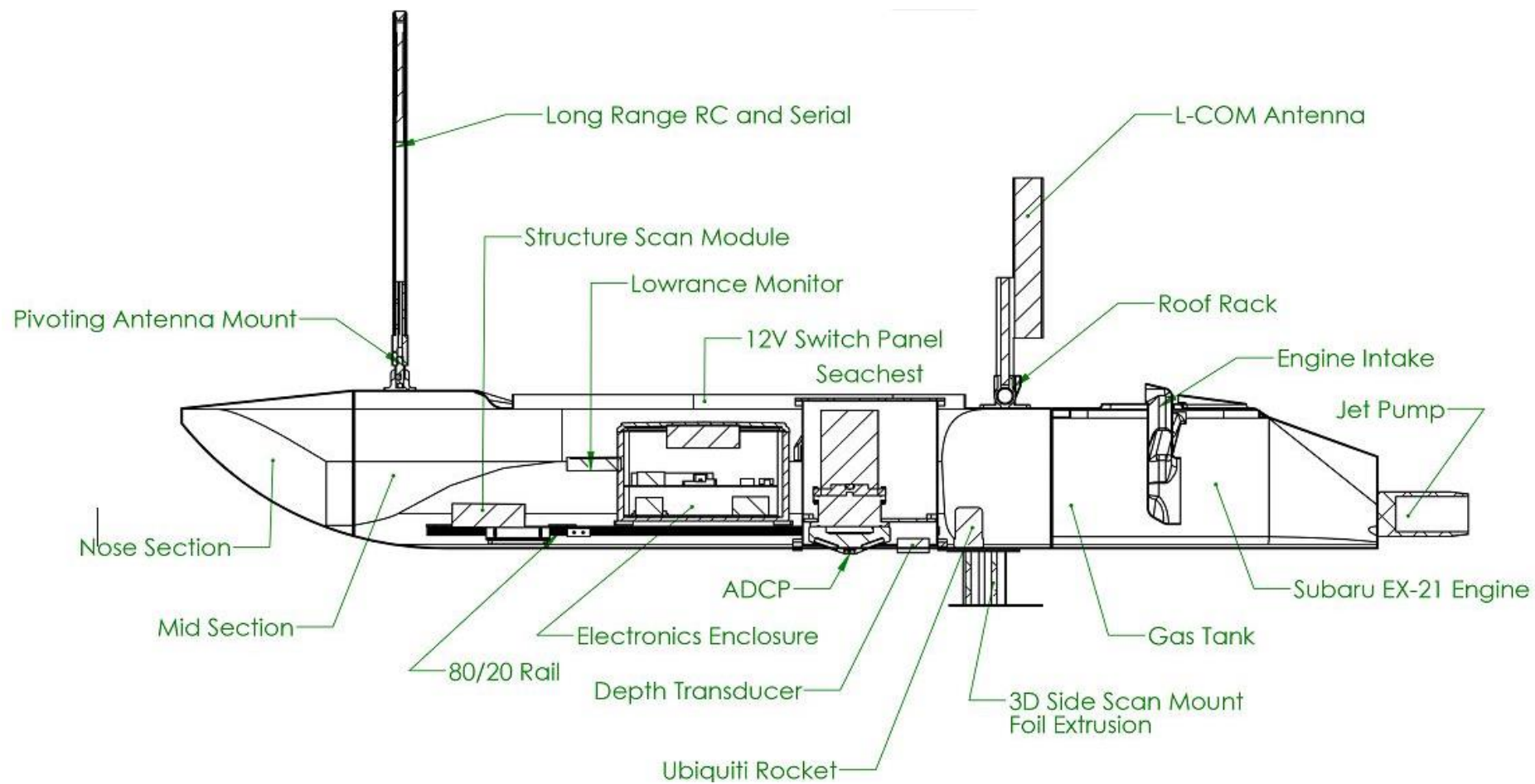Safety Case Number: S1507

Figure 1 Configuration of JetYak

# Appendix 1. Safe (Standard) operating procedures (SOPs)

Operational planning and USV checks procedures

| | Pre-deployment checks |
|---|---|
| | Roles of deployment participants (authorised) allocated, specifically, PIC (person in charge), operator, and observer/s. Depending on USV configuration (i.e. weight of payload and location and resources), min crew will be 1-3 as determined by PIC. |
| | PIC and operators familiar with procedures contained in safety case |
| | Operating area review, i.e. anticipated vessel traffic, maritime charts checked, notice to mariners checked, VHF and mobile coverage harbourmaster, regional council bylaws etc. |
| | Notification and approvals completed |
| | Risk assessment completed |
| | Suitable chase vessel arranged |
| | Weather conditions relative to performance capability of USV checked |
| | Plan deployment duration within daylight hours |
| | Inspection of USV logbook and safety case documentation up-to-date |
| | Confirm that maintenance is up-to-date |
| | Bearing and coupler greased |
| | Trailer condition and WOF checked |
| | Oil level |
| | Inspection of USV engine and jet unit in accordance to manufacturers user's manual |
| | Fuel line leaks, cracks, or loose connections |
| | Visual hull check |
| | Is vessel clean? Is biosecurity a risk? Spray vessel with 2% bleach or 1% sodium hyperchlorite if required |
| | Sufficient premium 95 octane fuel (fresh with stabiliser added) |
| | Check engine |
| | Starter battery charged |
| | Instrumentation batteries charged |
| | RC transmitter charged |

| | Peripheral sensors checked and payload total < 136 kg |
|---|---|
| | Check Trello board for checklist items and tasks |
| | |

## At location set-up procedures

| **Pre-operation (setting up USV at deployment location) checks** |
|---|
| Team briefing. Discuss work flow, hazards and use of SAPP: stop, assess, plan, proceed |
| On-site weather ok |
| Modular sections attached and secure (see Mokai manual) |
| Engine installed and locking pin secured (see Mokai manual) |
| Oil checked in pre-deployment |
| Starter battery secured, connected and state of charge |
| Sufficient fuel (refuel on land with spill kit and fire extinguisher ready, if unable to refuel on land then extreme caution with water based refuelling taken, USV must be secured, towel must be placed around engine compartment, careful and slow delivery of fuel) |
| Check fuel line and connection |
| Check jet drive, intake grill, steering connection and overcenter v-band clamp |
| Check starboard cockpit (mid-section) drain plug |
| Instruments (e.g. echosounder/s, CTD, ADCP) connected and secure |
| Instrumentation batteries secure |
| Test throttle |
| Test steering |
| Fuel valve open |
| See EX21 manual pg 8 for additional startup information |
| Set throttle to 1/3 towards high |
| Choke can be open if temp/engine warm or closed ½ way |
| Pull starter until resistance is felt |
| Engage starter for 5 sec max (if engine is not running wait for starter battery to recover) |
| Run engine for a few minutes and slowly reduce revs |
| Test kill switch |

| | |
|---|---|
| | Engine cover fitted and lock secured |
| | Dorade fitted if necessary |
| **Vessel is ready to be launched** | |

## Launching

| | **During deployment checks** |
|---|---|
| | Prior checklists completed |
| | Bung |
| | Covers |
| | Prepare for quick release from trailer |
| | Connect ground control station (GCS) to base station |
| | Any parameters require checking? Compass? Failsafe? |
| | |

## During operation procedures

| | **During deployment checks** |
|---|---|
| | If vessel is not visible confirm vessel location on base station or gps tracker every 5minutes. |
| | If refuelling allow engine to cool for 2 minutes prior, spill kit and fire extinguisher on-hand |
| | Check USV performance at regular intervals and inspect compartments for water ingress |
| | |
| | |

## Shut down and storage procedures

| | |
|---|---|
| | Familiar with page 8 of EX manual |
| | Run engine at low speed for 1-2minutes |
| | Activate kill switch or disconnect fuel line |
| | Close fuel valve |
| | Pull starter handle until resistance is felt (prevent moisture entering combustion chamber) |
| | Clean USV with fresh soapy water or Windex type product |
| | Spray vessel with 2% bleach or 1% sodium hyperchlorite |
| | Remove engine (note engine must always be upright to prevent oil entering carburator) |
| | Rinse any salt spray |
| | Light spray of corrosion block to exterior of engine and linkage |
| | Remove jet drive and rinse |
| | Complete bearing and coupler manintenance (page 16 Mokai manual) |
| | Disconnect starter battery |
| | Team debriefing |
| | Long term storage – drain carburator |
| | Long term storage recharge battery 1x month |
| | Update documentation |

## Gear checklist

| Gear checklist |
|---|
| See Trello board checklist |
| |

**Log of completed drills**

| Date | Completed drill/s | Person/s present |
|---|---|---|
| 14/06/2018 | Fuel spill<br>Loss of propulsion<br>Loss of steering | Dean Sandwell, Julia Mullarney, Morgan Harvie |
|  |  |  |
|  |  |  |
|  |  |  |
|  |  |  |
|  |  |  |
|  |  |  |

# Maintenance record

Note : maintanance is also recorded in the vessel logbook located on the drive :

\IntegratedCoastalSolutions

JetYak\Docs\USV_logbook_hrs_issues_maintenance.xlsx

Furthermore, maintenance information is on the Trello management board for USV.

| Date | Maintenance completed | Engine hours | Completed by |
|---|---|---|---|
| 12/12/2018 | Salt away, silicon and corrosion spray applied | 12.5 | DeanS<br>MorganH<br>JuliaM |
| 23/05/19 | Oil change, bearings greased, silicon and corrosion spray applied | 13.5 | DeanS<br>MorganH |

## Log of completed training

| Date | Completed training | Person/s present |
|------|-------------------|------------------|
| 14/06/2018 | Vessel assembly, refuelling, oil checks, oil delivery, engine removal and installation. | Dean Sandwell, Julia Mullarney, Morgan Harvie |
| 13/09/2018 | Mission planner, startup and operating procedures | Dean Sandwell, Julia Mullarney, Morgan Harvie |
| 03/10/2018 | Mission planner FS, fire drill, loss of control, startup and operating procedures | Dean Sandwell, Morgan Harvie |
| 15/10/2018 | Mission planner settings, loss of control | Dean Sandwell, Julia Mullarney, Morgan Harvie |
| 14/11/2018 | Mission planner, startup and operating procedures | Dean Sandwell, Julia Mullarney, Morgan Harvie |
| 23/05/2019 | Maintenance – oil changing | Dean Sandwell, Morgan Harvie |
| 27/05/2019 | PID optimisation | Dean Sandwell, Morgan Harvie |

# List of qualified operators

| Name | Qualifications | Trained/assessed by: |
|---|---|---|
| Dean Sandwell | | n/a involved in development of USV and procedures |
| Julia Mullarney | | n/a involved in development of USV and procedures |
| Morgan Harvie | | n/a involved in development of USV and procedures |
| | | |
| | | |
| | | |
| | | |